Bioactivity evaluation of manno-oligosaccharides produced from spent coffee grounds using a *Bacillus sp.* derived endo-1,4-β-mannanase

A thesis submitted in fulfilment of the requirements for the degree of

Master of Science (Biochemistry)

At

Rhodes University

By

Mihle Magengelele

ORCID ID:

https://orcid.org/0000-0002-2947-6219

Supervisor: Prof. Brett. I. Pletschke

Co-supervisor: Dr. Samkelo Malgas

Febuary 2022

Abstract

Coffee is one of the most popular beverages produced worldwide; however, its processing results in the generation of spent coffee grounds (SCGs). SCG as an agro-industrial waste which leads to adverse environmental effects, such as carbon dioxide and methane production, when disposed of in landfills. SCGs contain high levels of polysaccharides such as mannan, specifically galactomannan; thus, the utilisation of this waste is an important subject. Recently, there has been a growing interest in the production of nutraceutical mannooligosaccharides (MOS) through the enzymatic hydrolysis of mannans. MOS have been reported to exhibit various bioactive properties, including prebiotic effects, the ability to inhibit pathogens and antioxidant activity.

In this study, a *Bacillus sp*. derived endo-1,4-β-mannanase, Man26A, was used for the production of MOS from model mannan substrates; ivory nut mannan (INM), locust bean gum (LBG) and guar gum (GG). After incubation, Man26A exhibited saccharification yields of 30.18, 36.86 and 34.93% for INM, LBG and GG, respectively. Kinetic studies showed that Man26A had a high binding affinity and catalytic efficiency for LBG (K_m = 10.8 mg/mL and k_{cat}/K_m = 8.8 min^{-1} mg^{-1}mL) than INM (K_m = 28.9 mg/mL and k_{cat}/K_m = 3.8 min^{-1} mg^{-1}mL) and GG (K_m = 50.2 mg/mL and k_{cat}/K_m = 2.6 min^{-1} mg^{-1}mL). The hydrolysis products from these model mannan substrates were quantitatively and qualitatively analysed using high-performance liquid chromatography (HPLC) and thin-layer chromatography (TLC), respectively. INM hydrolysis resulted in the production of mannose (M1) - mannotriose (M3), while LBG hydrolysis resulted in the generation of M1 - M2 (mannobiose) and mannopentaose (M5) - mannohexaose (M6) as the dominant sugars. On the other hand, GG hydrolysis mainly produced M5 - M6, and some oligosaccharides with a degree of polymerisation (DP > 6). Putative galactosyl-MOS; GM2 and GM3, were also observed in the HPLC chromatograms of both LBG and GG hydrolysates. The MOS produced from these model mannan substrates were stable over a broad pH range of 2 - 10. Furthermore, MOS produced by enzyme hydrolysis showed antioxidant properties, with MOS obtained from INM showing higher antioxidant activity than those from LBG and GG.

A mannan-rich agro-processing waste, SCG, was pretreated using NaOH and hydrolysed using Man26A under the optimised conditions obtained from the model mannan hydrolysis studies for MOS generation. Structural analysis studies performed using Fourier-transform infrared spectroscopy (FT-IR) and thermogravimetric analysis (TGA) confirmed the structure of

untreated and pretreated SCGs, and some chemical differences were observed in the untreated and pretreated SCGs. TGA analysis specifically showed that pretreated SCG was more resistant to temperature induced decomposition than untreated SCG. The removal of lignin during the pretreatment of SCG was observed by TGA, whereas the decomposition of lignin was only observed in untreated SCG. Using FT-IR, α-linked D-galactopyranose units (812 cm-1) and β-linked D-mannopyranose units (817 cm-1) were observed in both untreated and pretreated SCGs, confirming the galactomannan presence. MOS were successfully produced from the hydrolysis of NaOH pretreated SCG by Man26A, where M2 (1.04 mg/mL) and M3 (1.20 mg/mL) were the main products. The effect of bile salts, α-amylase, trypsin and hydrochloric acid on SCG-MOS was investigated, and they did not degrade SCG-MOS. The effect of SCG MOS on the *in vitro* survival of beneficial bacteria was investigated. SCG-MOS enhanced the growth of *Lactobacillus bulgaricus, Bacillus subtilis* and *Streptococcus thermophilus*, and led to the production of short chain fatty acids (SCFAs). The growth of beneficial bacteria in the presence of SCG-MOS was 2-fold higher than in the presence of the glucose control and sugar-free control. Bacterial SCFAs production was more in carbon source containing broth than sugar-free broth. In terms of autoaggregation influence, *L. bulgaricus, B. subtilis* and *S. thermophilus* grown in the presence of SCG-MOS showed aggregation percentages of 18.21, 20.98 and 17.99%, respectively. The formation of biofilms by these bacterial cells in the presence of SCG-MOS were approximately 2-fold higher than the values obtained in the positive mannose control and sugar-free control. Utilisation of SCG-MOS activated putative mannan degrading genes in beneficial bacteria, resulting in the production of mannan degrading enzymes, such as β-mannanase, β-mannosidase and α-galactosidase.

In conclusion, this study demonstrated that enzymatic hydrolysis of SCG using Man26A resulted in the production of M2 and M3 as the predominant MOS. These MOS have prebiotic effects, which may be essential for the improvement of animal and human health. The MOS possibly act in the digestive tracts of mammals by enhancing the production of beneficial secondary metabolites, such as SCFAs, and enhancing autoaggregation and biofilm formation of beneficial bacteria, which may likely lead to competitive exclusion of pathogenic bacteria in the host's digestive tract.

Keywords: mannanase, mannooligosaccharides, prebiotic, probiotic, spent coffee grounds

Declaration

I, Mihle Magengelele, declare that this thesis is my own, unaided work. It is hereby submitted for the degree of Master of Science at the Faculty of Science, Rhodes University. It has not been submitted before for any degree or examination at any other university.

Signature:  Date: 08 February 2022

Table of contents

List of Abbreviations

°C	Degree(s) Celsius
µM	Micromolar
µmol	Micromole
AA	Acetic acid
ABTS	2,2'-azino-bis(3-ethylbenzothiazoline-6-sulfonic acid)
AXOS	Arabinoxylan-oligosaccharides
BA	Butyric Acid
BSA	Bovine serum albumin
CBM	Carbohydrate binding domain
CDV	Cardiovascular disease
DNS	Dinitrosalicylic acid
DP	Degree of polymerization
DPPH	2,2-diphenyl-1-picrylhydrazyl
EC	Enzyme commission number
EPS	Exopolysaccharides
g	Gram
GH	Glycoside hydrolase
GG	Guar gum
HMO	Human mannooligosaccharides
HPLC	High-performance liquid chromatography
RID	Refractive index detector

h	Hour
INM	Ivory nut mannan
kDa	Kilo Daltons
LA	Lactic acid
LBG	Locust bean gum
Man26A	GH26 endo-1,4-β-mannanase
MOS	Mannooligosaccharide(s)
mg	Milligram
min	Minute
mL	Millilitre
mM	Millimolar
OD	Optical density
PBS	Phosphate-buffered saline
QS	Quorum sensing
SCG	Spent coffee grounds
SD	Standard deviation
SEM	Scanning electron microscopy
SCFA	Short-chain fatty acids
TLC	Thin-layer chromatography
U	Unit of enzyme activity
VAPs	Value-added products
XOS	Xylo-oligosaccharides

List of Figures

List of Tables

Dedication

My work is wholeheartedly dedicated to:

My mother, Bongiwe Magengelele,

My grandparents; Nowinile Constance Magengelele and the late Tutu Ndisindile Ruphus Magengelele,

And

My late father, Kwanele Martin Ndleleni, uFaku!

Acknowledgements

I would like to show my gratitude to Prof. Pletschke and Dr. Malgas for their supervision, support and guidance throughout the duration of this degree, and for giving me the opportunity to be part of the ESP research group.

I would also like to acknowledge my funder, the National Research Foundation (NRF). Any opinion, findings and conclusions or recommendations expressed in this material are mine and therefore the NRF does not accept any liability in regard thereto.

Personal acknowledgements:

To my family, Bongiwe, Nowinile (Nontandathu), Mfanelo, Nomfundo, Tembeka, Mzoxolo and Vukile Magengelele, for their undying support, love and encouragement throughout this journey.

To my friends, Zipho Sofute, Anathi Ngxakeni, Yamkelani Sopapaza, Namhla Bhenxa, Sivuyile Sitole, Tariro Sithole Lesley Mpofu, Wezo Sukwana, Sihle Sithole and Tavonga Chidavaenzi., I am very grateful for their support, friendship and for keeping me sane throughout this journey. I appreciate each and every one of you.

I am also grateful to my colleagues (Blessing Mabate, Lebogang Ramatsui, Nosipho Hlalukana, Lithalethu Mkabayi, Tariro Sithole, Chantal Daub, Happyness Ncoyi, Amy Anderson, Arryn Michaels and Yuchan Park) for their friendship, encouragement and support.

List of outputs emanating from this study

Publications:

Hlalukana, N., Magengelele, M., Malgas, S. and Pletschke, B.I., 2021. Enzymatic conversion of mannan-rich plant waste biomass into prebiotic mannooligosaccharides. *Foods*, *10*(9), p.2010. https://doi.org/10.3390/foods10092010

Magengelele, M., Hlalukana, N., Malgas, S., Rose, S.H., van Zyl, W.H. and Pletschke, B.I., 2021. Production and *in vitro* evaluation of prebiotic manno-oligosaccharides prepared with a recombinant *Aspergillus niger* endo-mannanase, Man26A. *Enzyme and Microbial Technology*, *150*, p.109893. https://doi.org/10.1016/j.enzmictec.2021.109893

Research paper in preparation:

Magengelele, M., Malgas, S. and Pletschke, B.I. Bioactivity evaluation of manno-oligosaccharides produced from spent coffee grounds using a *Bacillus sp.* derived endo-1,4-β-mannanase.

CHAPTER 1: General Introduction and Literature review

1.1. Introduction

1.1.1. Coffee

Coffee is the second most popular beverage globally, and it results in the generation of large amounts of spent coffee grounds (SCG). Approximately 6 megatons of coffee beans are produced globally per year, and 1 ton of beans results in 650 kilograms (kg) of SCG (Nguyen et al., 2019). The International Coffee Organization (ICO) estimated that about 8.5 billion kg and 9.3 billion kg of coffee was produced in 2014 and 2016, respectively, worldwide (McNutt & He, 2019). Rodr guez- r talejo and L p ez-Garc a 2017) linked coffee consumption with a decreased risk of cardiovascular disease (CVD), the leading cause of poor health globally; this could mean that the production of coffee will continue to increase.

During the preparation of coffee, coffee beans are first roasted and ground. Then, water is used to extract the coffee via a thermal water extraction technique at 100 and 180^{o}C (Jooste et al., 2013). The resulting water-soluble solids are evaporated and dried either by spray drying or freeze-drying to obtain instant coffee (Jooste et al., 2013). The waste, which is the insoluble material, is then discarded in landfills (Jooste et al., 2013).

1.1.2. Spent coffee grounds

SCG is the main agro-industrial waste generated during the production of instant coffee. It is composed of lignocellulosic biomass that is amenable to hydrolysis by lignocellulolytic enzymes (Van Zyl et al., 2010). This lignocellulosic biomass is composed of polysaccharides (cellulose and hemicellulose), protein and lignin (Mussatto et al., 2011; Sachslehner et al., 2000). Hydrolysis of hemicellulose and cellulose by lignocellulolytic enzymes results in fermentable sugars, which can be used as precursors for the synthesis of value-added products (VAPs) (Mussatto et al., 2011; Sachslehner et al., 2000; Wolfrom & Patin, 1965). Among the components, mannan is responsible for the high viscosity of coffee extract and is the major polysaccharide in SCG which forms about 20-30% of the dry matter and is water-

insoluble (Sachslehner et al., 2000). There are four types of mannans in nature; linear mannan, glucomannan, galactomannan and galactoglucomannan (Malgas et al., 2015a; Van Zyl, et al., 2010). The primary type of mannan found in SCG is galactomannan (Nguyen et al., 2019).

1.1.2.1. Spent coffee ground galactomannan

Galactomannan is the predominant component in coffee bean cell walls; it accounts for approximately 50% of the total polysaccharides (Redgwell & Fischer, 2006). Galactomannan is made up of linear chains of β-1,4-linked mannopyranose residues substituted with galactose units at the C-6 position via α-1,6-linkages (Redgwell & Fischer, 2006). Nunes et al. (2005) and Oosterveld et al. (2004) demonstrated that there are acetyl groups which may be attached to the O-2 and O-3 positions on the mannose residues of coffee bean galactomannans. Like galactose substituents, these substituents disrupt the inter-chain hydrogen bonds and increase substrate solubility (Redgwell & Fischer, 2006). Jiang et al. (2014) reported that as the ratio of acetylation increases, the enzymatic hydrolysis ratio of hemicellulose decreases. This is why SCG is pretreated with sodium hydroxide to remove acetyl substituents to create more sites for hydrolysis (Redgwell & Fischer, 2006). The hydrolysis of SCG galactomannan results in mannooligosaccharide (MOS) production, which can be used as prebiotics, which are important in preventing pathogenic bacteria from attaching to the gut (Nguyen et al., 2019).

1.1.3. Mannan and mannan-degrading enzymes

As described previously, mannans are divided into four groups, depending on which sugar(s) the β-1,4-linked backbone contains and the amount of α-1,6-linked galactose present (Sachslehner et al., 2000). These groups are linear mannans, glucomannans, galactomannans and galactoglucomannans Malgas et al., 2015a; Van Zyl, et al., 2010). The β-1,4-linked backbones of linear mannans and galactomannans exclusively contains D-mannose, while that of glucomannans and galactoglucomannans contain both D-mannose and D-glucose (Van Zyl, et al., 2010). Galactomannans generally contain more than 5% (w/w) D-galactose while galactoglucomannanans are glucomannans that contain more than 5% (w/w) D-galactose

(Van Zyl, et al., 2010). The structures of these types of mannans are illustrated in Figure 1.1 below.

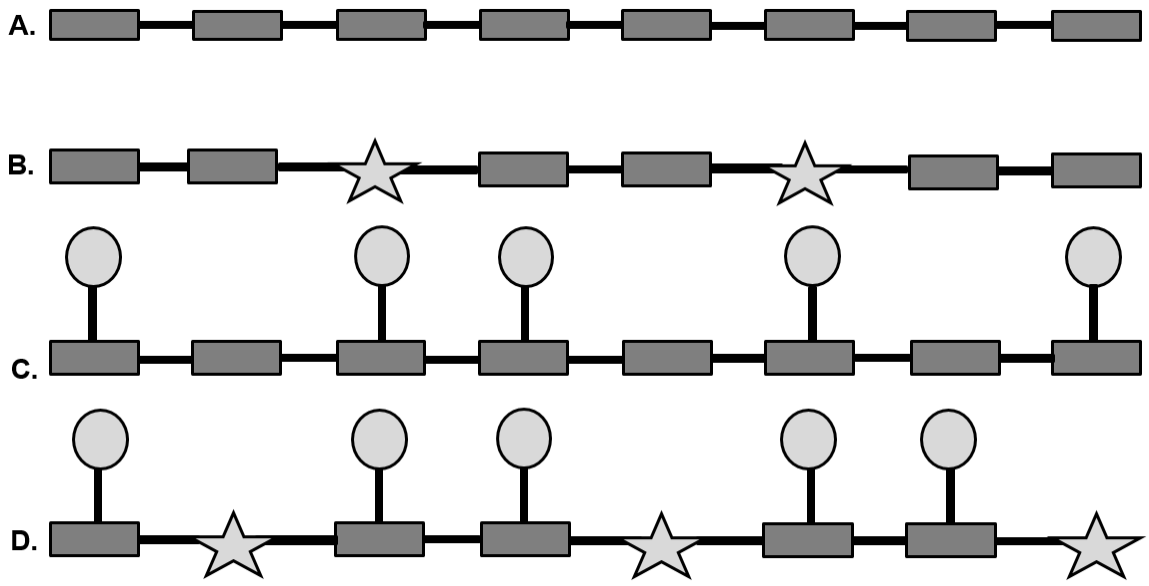

Figure 1.1: Structures of different mannans. A: linear mannan, B: glucomannan, C: galactomannan, and D: galactoglucomannan. The rectangles represent mannose; stars represent glucose; circles represent galactose and the lines between sugars represent glycosidic bonds. Adapted from Malgas et al. (2015a).

These mannans are hydrolysed by mannan-degrading enzymes, which are classified into glycosyl hydrolase (GH) families. GHs are enzymes that catalyse the hydrolysis of the glycosidic linkages of saccharides (Moreira & Filho, 2008). Hydrolysis of these glycosidic bonds require two important residues; the acid/base and the nucleophile (Van Zyl et al., 2010). These enzymes are classified into GH families based on the similarity of their amino acid sequences and three-dimensional structures (Van Zyl et al., 2010). Enzymes in GH families are further grouped into endo-acting hydrolases and exo-acting hydrolases (Moreira & Filho, 2008). The enzymes that contriute to mannan hydrolysis are β-mannanase, β-mannosidase, β-galactosidase, β-glucosidase, acetyl mannan esterase (Moreira & Filho, 2008; Van Zyl, et al., 2010) and mannobiohydrolase (Tsukagoshi, et al., 2014).

1.1.3.1. β-mannanases

β-mannanases (EC 3.2.1.78) are found in GH families 5, 26, 45, 113 and 134 in the Carbohydrate-Active enZyme (CAZy) system of annotation (www.cazy.org). β-Mannanases are endo-acting enzymes that randomly cleave the β-1,4-linked internal linkages of the mannan backbone, resulting in oligomers and small amounts of mannose (Moreira & Filho, 2008). GH families 5, 26 and 113 are from the GH- clan, a group of GHs with a $(\beta/\alpha)_8$-barrel fold (Bågenholm et al., 2019; Hlalukana et al., 2021; Zhang et al., 2008;) while the clan of GH134 mannanases is currently unknown (www.cazy.org). All CAZymes have an active site cleft which contains subsites, from the non-reducing end (-n) to reducing end (+n), for saccharide binding (Bågenholm et al., 2019). GH26 mannanases have conserved subsites that allow them to bind to substrates that contain six sugars (Kaira and Kapoor, 2019). GH26 mannanases have 7 substrate subsites; +2 to -5. The -5 subsite in GH26 enzymes contains Trp-112, which has been reported to bind mannosyl groups (Bågenholm et al., 2019). Tailford et al. (2009) reported that the GH26 mannanase derived from *Bacillus subtilis* has high specificity for mannose at its negative subsites. Srivastava and Kapoor (2017) reported that the substrate subsites important for GH5 mannanase binding range from +2 to -3. Some of the GH-A clan enzymes have been reported to exhibit transglycosylation activity, where a hydroxyl group of a carbohydrate acts an electron acceptor, resulting in oligosaccharides with higher degree of polymerisation (Couturier et al., 2013; Zhang et al., 2008). GH5 mannanases exhibit transglycosylation activity, while GH 26 mannanases do not transglycosylate (Couturier et al., 2013). The semi-conserved substrate subsite, +2, of GH5 mannanases plays an important role in transglycosylation (Couturier et al., 2013). Xia et al. (2016) reported that GH113 mannanases also exhibit transglycosylation activity.

β-Mannanases are produced by different microorganisms, such as fungi, yeast and bacteria, plants and animals Chauhan et al., 2012). β-Mannanases produced by microorganisms can be easily isolated since they tend to be produced extracellularly; this makes their commercial production cost-effective (Ozturk & Ogel, 2010). Chauhan et al. (2012) demonstrated that the optimum temperature and pH of β-mannanases range between 40-75^{o}C and pH 3-7.5, respectively. Tsukagoshi et al. (2014) showed that a mannobiohydrolase from *Reticulitermes speratus*, RsMan26H, has high activity on LBG than GG. RsMan26H mannobiohydrolase has an optimum pH and temperature range of of pH 5-6.5 and 40^{o}C, where 80% of the activity is retained. Mannobiohydrolase (EC 3.2.1.100) is an endo-processive mannanase with the

ability to hydrolyse polysaccharides and oligosaccharides to produce mannobiose (Tsukagoshi, et al., 2014). The fungus, *Sclerotium rolfsii*, uses cellulose or glucose as a carbon source for enzyme production (Van Zyl, et al., 2010). In *Aspergillus spp*., the production of β-mannanases is induced in the presence of substrates rich in mannan, e.g., copra meal and wheat bran (Alsarrani, 2011; Ozturk & Ogel, 2010; Van Zyl, et al., 2010). Gomes et al. (2017) reported that the enzyme activities of β-mannanase and β-mannosidase were high when their production was induced using locust bean gum and soybean in *Thermoascus aurantiacus.* This enzyme can hydrolyse inexpensive biomass, resulting in the production of mannooligosaccharides (MOS) used as prebiotics to enhance the growth of beneficial microflora in animals Harnpicharnchai et al., 2016). β-mannanases are also used in other processing steps such as in the extraction of oil from copra, improving clarity in juices, reducing viscosity in coffee extracts, and improving the quality of paper in the bio-bleaching of paper pulp (Ozturk & Ogel, 2010).

1.1.3.2. α-Galactosidases, β-glucosidases, acetyl mannan esterases and β-mannosidases

Complete hydrolysis of mannan also requires additional enzymes; acetyl mannan esterase, β-glucosidase and α-galactosidase, which are important for removing side-chain constituents attached to mannan, creating more sites for hydrolysis (Moreira & Filho, 2008). Acetyl mannan esterases (EC 3.1.1.72) remove acetyl groups from *O*-acetylated mannans (Van Zyl et al., 2010). α-Galactosidases (EC 3.2.1.22) are found in GH families 4, 27 and 36 in the CAZy database (Van Zyl et al., 2010) and are essential to remove galactose substituents from glycoproteins and glycolipids (Redgwell & Fischer, 2006). α-Galactosidases are also used to determine the degree of glycosylation by cleaving side-chain galactose from the primary synthetic product (Redgwell & Fischer, 2006). Ademark et al. (2001) showed that galactosidases from GH27 and GH36 are structurally different, contributing to the differences in their activities (Ademark et al., 2001). GH27, which is smaller and sometimes monomeric, has high activity on highly substituted galactomannan polymers; while GH37, which is large and tetrameric, is more specific to small galactosylated-oligosaccharides (Ademark et al., 2001).

β-Glucosidases (EC 3.2.1.21) are exo-acting hydrolases that catalyse the hydrolysis of the glycosidic bonds at the non-reducing ends in oligosaccharides, which result from the

hydrolysis of glucomannan and galactoglucomannan by β-mannanases, leading to the release of glucose Malgas et al., 2015a; Van Zyl, et al., 2010). β-Mannosidases (E.C. 3.2.1.25) are exo-acting enzymes found in GH families 1, 2, and 5. These enzymes attack the terminal non-reducing ends of MOS, such as mannobiose to mannose, to release mannose (Malgas et al., 2015a; Van Zyl, et al., 2010). It has been reported that GH 2 and 5 mannosidases contain a glycone binding site (-1), which is situated in a region that has hydrophobic residues in the family GH2 (Tailford et al., 2007). In family GH5, the glycone is not situated in a region containing hydrophobic residues (Tailford et al., 2007). Families GH 2 and 5 also have two aglycone binding sites (+1 and +2). Tailford et al. (2007) reported that *Bacteroides thetaiotaomicron* GH2 mannosidase, BtMan2A, draws its substrate-binding energy from the glycone binding site. Figure 1.2 below shows the putative cleavage sites of mannanolytic enzymes during mannan hydrolysis.

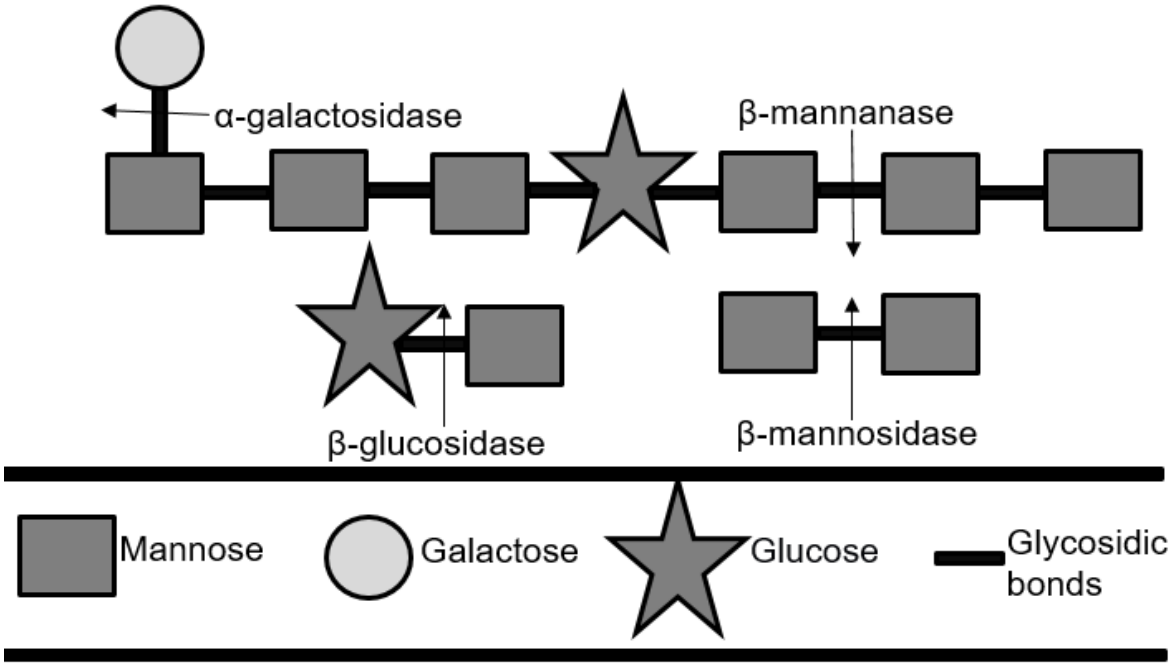

Figure 1.2: Diagram showing the putative cleavage sites of mannanolytic enzymes during mannan hydrolysis (Adapted from Malgas et al. (2015a) and Xu (2002).

1.1.4. Mannooligosaccharides (MOS)

MOS have gained attention as potential prebiotics over the years due to their ability to promote the growth of beneficial bacteria in the digestive tract and prevent pathogenic bacteria from attaching to the gut wall, without being digested by the host (Saeed et al., 2017). MOS can tolerate temperatures of up to 120^{o}C without losing their function (Chacher et al., 2017). This type of prebiotic modulates microorganisms found in the intestines and causes an increase in the length of the host intestinal villi (Chacher et al., 2017).

MOS are used as growth promoters in the animal feed industry instead of antibiotics, which the European Union banned in 2006, after being used for about 50 years (Castanon, 2007; Sultan et al., 2015). The use of antibiotics as growth promoters was banned, because of animals harbouring pathogenic bacteria that are resistant to the antibiotics and the antibiotic resistance genes being transferred from animals to the human microbiota (Castanon, 2007; Sultan et al., 2015). This, therefore, means that MOS are safer to use as growth promoters than antibiotics.

Oligosaccharides with a degree of polymerisation (DP) that is greater than six have been shown to be more effective at influencing the immune response and preventing allergic reactions (Bland et al., 2004, Ozaki et al. 2007). Allergic diseases involve multiple cells and factors, e.g. mast cells, cytokines and immunoglobulin E (IgE); which play a vital role in developing these diseases (Hu et al. 2018; Ozaki et al. 2007). Ozaki et al. (2007) demonstrated that MOS administered in ovalbumin-sensitized mice suppresses IgE, meaning that it had an anti-allergic function. MOS with a DP between five and seven could inhibit the production of reactive oxidising species (ROS), e.g. hydrogen peroxides and hydroxyl radicals, by neutrophils and monocytes (Ozaki et al. 2007). In Figure 1.3 below the mechanism of action of MOS is shown. There are many types of MOS, including β-MOS and α-MOS, produced from β-mannans and α-mannans, respectively (Nguyen et al., 2019). In this study, we sought to produce β-MOS from galactomannans found in SCG.

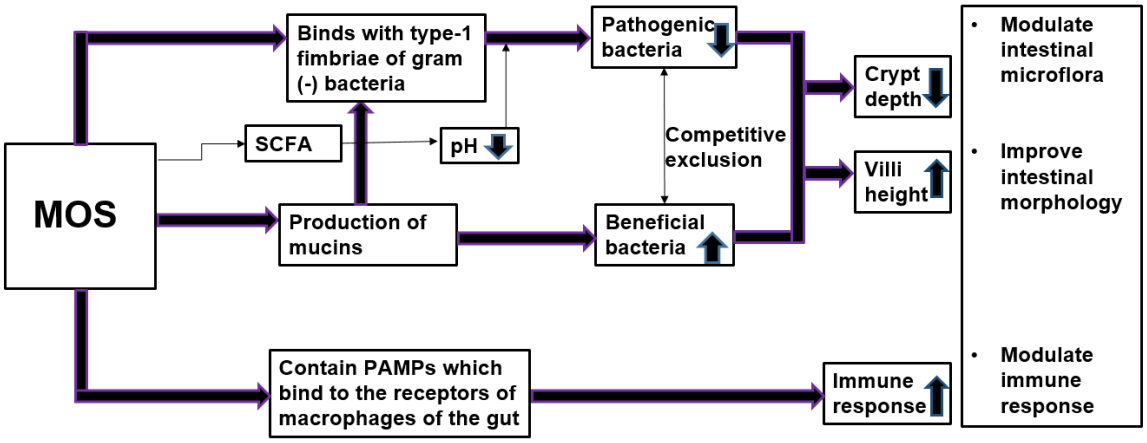

Figure 1.3: Mechanism of action of MOS. The diagram shows how MOS modulate the intestinal microflora, improve the intestinal morphology, and modulate an immune response. The black arrows pointing up represent an "increase" while the arrows pointing down imply a "decrease" (adapted from Chacher et al., 2017; Hlalukana et al., 2021).

1.1.4.1. Mechanism of action of MOS

Gram-negative bacteria such as *Escherichia coli* and *Salmonella* have type-1 fimbriae that contain mannose-specific lectins (FimH), which have a high binding affinity for mannose residues present on the intestinal mucosa (Chacher et al., 2017; Hlalukana et al., 2021). The presence of MOS decreases the number of bacteria attaching to the intestinal mucosa by binding to the bacterial FimH of type-1 fimbriae, thus inhibiting bacterial colonisation (Chacher et al., 2017; Hlalukana et al., 2021). MOS also increase the number of goblet cells produced, which, in turn, produce highly glycosylated proteins called mucins (Baurhoo et al., 2007; Chacher et al., 2017). Mucins act as the first line of defence against pathogenic bacteria in the digestive tract (Chacher et al., 2017). They have mannosyl receptors, which also bind to the type-1 fimbriae of pathogenic bacteria, which leads to bacterial removal from the intestines (Chacher et al., 2017). MOS, mucins, and pathogenic bacterial death together enhance the growth of beneficial bacteria (Chacher et al., 2017; Hlalukana et al., 2021). Baurhoo et al. (2007) reported that MOS enhanced the growth of *Bifidobacteria* and *Lactobacillus spp*. in broilers' intestines by increasing goblet cells and mucins. Magengelele et al. (2021) also demonstrated that MOS obtained from model substrates enhances the

growth of *B. subtilis* and *S. thermophilus* – see Figure 1.4 below for the influence of MOS on beneficial bacteria.

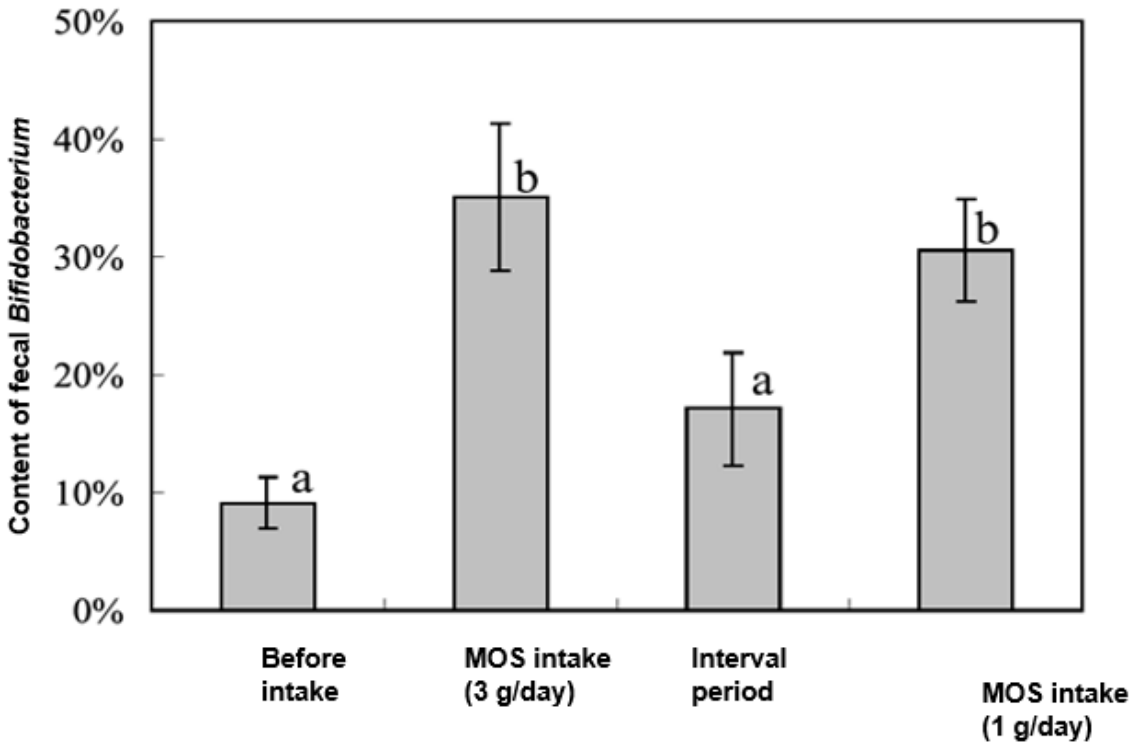

Figure 1.4: Graph showing amount of faecal *Bifidobacterium* after and before the intake of MOS. The intake of MOS (1 g/day and 3 g/ day) from coffee mannan resulted in *Bifidobacterium* being the most predominant bacteria in the faeces (Asano et al., 2004).

These beneficial bacteria then compete with pathogenic bacteria for nutrients. *Bifidobacteria* in the intestine produces lactic acid (LA) or short-chain fatty acids (SCFAs) and acetic acid (AA), which reduce the pH in the intestines and inhibit the adhesion of pathogenic bacteria (Asano et al., 2004; Chacher et al., 2017), while *Lactobacillus spp.* produce bacteriocins (Chacher et al., 2017). Bacteriocins are compounds that contain proteins and are harmful to bacteria, except the strain that produces them (Joerger, 2003). These componds are roduced by both beneficial and comensal bacterial strains (Joerger, 2003). The *Enterococcus faecium* J96 strain is one of the strains that produce bacteriocins, which in turn protects chickens from *Salmonella pullorum* (Audisio et al., 2000). *Bacteriocin microcin* 24 produced by genetically engineered *E. coli,* decreased *Salmonella typhimurium* counts, when it was administered

continuously with water, in chickens (Joerger, 2003). Audisio et al (2000) reported that *Lactobacillus spp.* can convert glucose to LA and AA in birds. This may lead to the competitive exclusion of pathogenic bacteria from colonising the gastrointestinal tract of birds.

1.1.4.2. Antioxidant activity of MOS

Oxidants are reactive molecules that bind to cellular molecules in the body (Birben et al., 2012). Their binding to cellular molecules damages these cellular molecules and may result in a person being prone to heart diseases, diabetes and liver disease (Birben et al., 2012). Antioxidants are, therefore, required to prevent the binding of oxidants to cellular molecules. They prevent oxidants from binding to cellular molecules by either transferring a hydrogen atom or an arbitrary single atom and/or chelating transition metals, to interact or stabilise reactive radicals in oxidants (Birben et al., 2012; Santos-Sanchez et al., 2019). For example, in the presence of Cu^{2+} and Fe^{2+}, hydrogen peroxide (which is an oxidant) is converted to OH^{-} (Birben et al., 2012).

Multiple studies have reported that some sugars have antioxidant activity, and this has been demonstrated using a number of substrates: 2,2-diphenyl-1-picrylhydrazyl DPPH), 2,2'-azino-bis(3-ethylbenzothiazoline-6-sulfonic acid) BTS+•), ferric reducing antioxidant power (FRAP) and hydroxyl radical scavenging (Amna et al., 2018; Jana & Kango, 2020; Haghparast et al., 2013). DPPH is a free radical that is widely used to determine antioxidant activity because of its ability to donate a hydrogen atom, especially in plant samples (Amna et al., 2018). DPPH results in a violet colour in ethanol but turns colourless in the presence of antioxidants. Haghparast et al. (2013) reported that D-glucose, D-mannose and D-arabinose have DPPH scavenging activity, with the D-glucose and D-mannose activities being 0.7 times higher than that of D-arabinose. The free hydroxyl groups in polymers are responsible for the antioxidant activity of polysaccharides (Jana & Kango, 2020). Hydrolysis of polysaccharides increases the number of free hydroxyl groups, which means that the antioxidant activity will also increase (Haghparast et al., 2013; Jana & Kango, 2020). Amna et al. (2018) reported that the ABTS radical scavenging method shows high antioxidant activity in MOS derived from β-mannans (such as konjac gum and galactomannan) compared to the FRAP and DPPH methods, and this is because it is highly reactive to many antioxidants. Thaipong et al. (2006)

reported that ABTS, FRAP and DPPH give comparable results for the antioxidant activities in methanol extract of guava fruit juice, but FRAP method showed high reproducibility.

1.1.4.3. Autoaggregation and biofilm formation

Autoaggregation occurs when microorganisms of the same strain cluster together and form aggregates (Solano et al., 2014; Trunk et al., 2018). Autoaggregation plays a crucial role in both beneficial and pathogenic bacteria, as it protects these cells from external stress such as oxidative stress (Trunk et al., 2018). Microorganisms form aggregates using self-recognising surface structures such as exopolysaccharides (EPS) (Trunk et al., 2018). The formation of aggregates is important for adherence and the prevention of bacterial cells from being eliminated on the surface (Galdiero et al., 1988). Autoaggregation forms part of biofilm formation, which is the attachment of a community of bacterial cells to surfaces or substrates (Solano et al., 2014; Trunk et al., 2018). The various mechanisms of autoaggregation are outlined in the diagram below (Figure 1.5).

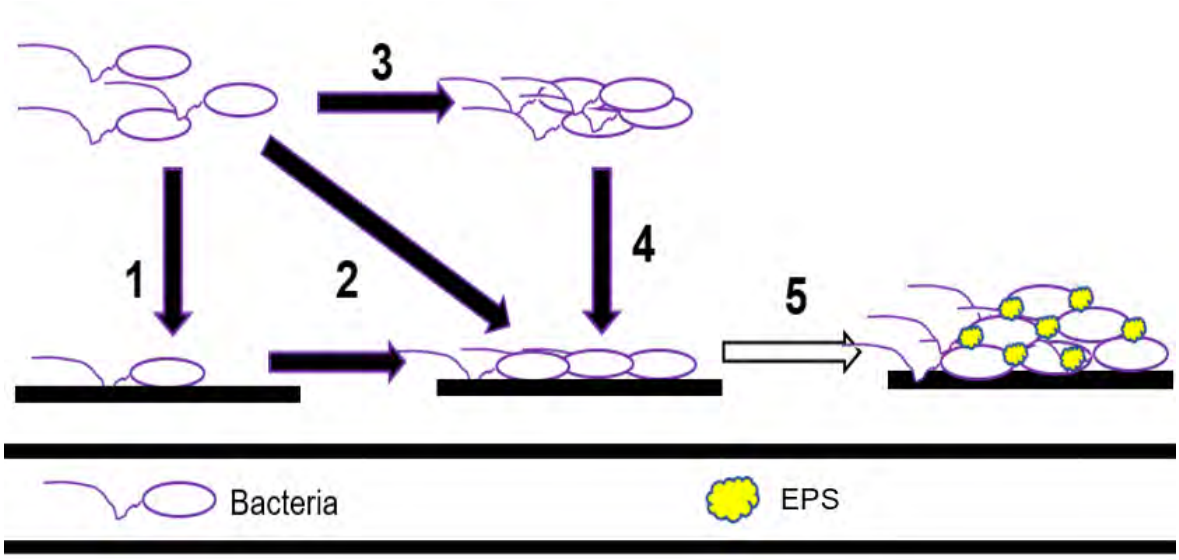

Figure 1.5: Mechanisms in which the autoaggregation of cells lead to biofilm formation. A single cell can bind directly to the surface and recruit other cells to where it is bound. Cells can also form aggregates, sediment to surfaces as aggregates, and produce biofilms. 1-adhesion, 2-recruitment, 3-aggregation, 4-sedimentation, 5-biofilm formation and the yellow blobs represent EPS (Adapted from Trunk et al., 2018).

The two mechanisms of autoaggregation in Figure 1.5 can occur at the same time, and both mechanisms result in the production of biofilm (Trunk et al., 2018). In the first mechanism, planktonic cells attach to the surface as single cells, e.g. using type IV pili. They then use autoagglutannins to recruit other planktonic cells to attach to the surface. This results in the formation of microcolonies, which further produces biofilm. The second mechanism the switching of planktonic cells to aggregates, in a solution. The aggregates formed sediment, and attach to the surface. The aggregates attached on the surface start producing biofilm.

The genes involved in microbial biofilm formation are regulated by quorum sensing (QS) (Solano et al., 2014; Trunk et al., 2018). QS is the regulation of genes involved in the development of biofilms and their dispersion (Solano et al., 2014). For example, in *E. coli*, the autoinducer-2 (AI-2) molecule is responsible for autoaggregation and biofilm formation, as this molecule causes QS (Trunk et al., 2018). In QS, bacteria produce chemical signal molecules called autoinducers, which increase in concentration until they reach a certain threshold level (Pena et al., 2019). When autoinducers reach this threshold level, quorum

sensing genes in bacteria are activated, allowing bacteria to act as a multicellular population instead of individual single-celled organisms (Pena et al., 2019).

Oligosaccharides can inhibit the adhesion and the biofilm formation of pathogenic bacteria (Chacher et al., 2017). Human milk oligosaccharides (HMOs) contain structural shapes that mimic the digestive wall patterns; their presence competitively prevents pathogenic bacteria from attaching to the intestinal surface (Asadpoor et al., 2020; Chacher et al., 2017). HMOs are indigestible sugars that form part of human milk (Asadpoor et al., 2020). These oligosaccharides are important in developing the immune system of infants (Asadpoor et al., 2020). Asadpoor et al. (2020) also reported that alginate oligosaccharides (AOS), another type of biomass-derived oligosaccharide, can also affect the genes responsible for QS regulation, inhibiting biofilm formation of pathogenic bacteria.

1.1.5. Production of MOS from agro-industrial waste

Lignocellulosic biomass contains cellulose, hemicellulose and lignin. Cellulose and hemicellulose are sources of fermentable sugars but these two components are enclosed by the cell wall made up of lignin (Mosier et al., 2005; Van Zyl et al., 2010). The presence of lignin in the cell wall makes hemicellulose and cellulose inaccessible to lignocellulosic enzymes (Mosier et al., 2005). Pretreatment of lignocellulosic biomass results in the breakdown of lignin and disruption of the complex structure of cellulose, making polysaccharides more exposed (Mosier et al., 2005). There are many methods available for pretreating agro-industrial wastes, and these include acid, alkali, lime, and liquid hot water pretreatments, steam explosion and microwave radiation (Amin et al., 2017; Mosier et al., 2005; Wongsiridetchai et al., 2018). The type of method used depends on the type of substrate, its intended use and the costs associated with the pretreatment method (Wongsiridetchai et al., 2018). Figure 1.6 below illustrates the process of pretreatment.

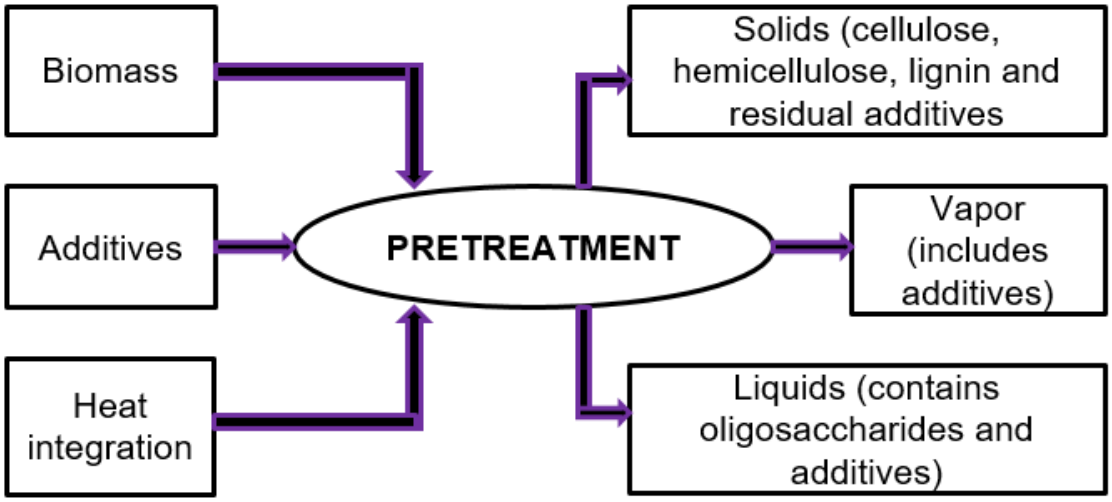

Figure 1.6: The pretreatment process of lignocellulosic biomass (adapted from Mosier et al., 2005).

During the pretreatment of lignocellulosic biomass, additives are added and heat is applied for a certain amount of time, which depends on the method of pretreatment and substrate being pretreated (Mosier et al., 2005). Pretreatment of lignocellulosic biomass then results in solids; which include lignin, cellulose, hemicellulose and residual additives, vapor is also released, as well as oligosaccharides (Mosier et al., 2005). During this process, melanoidins, which are discussed in detail in chapter 4, are also formed as a result of structural changes (Moreira et al., 2015).

MOS can be enzymatically produced from spruce galactoglucomannan (spruce GGM), palm kernel cake (PKC), copra meal (CM), konjac gum (KG) and guar gum (GG), which are low-value mannan-rich and pure mannan substrates (Bååth et al., 2018; Jana and Kango, 2020; Soni et al., 2016). Bååth et al. (2018) reported that enzymatic hydrolysis of spruce GGM using *Cj*Man5A and *Cj*Man26A, mannanases from *Cellvibrio japonicas,* results in MOS. Spruce GGM hydrolysis using *Cj*Man5A results in M3 and M4 as predominant sugars, while *Cj*Man26A results in M1 and M2 as the predominant sugars (Bååth et al., 2018). The presence of acetyl residues attached to spruce GGM reduces the activities of both *Cj*Man5A and *Cj*Man26A (Bååth et al., 2018). LBG, GG and KG mannan hydrolysis using *Aspergillus terreus* FBCC 1369 resulted in MOS with DP 2, 3 and 4 oligomers, respectively, as the predominant sugars (Soni et al., 2016).

1.1.5.1. Pretreatment and production of MOS from spent coffee grounds

SCG is an abundant agro-industrial waste mainly composed of cellulose, hemicellulose and lignin (Mosier et al., 2005; Wongsiridetchai et al., 2018). Lignin availability in SCG prevents CAZymes from accessing holocellulose to produce fermentable sugars (Wongsiridetchai et al., 2018). This, therefore, means that this agro-industrial waste needs to be pretreated to alter its complex lignocellulose structure to make holocellulose accessible to enzymes. Figure 1.7 below illustrates the importance of the pretreatment step before enzymatic hydrolysis.

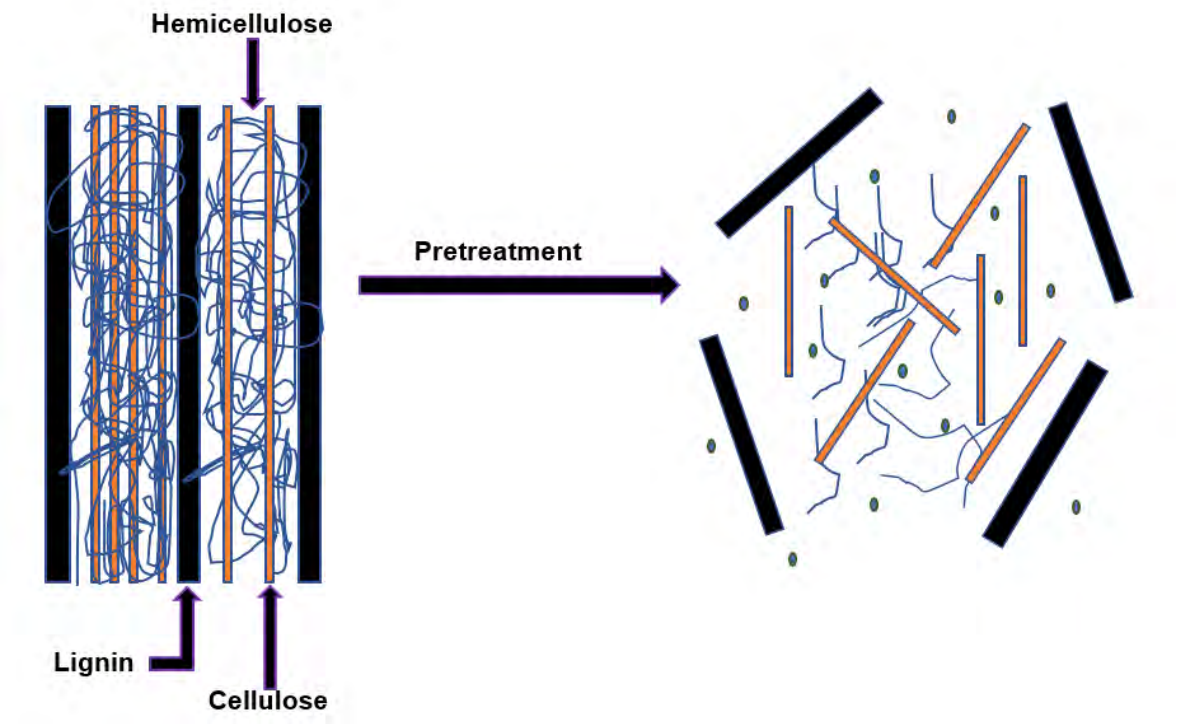

Figure 1.7: The impact of lignocellulosic biomass pretreatment on its recalcitrance (adapted from Mosier et al., 2005).

There are a number of different methods reported for pretreating SCG and these include using acids such as sulphuric acid (H_2SO_4), an alkali such as sodium hydroxide (NaOH) and steam pretreatment (Chiyanzu et al., 2014; Mosier et al., 2005). For this study, alkaline pretreatment using sodium hydroxide (NaOH) was used to pretreat SCG, because of its low severity and its ability to generate more reducing sugars compared to methods such as acid pretreatment (Wongsiridetchai et al., 2018). Wongsiridetchai et al. (2018) reported that SCG pretreated with NaOH, at 50^{o}C, creates more pores in the surface of SCG, than SCG pretreated at other temperatures (60 – 121^{o}C), which explains why more reducing sugars were produced in

NaOH pretreated SCG samples compared to untreated SCG. Another pretreatment method reported for SCG involves two steps: (1) Soxhlet extraction, for the removal of lipids from coffee and (2) delignification (at 80^{o}C) using sodium chlorite and acetic acid (Nguyen et al., 2019; Sachslehner et al., 2000). Pretreatment of SCG using this two-step method was efficient as it resulted in a decrease in soluble and insoluble lignin, from 27.5% to 2.9% and from 38.6% to 2.3% dry weight, respectively (Nguyen et al., 2019). Pores were also observed on the surface of pretreated SCG using SEM, and Fourier-transform infrared (FT-IR) spectra showed the disappearance of some peaks during pretreatment (Nguyen et al., 2019). Peaks at 3291.63 cm^{-1} – 3329.14 cm^{-1} were observed in SCG and associated with –OH vibration. A prominent peak in untreated SCG was observed at 2919.4 cm^{-1}, and was assigned to the vibration of the lignin C-H group. This peak (2919.4 cm^{-1}) was absent in delignified and defatted SCG. Nguyen and colleagues (2019) obtained a total sugar content of 92.5% dry weight in pretreated and 43% dry weight in untreated SCG. Extraction of mannan using NaOH (after pretreating SCG using the steps stated above) resulted in only a 12.8% (on a dry weight basis) yield of mannan (Sachslehner et al., 2000). Chiyanzu et al. (2014) also reported that steam pretreatment (at 150, 190 and 200^{o}C) improved the yields of reducing sugars produced from enzymatic hydrolysis. Enzymatic hydrolysis of steam pretreated (10 minutes) SCG using enzyme cocktail (1% (g/100 g) mannanase and 1% (g/100 g) cellulase) produced 10.1% MOS, which is lower than MOS produced from untreated SCG (8.76 %) (Chiyanzu et al., 2014).

Listed below are some of the SCG MOS production and prebiotic studies that have been reported in the literature on SCG MOS:

- Chiyanzu et al. (2014) reported that MOS (M2-M6) can be produced from enzymatically hydrolysed steam pretreated SCG. Chiyanzu et al. (2014) used a mannanase and cellulase cocktail to hydrolyse steam pretreated SCG, and M2 and M3 or M4 were the produced as predominant MOS.

- Nguyen et al. (2016) also demonstrated that delignified (sodium chlorite and acetic acid) and defatted (hexane) SCG hydrolysis using in house produced pectinase resulted in M2 and M6 as the predominant sugars produced.

- Wongsiridetchai et al. (2018, 2021) demonstrated that enzymatic hydrolysis of pretreated SCG using *Bacillus subtilis* GA2 (1) derived Man26A resulted in the production of M2 and M3 as predominant sugars. The SCG MOS produced from both

studies enhanced the growth of beneficial bacteria (*L. acidophilus*, *L. casei* and *L. plantarum*). Wongsiridetchai et al. (2021) also demonstrated that beneficial bacteria could tolerate gastrointestinal (GI) tract conditions, where the bacteria survived in the presence of α-amylase and hydrochloric acid.

This thesis investigated the properties of MOS produced enzymatically from pretreated SCG using an endo-1,4-β-mannanase, Man26A, from a *Bacillus sp*. source.

1.2. Motivation

Coffee is one of the most popular and consumed beverages globally, and large amounts of an agro-industrial residue, called SCG, are generated during its processing (Jooste et al., 2013; McNutt & He, 2019). This agro-industrial waste is associated with a sizeable environmental burden, and its utilisation is therefore a very relevant subject. SCG is rich in lignin, lipids, and polysaccharides. Mannans and arabinogalactans are the main hemicellulosic polysaccharides in SCG (Redgwell & Fischer, 2006). SCG can be used to produce value-added products (VAPs) such as MOS, which are prebiotics that enhance the growth and proliferation of beneficial bacteria, while reducing the number of pathogenic bacteria in the digestive tract (Chacher et al., 2017). MOS are safe to use and have a range of biological activities, including their application as an alternative to antibiotic growth promoters (Castanon, 2007; Sultan et al., 2015). Therefore, this study sought to produce MOS via the hydrolysis of mannan obtained from inexpensive and readily accessible SCG using endo-1,4-β-mannanase from a *Bacillus sp*., and evaluating their prebiotic potential.

1.3. Research question

Can mannooligosaccharides (MOS) be produced from spent coffee ground (SCG) mannan, using an endo-1,4-β-mannanase from *Bacillus sp*., and do these MOS demonstrate prebiotic potential?

1.4. Aims and objectives

The overall aim of this study was to produce MOS from SCG mannan using an endo-1,4-β-mannanase, Man26A, from *Bacillus sp*. and to investigate their prebiotic properties. For this aim to be achieved, the following objectives were addressed:

1. To biochemically characterise Man26A derived from *Bacillus sp*.;

2. To pre-treat and characterise SCG for its effective enzymatic hydrolysis by Man26A to generate MOS;

3. To develop a high-performance liquid chromatography (HPLC) protocol to quantify the MOS produced;

4. To investigate the prebiotic properties of SCG derived MOS.

1.5. Overview of thesis

Chapter 1 covers the general introduction to the study. The development and validation of a HPLC method for the simultaneous separation of MOS is detailed in Chapter 2. Characterisation of the endo-1,4-β-mannanase, Man26A, derived from *Bacillus sp*., is detailed in Chapter 3, where ivory nut mannan, locust bean gum and guar gum were used as model substrates for the production of prebiotic MOS. The prebiotic MOS produced from these three different substrates were then characterised. In Chapter 4, the agro-industrial waste, SCG, is pretreated and characterised, and Man26A is used to produce MOS. In Chapter 5, the prebiotic MOS produced from the enzymatic hydrolysis of SCG are assessed for their prebiotic activity, their ability to tolerate gastrointestinal tract conditions and their ability to activate mannan utilisation genes. Chapter 6 entails the general discussion, highlighting the conclusions of the study and suggestions for future work.

CHAPTER 2: HPLC analysis: method development and validation

2.1 Introduction

High-performance liquid chromatography (HPLC) is a quantitative and qualitative analytical technique used for identifying, separating and simultaneously quantifying different individual components in liquid samples (Malviya et al., 2010). Essential HPLC components include a column that holds the stationary phase, a liquid mobile phase, a pump to pass the mobile phase into the column and a detector to identify the analyte molecules (Lakka & Kuppan, 2019; Malviya et al., 2010; Sabir et al., 2013). The retention times of molecules being identified or quantified are shown by the detector and these differ depending on how these molecules interact with the stationary phase and the components of the mobile phase. The most commonly used solvents for HPLC are methanol and acetonitrile (Malviya et al., 2010).

HPLC is a very sensitive analytical technique used in biological and chemical analyses. The use of contaminated samples or solvent(s) negatively affects an already successful method, making it unusable (Bird, 1989). HPLC requires the use of highly pure samples and solvents. The method has to be validated to ensure that it gives accurate and reliable results that can be reproduced (Bird, 1989; Lakka & Kuppan, 2019). The quantification of MOS requires analytical techniques such as HPLC and gas chromatography-mass spectrophotometry (GC-MS). HPLC systems with a refractive index (RI) detector or pulsed amperometric detector (PAD) have been used for the identification and quantification of sugars such as glucose and fructose (Correia et al., 2014).

Oligosaccharides lack chromophores (such as azo, nitro and nitroso groups) in their structures and this makes it impossible to use an ultraviolet (UV) detector for their identification; this limits their detection via RI, PAD and evaporative light scattering detection (ELSD) (Bai et al., 2015; Vidushi & Meenakshi, 2017). Chromophores are chemical groups or structures responsible for absorbing visible light, causing the sample mixture to have colour absorption properties at a given wavelength (Bai et al., 2015). ELSD is a very expensive sample detection tool for HPLC, while an RI detector is a fast, cost-effective method that may be used for quantification of sugars. (Bai et al., 2015).

The overall aim of this chapter was to develop and validate a HPLC method for the separation, identification and quantification of MOS produced from the hydrolysis of mannan substrates in the subsequent chapters.

2.2. HPLC method development

Method development is a process used to determine whether a developed method is suitable for analysing certain samples. There are many factors that need to be considered when developing a method and these include the samples to be used, mode of chromatography, type of detector, appropriateness of the column, composition of the mobile phase, selection of flow rate and injection volume, robustness of the method, etc. (Lakka & Kuppan, 2019).

2.2.1. Selection of sugars for analysis

A sample used in HPLC analysis should not have contaminants as this could damage the column. It is important that the sample is filtered using 0.22 or 0.45 µm pore-sized filters before analysis. Mannose and MOS (mannobiose (M2), mannotriose (M3), mannotetraose (M4), mannopentaose (M5) and mannohexaose (M6)) were selected for analysis since these were the expected products from the enzymatic hydrolysis of agricultural biomass. The standards were filtered before sample injection onto the column to ensure purity. M2-M6 were purchased from Megazyme™ Bray, Ireland), and M1 from Sigma-Aldrich (St. Louis, USA).

2.2.2. Mode of chromatography

There are two modes of HPLC separation techniques: normal phase HPLC and reverse phase HPLC (Lakka & Kuppan, 2019). The mode of chromatography depends on the samples to be analysed. In this study, the sugars were analysed using ligand exchange chromatography, an ion-exchange technique used mostly for pretreated biomass hydrolysates (Becker et al. 2010). In

ligand exchange chromatography, the stationary phase is a cation resin with a metal ion (Becker et al. 2010).

2.2.3. Mode of detection

For detecting mannose and MOS produced via the enzymatic hydrolysis of mannan, a RI detector attached to a Shimadzu LC system (Shimadzu Corp, Kyoto, Japan) was selected. RI is an easy and effective way of determining analyte molecules in sample mixtures. This is due to its stable baselines and rapid equilibrium. This detector is used for detecting individual components that have limited or no UV absorption (Vidushi & Meenakshi, 2017). Like ELSD, RI detection is used for detecting and analysing compounds such as polymers and saccharides.

2.2.4. Analytical column

In this study, a CarboSep CHO 411 column (Concise Separations, San Jose, California, USA) was used for analysis. The column/stationary phase is the site where the separation of the molecules occurs. Different columns are made from different materials such as silica, charcoal and alumina. Silica is the most widely used column because it is highly stable to most organic solvents (Sabir et al., 2013). When selecting an appropriate column, the column's length and diameter, particle size, and shape of the particles need to be considered. Longer columns (i.e. 250-300 mm) result in high peak resolution but longer run times than shorter columns (i.e. 30-50 mm) (Lakka & Kuppan, 2019). It is impossible to develop a reproducible, reliable method without a stable column. The CarboSep CHO 411 column selected for use in this study separated components according to their sizes and via ligand exchange. Becker et al. (2010) reported that ligand chromatography is important and widely used for the analysis of sugars obtained from the hydrolysis of biomass.

2.2.5. Mobile phase

Appropriate mobile phase selection in HPLC separation is vital, because resolution and selectivity depend on it (Vidushi & Meenakshi, 2017). Many organic solvents are used as mobile phases and these include acetonitrile and methanol. Acetonitrile is mostly preferred over methanol, as it results in better spectral interpretation (Vidushi & Meenakshi, 2017). However, in this study, filtered (0.45 µm pore-size) and degassed Milli-Q water was used as the mobile phase in isocratic mode.

2.3. HPLC method validation

2.3.1. Analytical standards

HPLC standards are important for accurate results. The required standards also need to be pure and well characterised. These are selected based on the expected products of the enzymatic hydrolysis of mannan. The standard concentrations and peaks (areas) were used to plot standard curves, which were then used to determine which oligosaccharides and their concentrations are produced from the enzymatic hydrolysis of SCG.

2.3.2. Linearity and range

Linearity is determined by analysing the concentrations of different standards and plotting a standard curve or linearity graph either manually, using Microsoft Excel or any other computer software. The linearity of the standard curve is demonstrated using the coefficient correlation (R^2). A correlation coefficient close to 1.0 is sufficient evidence to show that the standard curve is linear (Moosavi & Ghassabian, 2018). The range is the difference between the lower and upper values in the standard curve. The concentration range of the standards used to determine linearity was 0.135 to 2.67 mg/mL of each MOS standard.

2.3.3. Accuracy

Accuracy is defined as the closeness of the measured values to that of the standard or known sample. It is usually expressed as a percentage (%) recovery (Abboo, 2016). Accuracy is measured by using a validated method to analyse samples that have been spiked with known amounts of the analytes (standards) (Swartz & Krull, 2005; Vidushi & Meenakshi, 2017). It is also suggested that accuracy be assessed with a minimum of nine determinations over a specified range of at least three concentrations (Swartz & Krull, 2005; Abboo, 2016).

2.3.4. Precision

Precision is defined as the closeness of the measured values to each other. The relative standard deviation (RSD, %) is calculated to determine how precise the results obtained are. The following formula is used to calculate RSD (%):

$$RSD\ (\%) = \frac{}{\mu} \times 100$$

Where σ is the standard deviation and μ is the mean.
The smaller the RSD (%) value, the higher the precision.

2.3.5. Limit of Detection (LOD) and Limit of Quantification (LOQ)

LOD is the lowest concentration of a substance that can be detected using HPLC. It involves measuring samples in replicates, determining the mean and the standard deviation of each component present in the sample. LOQ is the lowest concentration of a substance that can be quantified with acceptable repeatability. LOQ is always at a higher (or equal) concentration than LOD (Armbruster & Pry, 2008). The formulas for determining the LOD and LOQ are:

$$LOD = 3.3 \times \frac{m}{SD}$$

$$LOQ = 10 \times \frac{m}{SD}$$

where *m* is the slope of the calibration curve, and SD is the standard deviation.

2.4. Optimum parameters developed for the simultaneous separation of mannooligosaccharides (MOS)

2.4.1. Instrumentation, materials and reagents

Mobile phase: filtered using Whatman filter (0.45 µm) and degassed Milli-Q water

Analytical column: CarboSep CHO 411 column (7.8 X 300 mm)

Flow rate: 0.3 mL/min

Detection: Refractive Index (RI)

Column temperature: 80^{o}C

Injection volume: 20 µL

Column back pressure: 470 psi

The following instrumentation was used:

1. Shimadzu Differential Refractive Index Detector (Shimadzu Corp, Kyoto, Japan)

2. Shimadzu autosampler (Shimadzu Corp, Kyoto, Japan), injection range: 0.1-100 µL

3. CarboSep CHO 411 column (Concise Separations, San Jose, USA)

4. Shimadzu column oven, temperature range: -15^{o}C to 80^{o}C (Shimadzu Corp, Kyoto, Japan)

5. Milli-Q water purification system

6. Pump for filtering and degassing the mobile phase

The following reagents were used:

1. Standards: M1-M6 Megazyme™, Bray, Ireland)

2. Fifty mM sodium phosphate buffer (pH 7.0) and Milli-Q water

2.4.2 Standard preparation

Different concentrations of standards; M1, M2, M3, M4, M5 and M6, were prepared in Milli-Q water and filtered into the vials using 0.45 µm pore-size filters. The samples were then run on HPLC. The concentrations of the standards were plotted against the obtained peak area. The concentrations of the prepared MOS standards ranged from 0.135 to 2.67 mg/mL.

2.6 Results and discussion

Chromatograms obtained after running the MOS standards showed clear and distinct peaks. These peaks were detected and separated using the validated and developed parameters. The retention time, linear regression equation and coefficient of correlation of each of the MOS standards are shown below in Table 2.1.

Table 2.1: Retention times of MOS (M1-M6), linear regression and coefficient of correlation (R^2) obtained from their standard curves (n=2)

Standards	Retention time (minutes)	Linear regression	Coefficient of correlation (R^2)
M1	31.809	y=500113x+15687	0.9988
M2	26.775	y=464015x+19060	0.9942
M3	22.642	y=534418x-3815.8	0.9983
M4	19.692	y=514303x-7900.8	0.9978
M5	17.499	y=531012x-4574.5	0.9987
M6	15.847	y=495319x-6105.7	0.9958

M1-mannose, M2-mannobiose, M3-mannotriose, M4-mannotetraose, M5- mannopentaose and M6-mannohexaose

2.6.1 Linearity

The linearity was tested using six standards solutions (M1-M6) with concentrations ranging from 0.135 to 2.67 mg/mL (Appendix B, Figure B.5). The standard concentrations were performed in duplicate. The average peak areas were calculated and plotted against the standard concentrations, and standard curves for the standards were constructed (Appendix B, Figure B.5). The correlation coefficients of the standard curves showed that the developed and validated parameters were reliable. All the correlation coefficient values were close to 1.0, with all values greater than 0.99. When the R^2 value is closer to zero instead of 1.0, it means there is no linearity (Vidushi & Meenakshi, 2017).

2.6.2 Specificity

The ability of the HPLC method to separate and quantify the products of interest was confirmed by mixing six different standard solutions (M1-M6). The standards were separated effectively with different retention times, and there was linearity between the peak area and concentration of each standard. There was one unknown peak observed at retention time, 11.653. This peak was shown to be due to the water that was used during the dilution of the standards, but this peak did not interfere with the peaks of the standards (M1-M6). Overall, the method was shown to be specific for the identification, separation and quantification of the oligosaccharides.

2.6.3 Limits of Detection (LOD) and Limits of Quantification (LOQ)

The LOD and LOQ values determined for M1 were 0.0343 and 0.1039 mg/mL, respectively, which were lower than the values reported by Pitsch & Weghuber (2019) who reported that the LOD and LOQ values of M1 were 0.6 and 2.12 mg/mL. The difference in these values may be due to the difference in the oven temperature used (40^{o}C vs 80^{o}C), the difference in the mobile phase used, and the column. Pitsch & Weghuber (2019) used a mixture of acetonitrile and water as the mobile phase and a WATERS Acquity UPLC BEH amide column (2.1 mm x 150 mm). Pitsch & Weghuber (2019) also used a corona charged aerosol detector (CAD), which was different from the detector used in this study (RI detector). There are no literature results available regarding the LOD and LOQ values of M2-M6 in literature. Table 2.2 below summarises the LOD and LOQ values of the MOS standards (M1-M6).

Table 2.2: Limit of Detection and Limit of Quantification values for MOS determined using the optimised HPLC method

MOS standards	Limit of detection (LOD) (mg/mL)	Limit of quantification (LOQ) (mg/mL)
M1	0.034	0.104
M2	0.005	0.017
M3	0.006	0.017
M4	0.004	0.011
M5	0.007	0.022
M6	0.013	0.031

2.6.4. Precision, accuracy and reproducibility

Precision, accuracy and reproducibility were evaluated by determining the relative standard deviation (RSD %). Two injection replicates showed reproducibility for each of the six sugar standards. The RSD (%) demonstrates the dispersion around the mean. The RSD (%) is reported in Table 2.3 below. The RSD (%) of M1, M2, M3, M4, M5 and M6 ranged from 0-2.66, 0.01-1.43, 0.06-1.71, 0-5.15, 0.09-7.15 and 0.02-3.91 mg/mL, respectively. Most of these RSD percentage values were low, confirming that the method demonstrated high accuracy, precision and reproducibility.

Table 2.3: Relative standard deviation (%) of the standard solutions at different concentrations (mg/mL) (n=2)

Concentration (mg/mL)	M1	M2	M3	M4	M4	M6
0.135	2.66	1.43	1.71	1.29	1.85	3.91
0.25	1.10	0.01	0.72	0.40	0.87	1.18
0.3	0	0.28	0.23	0.01	4.45	0.02
0.67	0.51	0.05	0.24	5.15	7.15	2.59
1.3	0.18	0.14	0.06	0	0.09	0.02
2.67	0.05	0.10	0.46	0.52	0.12	0.05

2.7. Conclusion

An HPLC method was developed and validated for the separation, detection and quantification of MOS. The developed and validated method displayed linearity, where all the coefficients of correlation values were all close to 1.0. The method also showed specificity and high precision, accuracy and reproducibility. All the standards separated effectively, with peaks observed at different and distinct retention times with no interference.

CHAPTER 3: Production of MOS from model substrates using *Bacillus sp* endo-1,4-β-mannanase, Man26A

3.1. Introduction

β-mannanases (EC 3.2.1.78) are endo-acting hydrolases found in GH families 5, 26, 113 and 134 according to the CAZy database (www.cazy.org). The GH 26 mannanase, Man26A, was the first mannanase reported to contain a mannan-binding domain responsible for binding to soluble mannan (Stoll et al., 2000). Man26A derived from the bacterium *Cellulomonas fimi* (*C. fimi*) is comprised of the mannan-binding module (MBM), catalytic module (CM), s-layer homology module (SLHM) and an unknown module (X) (Stoll et al., 2000) – see Figure 3.1 below.

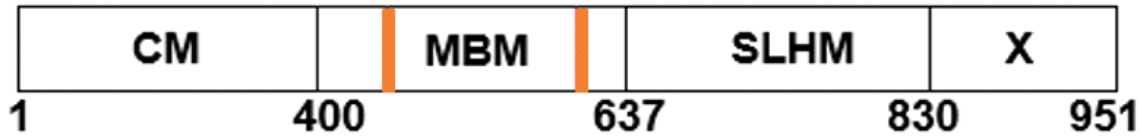

Figure 3.1: Composition of the modular structure of Man26A from bacterium *C. fimi.* CM-catalytic module, MBM-mannan-binding module, SLHM-S layer homology module, X-module with an unknown function, numbers = positions of modules in the amino acid sequence, orange lines-show that the exact termini of the MBM have not been identified yet (Stoll et al., 2000).

Below is a three-dimensional (3-D) structure of GH26 mannanase from *Reticulitermes speratus*, RsMan26C, which was obtained using X-ray crystallography at 1.3 Å resolution (Figure 3.2). The structures below show that RsMan26C has a $\beta/\alpha)_8$- barrel fold with a catalytic neucleophile, Glu^{288} and the acid/base Glu^{191} (Tsukagoshi et al., 2014).

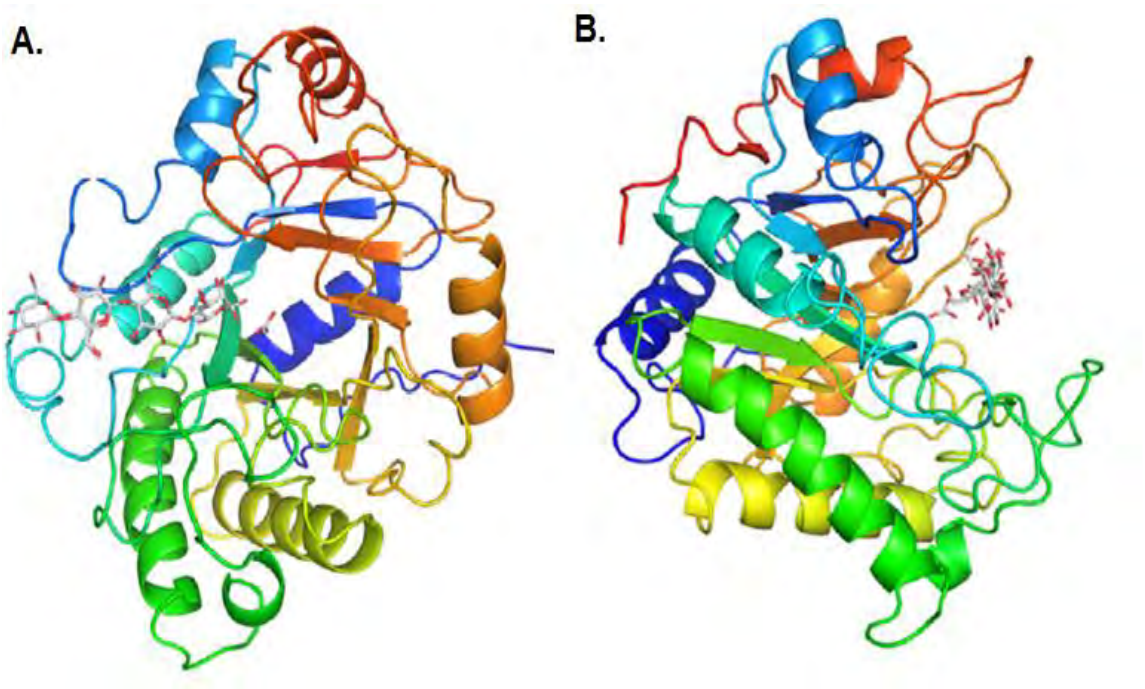

Figure 3.2: The 3-D structure of RsMan26C. The structure was obtained using X-ray crystallography. A: front view of the 3-D structure, B: side view of the 3-D structure (Tsukagoshi et al., 2014)

Yoon et al. (2008) reported that the endo-1,4-β-mannanase from *Bacillus subtilis* WL-3 has higher activity on LBG than konjac-glucomannan and guar gum, and does not hydrolyse carboxymethylcellulose. Bågenholm et al. (2019) reported that *Bacteroids ovatus* derived GH26 endo-1,4-β-mannanase, *Bo*Man26B, is highly tolerant of galactosyl residues. Endo-1,4-β-mannanase shows high binding affinity for LBG (K_m value = 10±1.1 g/L) than GG (K_m value = 12.9±1.7 g/L) (Bågenholm et al., 2019).

Hydrolysis of mannan by endo-1,4-β-mannanase results in MOS production (Dhawan & Kaur, 2007; Moreira & Filho, 2008). Kulcinskaja et al. (2013) reported that the hydrolysis of linear mannan, INM, by *Bifidocterium adolescentis* derived GH26 endo-1,4-β-mannanase, resulted in the production of mannotriose (M3) as the predominant sugar, while mannobiose (M2) and mannotetraose (M4) are produced to a lesser extent. *Bifidocterium adolescentis* derived GH26 endo-1,4-β-mannanase could also hydrolyse M4 to M2, M5 to M2 and M3 and M6 to M3, but could not hydrolyse M2 and hydrolysed M3 at a very slow rate (Kulcinskaja et al., 2013).

Oxidants are bioactive molecules produced both inside the body and in the environment, and can react with other cellular molecules in the body (Birben et al., 2012). These molecules can bind to cellular molecules such as DNA and proteins, leading to adverse effects in the body such as CVD, liver diseases, diabetes, ageing, skin diseases, etc. (Birben et al., 2012). Damage to cells by these highly reactive oxygen and nitrogen species (ROS and RNS) occurs as a result of alterations of macromolecules (Birben et al., 2012). These include lipoperoxidation of polyunsaturated fatty acids in membrane lipids, protein oxidation and DNA strand breakage (Birben et al., 2012). Antioxidants are required to prevent and delay this binding of oxidants to cellular molecules by donating a hydroxyl group to the oxidant (Birben et al., 2012). Aerobic organisms have effective antioxidant systems that prevent oxidants from interacting with other cellular molecules; however, these systems may be overwhelmed (Birben et al., 2012). MOS have been reported to increase the antioxidant activity, because of the number of activated hydroxyl groups that are present in polysaccharides (Birben et al., 2012). They are also important for inhibiting the growth of pathogenic bacteria and enhancing the growth of beneficial bacteria in the digestive tracts of mammals (Saeed et al., 2017). MOS have been reported to play an essential role in producing antibodies and improving intestinal morphology in mammals (Chacher et al., 2017; Saeed et al., 2017). MOS could be produced via the acid or enzymatic hydrolysis (using β-mannanases) of agricultural waste residues such as copra meal, SCG and palm kernel cake (Moreira & Filho, 2008). This study sought to produce MOS from INM, LBG and GG using a *Bacillus*-derived Man26A and further characterise these MOS.

3.2. Aims and objectives

Aim

The overall aim of this chapter was to produce MOS from model mannan substrates using a *Bacillus* sp. derived endo-1,4-β-mannanase, Man26A. To achieve this, the following objectives were performed:

Objectives

- To biochemically characterise the Man26A from a *Bacillus* sp;
- To hydrolyse model mannan substrates using Man26A;
- To analyse the Man26A produced MOS using Thin Layer Chromatography (TLC) and High-Performance Liquid Chromatography (HPLC); and
- To evaluate the thermostability and pH stability of the MOS.

3.3. Materials and Methods

3.3.1. Endo-1,4-β-mannanase activity assay

Model mannan substrates; ivory nut mannan INM) Megazyme™, Bray, Ireland)), locust bean gum (LBG) (Sigma- ldr ich, St. Louis, US) and guar gum GG) Megazyme™, Bray, Ireland), at 4% (w/v) were prepared in phosphate buffer (50 mM, pH 7), and the Man26A enzyme (10 µg/mL) from Megazyme™ Bray, Ireland) was added to the reaction mixture. The samples were incubated at 50^{o}C for 15 minutes and 24 hours, for specific activity determination and MOS production, respectively. The hydrolysis reaction was terminated by heat inactivation by incubating the samples for 5 minutes at 100^{o}C in a Labnet c cuBlock™ digital dry bath Labnet International. Inc, Woodbridge, USA). Centrifugation of the samples in a desktop centrifuge - Biofuge Pico Heraeus (Hanau, Germany) for 5 min was performed to sediment undigested biomass. Subsequently, the reducing sugars in the samples were quantified using the DNS method as described by Miller 1959), where 150 µL aliquot of the supernatant was mixed with 300 µL of DNS reagent [1% w/v) NaOH; 1% w/v) dinitrosalicylic acid; 20 % w/v) sodium potassium tartrate; 0.2% (w/v) phenol and 0.05% (w/v) sodium metabisulphite] in a safe-lock Eppendorf tube. The samples were heated at 100^{o}C for 8 minutes in a Labnet c cuBlock™ digital dry bath (Labnet International. Inc, Woodbridge, USA) and the absorbance was measured at 540 nm (PowerwaveX microplate reader on KC Junior software). D-mannose of a known

concentration was used as a positive control. Enzyme and substrate controls were included as negative controls.

The enzyme control was composed of an enzyme and phosphate buffer, and the substrate control had the substrate and the phosphate buffer (no enzyme). The assays were performed in triplicate and the concentration of reducing sugars produced was determined using a mannose standard curve. The yield was calculated using the formula below:

$$Yield\ (\%) = \frac{Reducing\ sugars\ released\ by\ Man26A}{Amount\ of\ mannose\ present\ in\ the\ substrate\ before\ hydrolysis} \times 100$$

3.3.2. Determination of kinetic parameters

The kinetic parameters, K_m and V_{max}, were determined from hyperbolic Michaelis-Menten plots using five concentrations of each model mannan substrate (5-40 mg/mL) in 50 mM phosphate buffer, pH 7.0, as described in section 3.3.1. The data was processed using GraphPad Prism 6.05 software (San Diego, CA, USA).

3.3.3. Thin Layer Chromatography (TLC) analysis

The MOS produced during mannan hydrolysis were analysed using TLC to determine their DP. The method used was adapted from a method described by Sachslehner et al. (2000) and Wongsiridetchai et al. (2018). The mobile phase used to develop the plates was composed of butanol: acetic acid: deionised water in a ratio of 2:1:1. The samples (2.5 µL) were applied to TLC silica gel 60 F_{254} plates (10 x 10 cm aluminium sheets) (Merck, Darmstadt, Germany). The spots corresponding to the presence of sugars were detected by spraying the plate with a solution composed of 0.3% α-naphthol in 5% (v/v) sulphuric acid in methanol, followed by incubation at 100^{o}C for 10 minutes. The standards used were M1-M6.

3.3.4. Stability of MOS

3.3.4.1. Temperature stability of MOS

The temperature stability of MOS was determined by incubation in a Labnet c cuBlock™ digital dry bath (Labnet International. Inc, Woodbridge, USA) of MOS obtained from model mannan substrate hydrolysis at different temperatures (25-100^{o}C) for 3 hours. Reducing sugars were quantified using the DNS method described in section 3.3.1. D-Mannose, dissolved in 50 mM, phosphate buffer (pH 7.0), with a known concentration was used as a positive control and a phosphate buffer (pH 7.0) as a negative control, and incubated at different temperatures (37-100^{o}C).

3.3.4.2. pH stability of MOS

Universal buffer (boric acid (0.4 M), phosphoric acid (0.4 M) and acetic acid (0.4 M) was adjusted with sodium hydroxide (0.2 M) to five different pH readings (pH 2 - 10). MOS were incubated in the universal buffer of different pH readings for 3 hours at 25^{o}C, and reducing sugars were quantified using the DNS method described in section 3.3.1. D-Mannose dissolved in different universal buffer pH readings, with known concentrations (1, 2, 2.7 mg/mL) was used as a positive control and 50 mM phosphate buffer (pH 7.0), as a negative control.

3.3.5. ABTS radical scavenging activity

The antioxidant activity of MOS was determined using a method adapted from Amna et al. 2018), which involved the use of 2,2'-azinobis-(3-ethylbenzothiazoline-6-sulfonic acid) (ABTS) as a radical. ABTS (7 mM) and potassium persulfate (7.35 mM) were dissolved in distilled water. The resulting solution was covered with foil and kept at room temperature for 16 hours. Radicalised ABTS solution (225 µL) and MOS (25 µL) were mixed and the reaction mixture was allowed to continue at room temperature for 6 minutes. The absorbance of the solution was

then measured at 734 nm. For the negative control, radicalised ABTS solution was mixed with phosphate buffer (50 mM, pH 7.0) and in the positive control, radicalised ABTS solution was mixed with gallic acid (0.02 mg/mL).

The scavenging activity was calculated using the following formula:

$$RA\ (\%)\ =\ [1-(\frac{As}{Ac})]\ \times 100$$

where *As* is the absorbance of the sample and *Ac* the absorbance of the negative control.

3.3.6. Statistical Analysis

One-way analysis of variance (ANOVA) was used for statistical analysis. A p-value of less than 0.05 was considered statistically significant, while p-vale greater than 0.05 is not statistically significant. Data were analyzed using GraphPad Prism 6.05 software (San Diego, CA, USA).

3.4 Results and discussion

3.4.1 Yield determination and kinetic parameters of Man26A

The enzymatic activity and specific activity of Man26A from *Bacillus* sp. were determined using ivory nut mannan (INM), locust bean gum (LBG) and guar gum (GG) as substrates. This was performed to determine the ability of Man26A to tolerate galactose side chains. Hydrolysis of INM, LBG and GG using Man26A resulted in the production of reducing sugars where LBG (36.86%) and GG (34.93%) showed higher yields than INM (30.18%). It is known that *Bacillus sp.* derived Man26A can partially tolerate galactose side chains; however, the abundance of these galactose residues affects the enzyme's efficiency in hydrolysing the mannan backbone (Kurakake et al., 2006). Also, GG contains more galactose residues (38%) than LBG (23% galactose) (Kurakake et al., 2006). Our results are not in agreement with the results obtained by Jiang et al. (2006), which showed that a β-mannanase from *Bacillus subtilis WY34* had a higher

activity on LBG (100%) than on GG (10.7%). In this study, there is a small difference (1.93% difference) between the yield of LBG (36.86%) and GG (34.93%) (*P-value*>0.05), compared to Jiang et al. 2006)'s findings who reported 89.3% yield difference between these two substrates. Yoon et al. 2008) also reported that β-mannanase derived from *Bacillus subtilis WL-3* acted better on partially substituted mannan substrates. According to our results (Fig. 3.1 below), the substituted mannans (LBG and GG) were more amenable to hydrolytic activity than linear mannan (INM). INM is insoluble, while LBG and GG are water-soluble (Van Zyl et al., 2010). Stoll et al. (2000) also reported that Man26A from *C. fimi* was able to bind tightly to soluble mannans.

Table 3.1: Yield and specific activity of *Bacillus* Man26A (n=3). All reactions were performed at 50^{o}C.

	Yield (%)	Specific activity (µmol/min/mg)
INM	30.18±0.77	333.85±1.14
LBG	36.86±1.85	453.52 ±1.16
GG	34.93±2.09	194.14±0.98

INM-ivory nut mannan, LBG-locust bean gum & GG-guar gum.

Michaelis-Menten kinetics for *Bacillus sp.* Man26A with different model substrates were determined and the results are shown in Table 3.2. According to the results in Table 3.2, Man26A showed the highest catalytic efficiency with LBG (k_{cat}/K_m = 8.8 mL $min^{-1}mg^{-1}$) followed by INM (k_{cat}/K_m = 3.8 mL $min^{-1}mg^{-1}$) and the lowest with GG (k_{cat}/K_m = 2.6 mL $min^{-1}mg^{-1}$). These values are lower than the values reported by Jiang et al. (2006). Jiang and colleagues reported that β-mannanase from the *Bacillus subtilis WY34* have high catalytic efficiency with LBG than GG, with k_{cat}/K_m values of 5058- and 2100-mL $min^{-1}mg^{-1}$, respectively.

Man26A showed the highest affinity for LBG (K_m = 10.8 mg/mL), followed by INM (K_m = 28.9 mg/mL) and the lowest affinity for GG (K_m = 50.2 mg/mL). These results are comparable to the results reported by Bågenholm et al. (2019) and Kaira et al. (2019) with GH26 endo-mannanase

derived from *Bacteroides ovatus* (*Bo*Man26B) and GH26 endo-mannanase from *Bacillus sp*. (ManB-1601), respectively. Bågenholm et al. (2019) reported that *Bo*Man26B exhibited a K_m value of 10.7 mg/mL with LBG, while Kaira et al. (2019) reported a K_m value of 6.3 mg/mL for ManB-1601 with LBG. Jiang et al. 2006) also showed that a β-mannanase from the *Bacillus subtilis WY34* exhibited K_m values of 7.6 mg/mL and 27.4 mg/mL with LBG and GG, respectively. Bågenholm et al. (2019) also reported a *Bo*Man26B K_m value of 12.9 mg/mL with GG, which is lower than 50.2 mg/mL obtained for Man26A. The differences in the kinetic constants for Man26A and values in the literature (Bågenholm et al., 2019; Jiang et al., 2006; Kaira et al., 2019) may be due to the use of mannanases from different types of bacteria i.e., *Bacillus sp*. and *Bacteroides ovatus*. Bågenholm and colleagues (2019) performed their enzyme kinetic study by hydrolysing different concentrations (2.5-20 mg/mL) of LBG at 37^{o}C, and in the presence of 1 mM $CaCl_2$, while in our study, enzymatic hydrolysis of INM, LBG and GG (2-40 mg/mL) was performed at 50^{o}C with no $CaCl_2$ present. A different protocol that did not include $CaCl_2$ was used in our study.

Table 3.2: Enzyme kinetics of Man26A against various mannans

	K_m (mg/mL)	V_{max} (µmol/min/mg)	k_{cat} (min^{-1})	k_{cat}/K_m ($mL\ min^{-1}mg^{-1}$)
INM	28.9	702.80	110.8	3.8
LBG	10.8	825.80	95.10	8.8
GG	50.2	563.30	133.6	2.6

3.4.2. Analysis of reaction products on TLC and HPLC

Hydrolysis of the model mannan substrates - ivory nut mannan (INM), locust bean gum (LBG) and guar gum (GG) - by *Bacillus* Man26A resulted in the generation of products of different sizes, which were analysed by TLC (see Figure 3.3) and confirmed using HPLC (Figure 3.4

below). As can be seen in Figure 3.3 below, the enzymatic hydrolysis of INM (lane 1) using Man26A resulted in M2 and M3 as the predominant sugars, while M1 and M4-M6 were produced to a lesser extent. Enzymatic hydrolysis of LBG resulted in M5 and M6 as the predominant sugars, followed by M2, while GG hydrolysis produced MOS with a DP equal to or greater than 6, and could not resolve on the TLC plate. In the chromatograms of LBG and GG, an unknown spot was also observed between M5 and M6. This could be a galactosyl substituted MOS. These TLC results agree with the results obtained using HPLC.

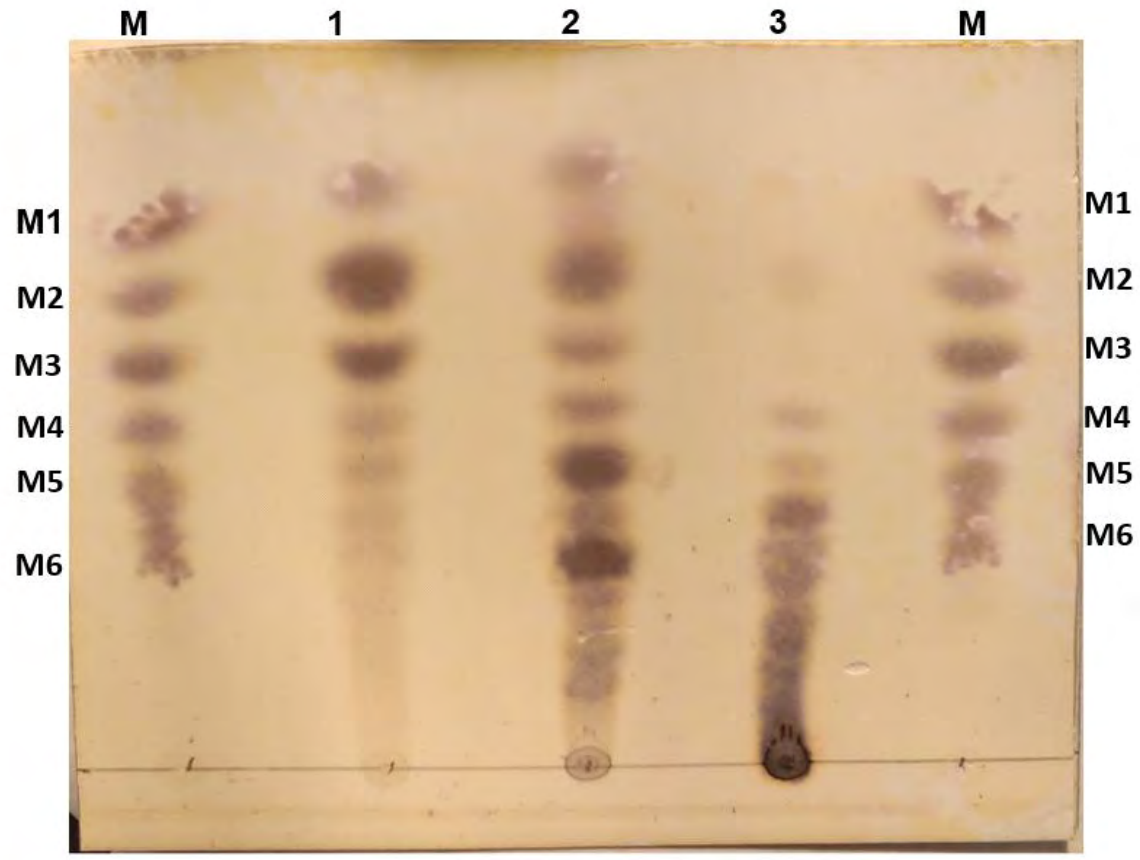

Figure 3.3: TLC plate showing the products produced during the hydrolysis of model mannans by Man26A. Lanes: M-MOS standards, 1-INM, 2-LBG and 3-GG. M1-mannose, M2-mannobiose, M3-mannotriose, M4-mannotetraose, M5-mannopentaose and M6-mannohexaose.

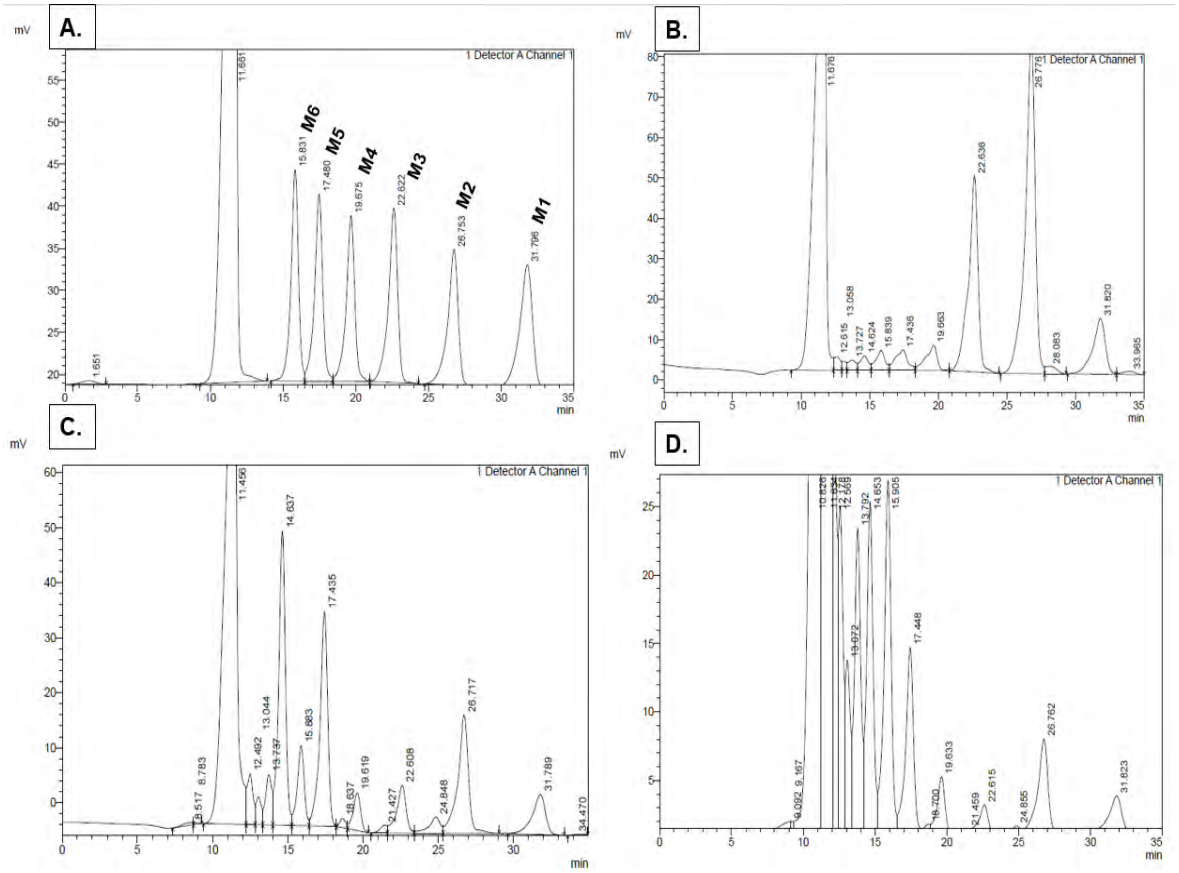

Figure 3.4: HPLC chromatograms displaying the MOS produced from the enzymatic hydrolysis of model mannan substrates (INM, LBG and GG). A: MOS standards (M1-M6) (0.17 mg/ml), B: INM MOS, C: LBG MOS and D: GG MOS. M1-mannose, M2-mannobiose, M3-mannotriose, M4-mannotetraose, M5-mannopentaose and M6-mannohexaose.

Bågenholm et al. (2017) reported only the production of M2 from INM, upon *Bacteroides ovatus* endo-1,4-β-mannanase hydrolysis, while, in our study, both M2 and M3 were produced as the predominant MOS. This difference could be due to the use of endo-1,4-β-mannanases derived from different bacteria. The predominant sugars obtained in the enzymatic hydrolysis of LBG were M5 and M6. This is different from the findings of Jiang et al. (2006) who reported that M2 and M3 were the predominant sugars obtained from *Bacillus subtilis WL-3* endo-1,4-β-mannanase hydrolysis of LBG. Srivastava et al. (2017) also reported M2, M3 and M5 as the predominant sugars obtained from LBG hydrolysis using a *Bacillus sp*. CFR1601 endo-1,4-β-mannanase, ManB-1601. These variations in results may be due to the different

hydrolysis/incubation times employed (hydrolysis in our study was performed for 24 hours) and the fact that the commercial Man26A used in our study may be from a different species of *Bacillus*. Hydrolysis of GG using Man26A resulted in oligosaccharides with a DP greater than 5. Some oligosaccharides could not resolve on TLC because of their size and the fact that the standards ranged from M1 to M6. Mannanases have been reported to only attack bonds between mannose residues that do not have galactose substituents, which explains why GG hydrolysis resulted in MOS with a higher DP than LBG. LBG galactomannan (23% galactose) has fewer galactose substituents than guar gum (38% galactose) (Kurakake et al., 2006). Hydrolysis of LBG and GG using Man26A also resulted in galactosyl substituted MOS. This agrees with the findings of Magengelele et al. (2021), where galactosyl substituted MOS was produced from LBG and GG using *A. niger* Man26A.

3.4.3. MOS stability

The temperature and pH stability of the MOS obtained from INM, LBG and GG was investigated to assess whether MOS can pass through the stomach and intestine without losing their structural integrity. Figure 3.5 shows that MOS were stable at temperatures ranging from 25^{o}C up to 100^{o}C, and at pH 2-10. The concentrations of MOS from INM, LBG and GG were 2.07, 2.74 and 1.22 mg/ml, respectively.

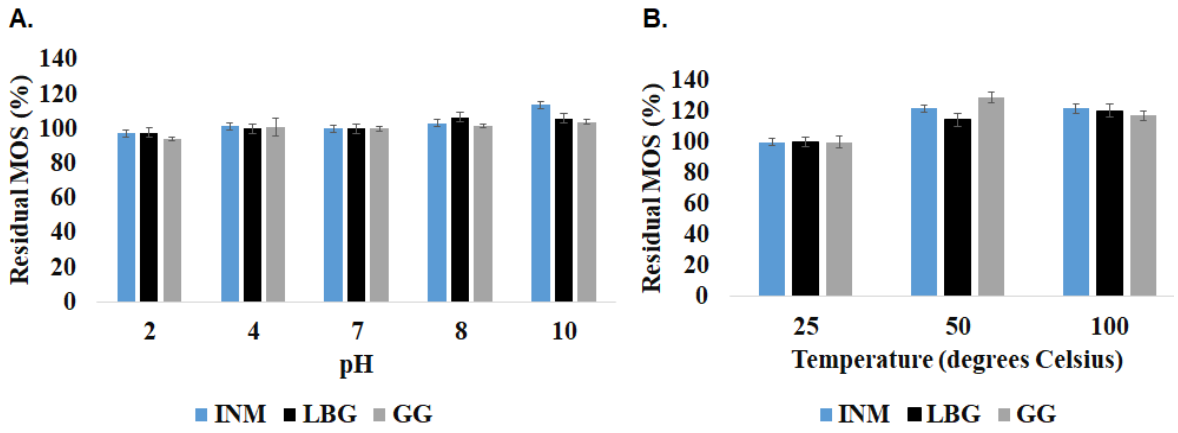

Figure 3.5: Temperature and pH stability of MOS produced from INM, LBG and GG hydrolysis using *Bacillus* Man26A. A: MOS generated from INM, LBG and GG were incubated with buffers of varying pH for 3 hours. B: MOS generated from INM, LBG and GG were incubated at different temperatures for 3 hours. INM-ivory nut mannan, LBG-locust bean gum and GG-guar gum. Values are represented as residual MOS relative to the mannose control (which is 100 %), and as means ± standard deviations (n=3).

The reducing sugar content from INM- and LBG-derived MOS slightly increased with temperature, but this increase was statistically significant ($P < 0.05$) to suggest MOS is not thermally stable or undergoes degradation. Chacher et al. (2017) reported that MOS tolerate temperatures of 120^{o}C without losing their function. It has been reported that MOS are highly stable against intestinal juice and gastric juice (Singh et al., 2018). Our results in Figure 3.3A reflected this pH stability of MOS, as they were stable at different pH (2-10) points. These characteristics are essential for oligosaccharides which may be used as prebiotics.

3.4.4. ABTS radical scavenging activity

The antioxidant activity of the MOS obtained from model mannan substrates was determined using the ABTS radical as described by Amna et al. (2018). Oligosaccharides such as xylo-oligosaccharides (XOS) and arabinoxylan-oligosaccharides (AXOS) have been reported to prevent oxidation of lipids, which is caused by gastric juice, in the stomach of humans (Van de

Ende et al., 2011). The ability of these oligosaccharides (XOS and AXOS) to counteract oxidation results in the inhibiton of ROS-related diseases (Van de Ende et al., 2011). Van de Ende et al. (2011) also reported that prevention of oxidation by oligosaccharides results in the inhibition of the growth of pathogens and enhancement of beneficial bacteria.

The antioxidant activity of MOS was investigated to test if MOS also have an oxidation potential. Discolouration in the assay was observed as a result of the interaction of this radical with free hydroxyls in the solution and was quantified. The amounts of reducing sugars used in Fig. 3.6A, derived from INM, LBG and GG, were 4.11, 4.24 and 3.29 mg/mL, respectively. In Fig. 3.6B, reducing sugars from all three substrates were diluted to the same concentration of 3 mg/mL. From Fig. 3.4A it can be seen that the MOS from INM have the highest scavenging activity of 34.96%, followed by those from LBG with 24.45% and GG, which had a scavenging activity of 6.69%. The results in Fig. 3.6B indicate that the relative scavenging activity of INM MOS is 26.20% and is not significantly different from those from LBG hydrolysis (24.83%) at 3 mg/mL concentration. Reducing sugars from GG hydrolysis resulted in scavenging relative activity of 10.01%, which is less than half the activity obtained from INM and LBG reducing sugars at 3 mg/mL. Gallic acid (0.02 mg/ml) was used a positive control and resulted in 61.12% scavenging relative activity. Du et al. (2014) reported that 0.1 mg/mL of gallic acid resulted in 92.9 and 91.3% scavenging relative activity, when using the DPPH and ABTS radical methods, respectively. The difference in the scavenging relative activity of our study and that in the literature may be due the difference in the concentrations used (0.02 mg/mL vs 0.1 mg/mL). A smaller concentration of gallic acid was used because it is known to have a very high antioxidant activity. Gallic acid was used as positive control because it is a known antioxidant (Du et al., 2014).

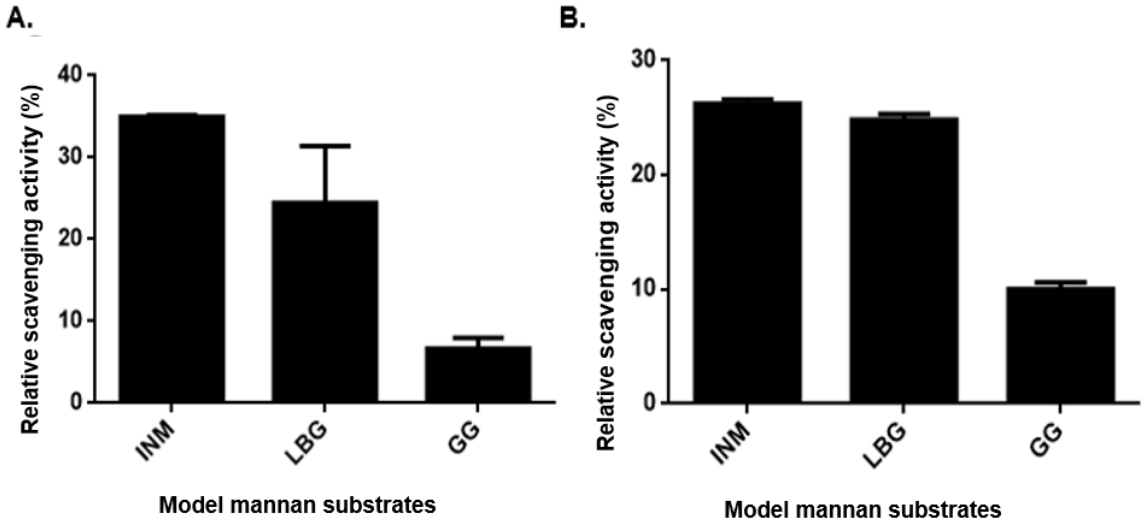

Figure 3.6: Relative ABTS scavenging activity of MOS produced using *Bacillus* Man26A from model substrates. INM-ivory nut mannan, LBG-locust bean gum and GG-guar gum. A: The amounts of reducing sugars (mg/mL) were different for each substrate (INM, LBG and GG, were 4.1112, 4.2409 and 3.2859 mg/mL, respectively), and in B: the amounts of reducing sugars of all the substrates (INM. LBG and GG) were standardised to 3 mg/mL. ABTS was radicalised for 16 hs in the dark, using potassium persulfate. Values are represented as means ± standard deviations (n=3).

The chemical structure of gallic acid is composed of an aromatic ring with three phenolic hydroxyl groups and one carboxylic group (Badhani et al., 2015). An increase in the number of hydroxyl groups causes an increase in the antioxidant activity/ scavenging relative activity (Badhani et al., 2015; Du et al., 2014). INM has a ratio of mannose: galactose of 19:1, LBG has a ratio of mannose: galactose of 1:4, and GG has a ratio of mannose: galactose of 2:1 (Malgas et al., 2015a; Singh et al., 2018). These substrates were enzymatically hydrolysed to produce MOS, and the presence of hydroxyl groups in these reducing sugars were the source of antioxidant activity. It has also been reported that the free hydroxyl groups from polymers are the main source of antioxidant activity in saccharides (Jana & Kango 2020). The results obtained in this study are in agreement with the findings of Jana & Kango (2020). INM and LBG hydrolysis which resulted in more reducing sugars (and hydroxyl groups) showed more antioxidant activity,

than GG which displayed higher DP in TLC and HPLC. The antioxidant activity of MOS is affected by its length (DP).

3.5. Conclusion

Man26A demonstrated high specific activity and MOS product yield for partially substituted LBG. The enzymatic hydrolysis of model mannan substrates (INM, LBG and GG) resulted in MOS of variable DP and, possibly, galactose substituents. These MOS were not stable at different temperatures but may pass through the digestive tract without being degraded as they could withstand both acidic and alkaline pH conditions. Unsubstituted MOS and MOS with a low DP demonstrated high antioxidant activity.

CHAPTER 4: Pretreatment and hydrolysis of SCG by Man26A, and characterisation of SCG-derived MOS

4.1. Introduction

With tons of coffee being generated worldwide, the beneficiation of its by-product, SCG, for the production of value-added products is essential. In 2014 and 2016, 8.5 and 9.3 billion kilograms of coffee were generated worldwide (McNutt & He, 2019). SCG is currently used as compost, fertiliser and fuel, and these are low-value applications (Mussatto et al., 2011, Sachslehner et al., 2000). This agro-industrial waste is mainly composed of insoluble cellulose and galactomannan as its main polysaccharides (Jooste et al., 2013; Redgwell & Fischer, 2006). Enzymatic hydrolysis of SCG galactomannan results in the production of MOS, which are defined as indigestible oligosaccharides important for the enhancement of beneficial bacteria in the digestive tracts of mammals (Redgwell & Fischer, 2006).

β-Mannanase from *Bacillus* sp. G 2 1) can hydrolyse the β-1,4-mannosidic bonds present in SCG galactomannan and results in the production of M2 and M3 (Wongsiridetchai et al., 2018). Asano et al. (2003) also reported that thermal hydrolysis of SCG results in the generation of M2 – M5. MOS are reported to not only promote the proliferation of beneficial bacteria, but also act as antioxidants, exhibit anticancer effects and trigger an immune response (Chacher et al., 2017; Saeed et al., 2017).

The availability of complex, high molecular lignin (39.4%, on a dry basis) in SCG lignocellulose makes it difficult for CAZymes to access the polysaccharides (Tsai et al., 2012). Therefore, pretreatment of SCG before hydrolysis is required to increase the efficiency of enzymes during the hydrolysis of the substrate by creating pores on the surface of SCG (Wongsiridetchai et al., 2018). The structural changes occurring upon biomass pretreatment can be observed using techniques such as scanning electron microscopy (SEM) (Wongsiridetchai et al., 2018). There are many methods that have been used for the pretreatment of agricultural biomass, including acid pretreatment, alkaline pretreatment and steam explosion (McNutt & He, 2019; Wongsiridetchai et al., 2018). Alkaline pretreatment using sodium hydroxide (NaOH) was used

in this study because it is more efficient and results in more reducing sugars being produced with than acid pretreatment (Wongsiridetchai et al., 2018).

Pretreatment of lignocellulosic biomass solubilises lignin and hemicellulose without degrading cellulose (Loow et al., 2016; Oriez et al., 2020). In the presence of an alkaline solution, intermolecular hydrogen bonds that hold cellulose molecules together are disrupted, resulting in the swelling of the biomass (Oriez et al., 2020; Wongsiridetchai et al., 2018). Motifs that are sensitive to alkaline solutions, and present between monomers of lignin and polysaccharides are broken down (Oriez et al., 2020). Jiang et al. (2014) reported that NaOH is also important for the removal of acetyl groups, which negatively affect the efficiency of enzymes during hydrolysis, from agricultural biomass such as corn stalk (Jiang et al., 2014). After SCG pretreatment, melanoidins are formed resulting in SCG being darker (Moreira et al., 2015). Figure 4.1 below shows how the structural changes in galactomannan, arabinogalactan, chlorogenic acids and proteins result in the formation of melanoidins

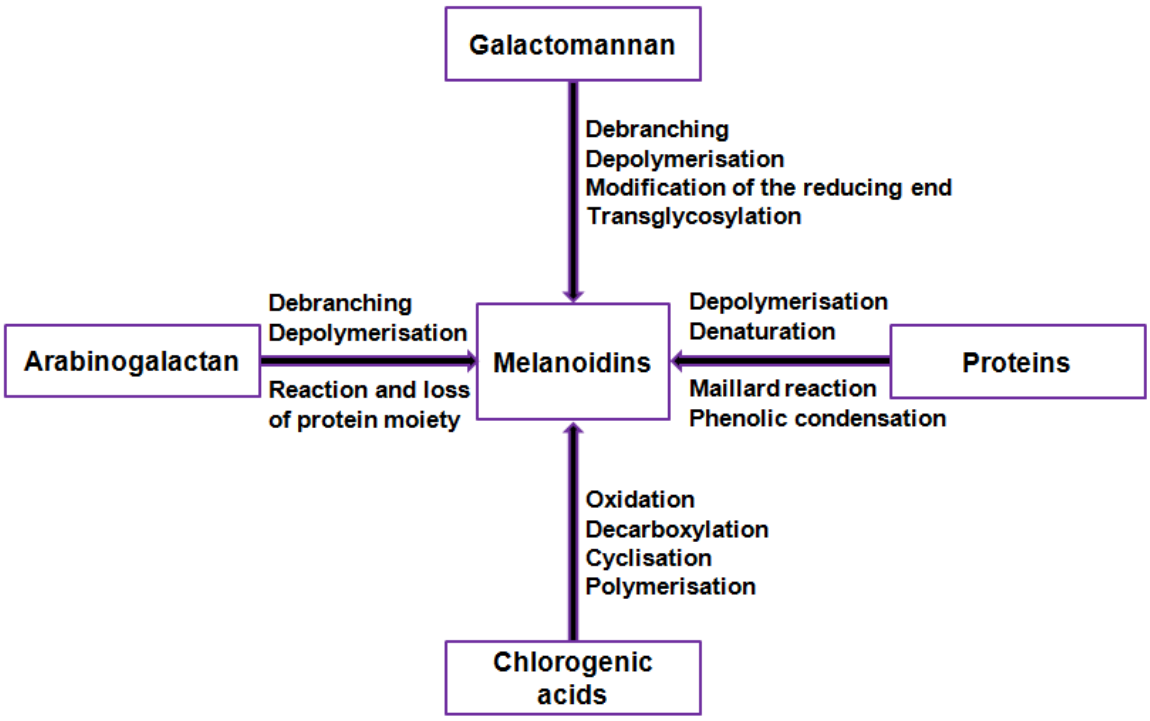

Figure 4.1: The formation of melanoidins as a result of structural changes in coffee. The debrancing, depolymerisation, polymerisation denaturation, amongst other things, that occur in galactomannan, arabinogalactan, proteins and chlorogenic acids result in the formation of melanoidins (adapted from Moreira et al., 2015).

In this chapter, the structural changes due to pretreatment and the hydrolysates produced by Man26A from pretreated SCG were analysed using FT-IR, TGA, SEM, TLC and HPLC.

4.2. Aims and objectives

4.2.1. Aims

To produce MOS from alkaline pretreated SCG using an endo-1,4-β-mannanase derived from *Bacillus* sp., Man26A and characterise these oligosaccharides. To achieve this, the following objectives were addressed:

4.2.2. Objectives

1. To pretreat SCG using sodium hydroxide (NaOH);
2. To analyse the composition and morphology of SCG before and after pretreatment;
3. To hydrolyse SCG mannan using Man26A from *Bacillus sp*.; and
4. To analyse of the hydrolysis products of Man26A using TLC and HPLC.

4.3. Materials and Methods

4.3.1. Pretreatment of SCG

SCG was supplied by National Brands Limited (Isando, South Africa). For the pretreatment of SCG, 12.5 g of NaOH, 1 L of distilled water and 50 g of SCG were combined in a Schott bottle. The slurry was incubated at 70^{o}C with occasional stirring for 4 hours in a 6-litre water bath (Labnet International. Inc, Woodbridge, USA). After incubation, the slurry was cooled down to room temperature, filtered using a cheesecloth and washed three times with 500 mL distilled water. The SCG was then dried at 50^{o}C for 24 hours or until a constant weight was obtained. Dried SCG was pulverised using a pestle and mortar, passed through a sieve (mesh size 0.5 mm) and stored at room temperature for further studies. Untreated SCG (50 g) was also washed and dried in the same manner as the pretreated SCG.

4.3.2. Structural analysis

4.3.2.1. Fourier transform infrared spectrometer (FT-IR) analysis

A Spectrum 100 FT-IR spectrometer system (Perkin Elmer, Welles-ley, MA) was used to characterise the pretreated and untreated SCG. The spring-loaded anvil was used to evenly press the samples against the spotting surface. FT-IR spectra were obtained by averaging four scans

from 4000 to 600 cm^{-1}. Spectrum™ One software was used for baseline and TR corrections for penetration depth and frequency.

4.3.2.2. Thermogravimetric (TGA) and derivative thermogravimetric (DTA) analysis

TGA was performed using a Perkin-Elmer analyser (PerkinElmer, Shelton, CT, USA). For both analyses, around 3 mg of the samples (pretreated and untreated SCG) were placed in a platinum pan. A stream of nitrogen at 20 ml/min was allowed to run over the incubation chamber during analysis. The heat was applied from 30°C to 750°C, with an increase of 30°C/min under nitrogen gas.

4.3.3. Scanning Electron Microscopy (SEM)

Untreated and pretreated SCG samples were analysed on a SEM (JEOL JSM 840) to observe the effect of NaOH pretreatment on the structure of the biomass. The samples were placed on metal pin stubs, coated with gold and dried using a critical point-drying process in a Quorum (Q150RS) metal coater (Advanced Laboratory Solutions, Johannesburg, South Africa) before they were analysed (Cross, 2001).

4.3.4. Investigating the efficiency of SCG pretreatment

Prior to hydrolysis, the pretreated and untreated SCG samples were pre-wetted in 50 mM phosphate buffer (pH 7) for 5 hours. After this, the SCG (at a final concentration of 4% (w/v)) was hydrolysed with 0.25 mg enzyme/g SCG. The reaction mixture also contained bovine serum albumin (BSA; 1 mg/mL) to keep the enzyme stable and minimise non-productive binding of the enzyme to SCG. The reactions were allowed to proceed for 48 hours at 50^{o}C, at 70 rpm. After the 48-hour incubation period, the reaction was terminated by incubating the samples at 100^{o}C for 5 minutes. The samples were then centrifuged at 16 060 *g* for 5 minutes (Biofuge Pico

Heraeus (Hanau, Germany)) and the reducing sugars were subsequently quantified using the DNS method described in section 3.3.1.

4.3.5. Optimisation of enzyme and substrate loading

SCG was hydrolysed using different concentrations of Man26A (0.25 – 2 mg enzyme/g SCG) in 50 mM phosphate buffer (pH 7.0). The reaction mixtures were incubated at 50^{o}C for 48 hours. The optimised enzyme load of Man26A (2 mg enzyme/g SCG) was used to hydrolyse different concentrations of SCG (2-10% (w/v)). The reaction mixtures were incubated at 50^{o}C for 48 hours, at 70 rpm.

4.3.6. Analysis of hydrolysis products on TLC

The MOS produced during SCG mannan hydrolysis were analysed using TLC to determine which sugars were present by comparing the observed sample spots with the standards M1 – M6. This experiment was performed according to the protocol described in section 3.3.3.

4.3.7. Analysis of hydrolysis products on HPLC

After TLC analysis, MOS from enzymatic hydrolysis of SCG were also separated, identified and quantified using the HPLC method developed in Chapter 2.

4.3.8. Gastrointestinal tolerance test

4.3.8.1. Effect of bile salts, α-amylase, trypsin and hydrochloric acid on MOS

Bile salts (0.3% w/v) (Sigma-Aldrich, St. Louis, USA), α-amylase (1 mg/ml) (Sigma-Aldrich, St. Louis, USA) and trypsin (1 mg/ml) (Sigma-Aldrich, St. Louis, USA) were prepared in 50 mM phosphate buffer (pH 7.0). The prepared solutions of bile salts, α-amylase and trypsin were mixed with MOS derived from SCG (1.7 mg/ml), in a 1:1 ratio. Mannose was used as a positive control, and 50 mM phosphate buffer (pH 7.0) was used as the negative control. For hydrochloric acid, the phosphate buffer (used to prepare SCG MOS) was removed using a CentriVap, and 1 ml of 0.1 M HCl (pH 1.5) was added to the Eppendorf tubes. The solutions were all incubated at 37˚C for 4 h. fter incubation, the Eppendorf tubes with α-amylase and trypsin were incubated at 100˚C for 5 minutes to inactivate the enzymes, and HCl was removed using the CentriVap and replaced with 1 ml phosphate buffer. The reducing sugars were quantified using the DNS method described in section 3.3.1.

4.3.9. Thermogravimetric (TGA) and derivative thermogravimetric (DTA) analysis of SCG MOS

TGA was performed using a Perkin-Elmer analyser (PerkinElmer, Shelton, CT, USA) as described previously (Section 4.3.2.2). SCG MOS was freeze-dried before it was used for analysis

4.4. Results and discussion

4.4.1. Pretreatment of SCG

SCG was pretreated using NaOH to make it easier for the endo-1,4-β-mannanase to access SCG mannan by creating pores and increasing the surface area of the biomass. In Fig. 4.2 below, it can be observed that SCG pretreated with NaOH is black and untreated SCG is brown.

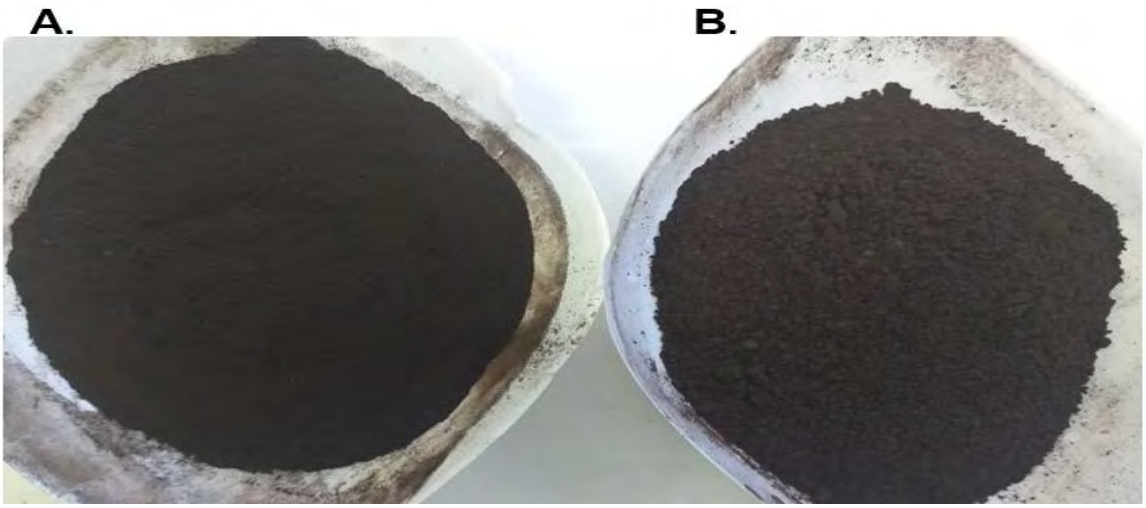

Figure 4.2: Visual differences observed in the NaOH pretreated (A) and untreated (B) spent coffee ground (SCG)

This could perhaps indicate that the structural changes of SCG during NaOH pretreatment resulted in the formation of more melanoidins. Melanoidins are brown coloured compounds usually formed as a result of coffee bean structural changes during roasting (Moreira et al., 2012; Moreira et al., 2015).

During the pretreatment of SCG using NaOH, the removal of phenolics, and possible debranching and depolymerisation of polysaccharides resulted in SCG to become black/darker than untreated SCG. The mass of SCG decreased after pretreatment, from 50 g to 30.3 g, while the untreated SCG mass only marginally decreased from 50 g to 47.14 g. This decrease in the mass of the pretreated SCG (39.41% (w/w)) was due to the removal of lignin, lipids and acid insoluble phenolics from SCG (Wongsiridetchai et al., 2018). Tsai et al (2012) reported that SCG contains 39.4% total lignin while Ballesteros et al. (2014) reported a lignin content of 23.90%. Layao et al. (2014) reported 16.07% lipid content in SCG, while Ballesteros et al. (2014) reported 2.29% lipids.

SCG also contains 16.07% of lipids (Loyao et al., 2018). Hemicellulose and cellulose contents in lignocellulosic biomass are generally not affected by NaOH pretreatment (Wongsiridetchai et al., 2018). McNutt & He (2019) reported that these polysaccharides make up 50% of the dry mass of SCG. Ballesteros et al. (2014), in turn, reported that SCG contains 12.40% and 39.10% of

cellulose and hemicellulose, respectively. The slight decrease in mass of the untreated SCG (5.72% (w/w)) was due to small particles of the SCG that pass through the cheese cloth, as well as lignins (soluble and insoluble), proteins and lipids.

4.4.2. Structural analysis of SCG

4.4.2.1. FT-IR analysis

FT-IR analysis was conducted to analyse the functional group differences in the structures of untreated and NaOH pretreated SCG samples (Figure 4.3).

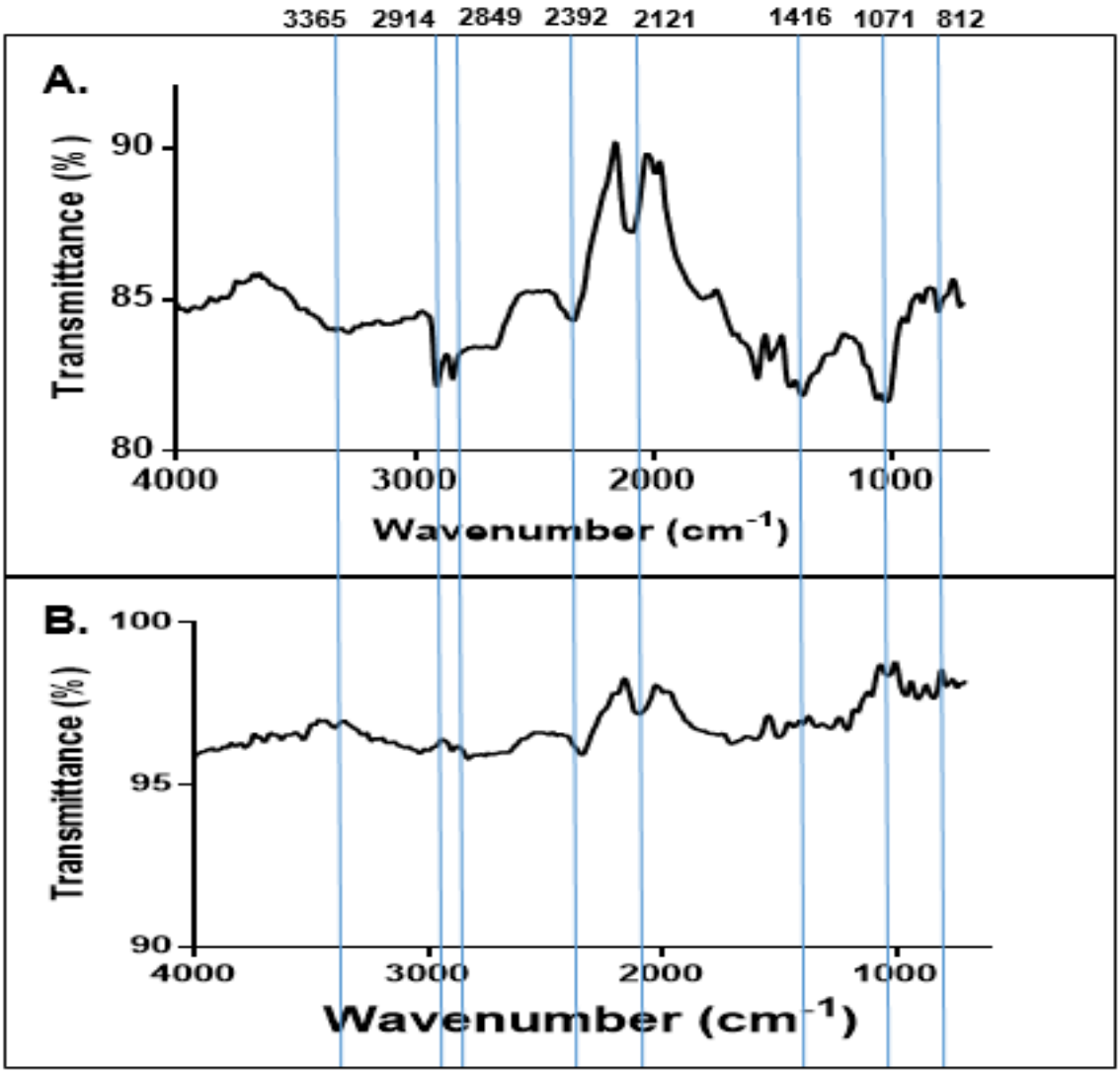

Figure 4.3: FT-IR spectra of NaOH pretreated SCG and untreated SCG. A: pretreated SCG, B: untreated SCG.

As shown in Figure 4.3, the broad peak 3364 cm^{-1} is attributed to the O-H vibration in pretreated SCG. In the untreated sample, the peak at 3364 cm^{-1} is very small. This is a peak usually found in all carbohydrate samples and has also been reported at 3277 and 3276 cm^{-1} in coffee waste before oil extraction (CWBE) and coffee waste after extraction (CWAE) samples (Atabani et al., 2018). Pandey et al. (2020) reported that the band at 3426 cm^{-1} is associated with the primary (-CH-OH) and secondary (-CH_2-OH) stretch of hydroxyl vibration. The peak at 2914 and 2849

cm^{-1} is associated with CH and CH_2 stretching vibration and this peak is similar to the peak observed by Pandey et al. (2020) at 2927 cm^{-1} for locust bean gum. Pandey et al. (2020) described the peak observed at 1383 cm^{-1} as the peak formed as a result of deformation of the CH-OH group, and a similar peak was observed at 1416 cm^{-1} in pretreated SCG. There is a very small peak observed at 1080 cm^{-1} in untreated SCG and a big scissor peak at 1071 cm^{-1} in pretreated SCG, and these peaks are associated with the C-O (carbon-oxygen stretch) vibration in C-O-H bonds (glycosidic bonds). These bands are associated with galactomannan in SCG (Atabani et al., 2018; Ballesteros et al., 2014). Similar peaks were observed in CWBE and CWAE samples (Atabani et al., 2018). Pandey et al. (2020) reported that the peaks at 812 and 817 cm^{-1} show the presence of α-linked D-galactopyranose units and β-linked D-mannopyranose units, respectively. These peaks (812 and 817 cm^{-1}) could also be observed in the untreated and pretreated SCG samples above. The peaks observed in both pretreated and untreated SCG (2392, 2121, 1071, 812 cm^{-1}) are clearer in Figure 4.3A. Peaks 3365, 2914 and 1416 cm^{-1} could only be observed in the pretreated SCG (Figure 4.3B). All the peaks were more clearly visible in the pretreated SCG than the untreated sample.

4.4.2.2. Thermogravimetric (TGA) and derivative thermogravimetric (DTA) analysis

TGA analysis was performed on pretreated and untreated SCG. The results obtained are shown in Figure 4.4 below.

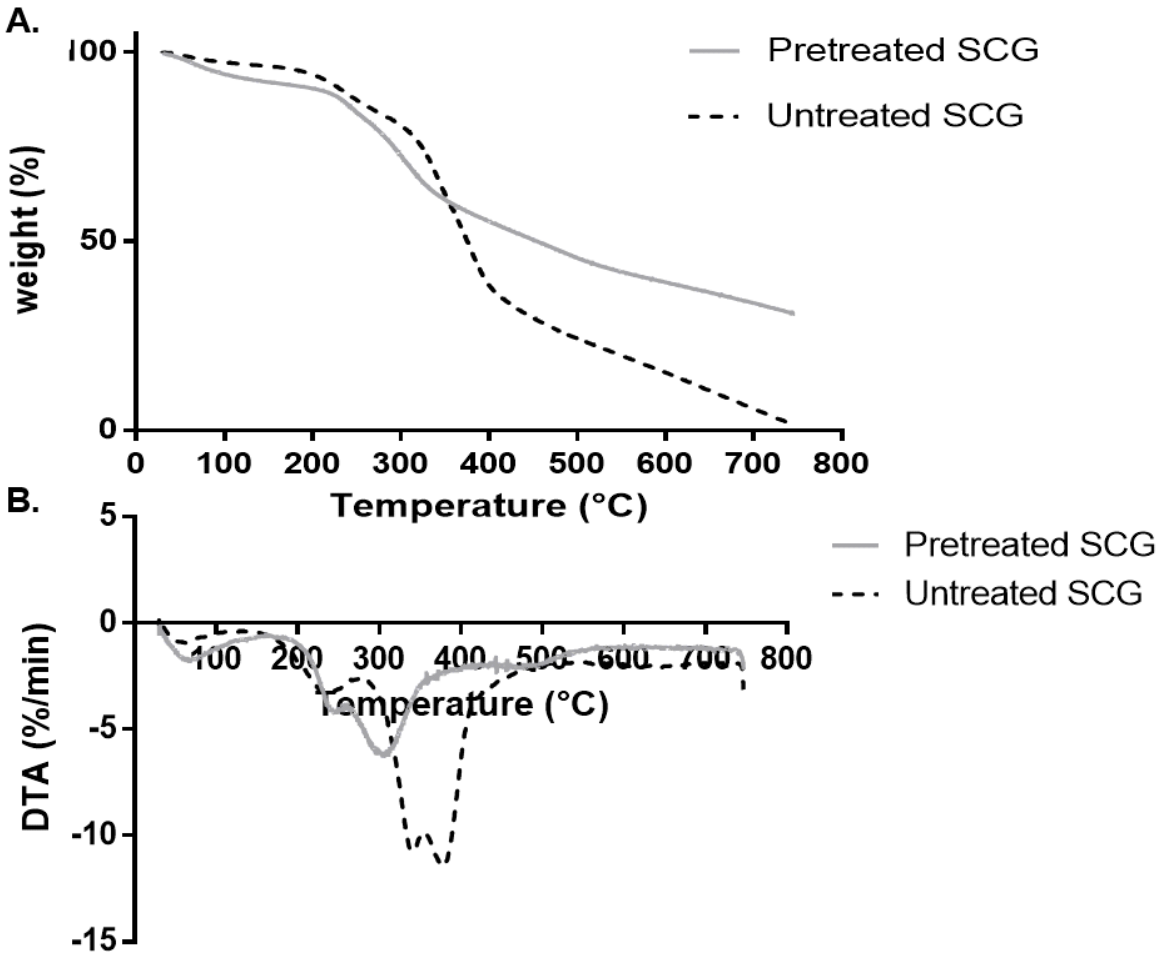

Figure 4.4: TGA (A) and DTA (B) curves of weight and different temperatures of pretreated SCG and untreated SCG

Figure 4.4A displays the TGA curves, while Fig. 4.4B shows the curves of the derivatives of TGA. Pretreated SCG and untreated SCG samples slightly lost weight at approximately 50°C and this was due to dehydration of the sample. Water and volatile substances are lost at this stage of TGA (Atabani et al., 2018; Ballesteros et al., 2014; Carrier et al., 2011). These findings are similar to the findings of Atabani et al. (2018) and Ballesteros et al. (2014) who reported that SCG (untreated), SCG before oil extraction and SCG after extraction first experienced a loss in weight at approximately 60, 60.38 and 77.03°C, respectively. The pretreated and untreated SCG samples, especially untreated SCG, then underwent an immense loss in weight between 200°C and 400°C. This is the second stage of TGA, where decomposition and depolymerisation occurs

(Atabani et al., 2018; Ballesteros et al., 2014; Carrier et al., 2011). Ballesteros et al. (2014) also reported that SCG undergoes an immense weight loss at approximately 300°C. Between 200°C and 400°C, there are two and three peaks observed in DTA curves of pretreated and untreated SCG, respectively. There is a hemicellulose peak in both pretreated and untreated SCG at approximately 250°C, with that of pretreated SCG increased slightly. DTA also displayed a cellulose peak at 300°C in pretreated SCG, but there was no peak in the untreated SCG sample. This peak was also observed for SCG MOS. DTA then showed a major peak in the untreated SCG sample, between 310 and 400°C, and this was indicative of a lignin peak. The presence of a major lignin peak in untreated SCG and its absence in pretreated SCG shows that the removal of lignin via pretreatment of SCG with NaOH was successful. These results are similar to the findings of Carrier et al. (2011) on lignin, hemicellulose and cellulose extracted from fern. Carrier et al. (2011) reported that in TGA, decomposition of biomass occurs at 200-300°C for hemicellulose, followed by decomposition of cellulose at 250-350°C and lignin at 300-500°C. Based on the results above, pretreated SCG was more stable than untreated SCG against temperature change.

4.4.3. Microscopy

4.4.3.1. Scanning Electron Microscopy (SEM)

The structural changes in SCG after NaOH pretreatment were assessed using SEM in order to better understand how NaOH pretreatment allows efficient enzymatic hydrolysis, and this is depicted in Figure 4.5.

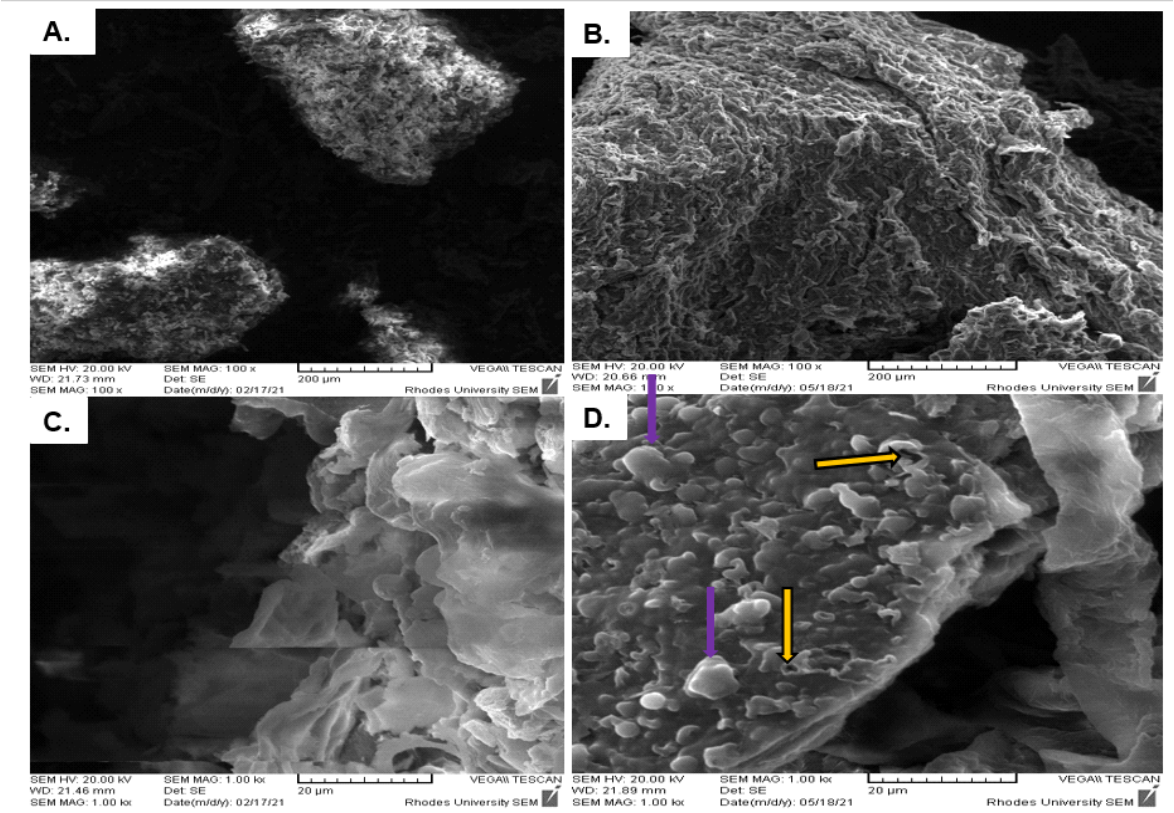

Figure 4.5: SEM images of pretreated and untreated SCG at different magnifications. (A): Untreated SCG at 100x magnification. (B): NaOH pretreated SCG at 100x magnification. (C): Untreated SCG at 1000x magnification. (D): NaOH pretreated SCG at 1000x magnification. Purple arrows indicate swelling, yellow arrows: pores.

Pores (indicated by the yellow arrows) were observed on the surface of NaOH pretreated SCG particles and not on the untreated SCG. Wongsiridetchai et al. (2018) reported that the swelling caused by NaOH pretreatment increases the surface area of the substrate, allowing easy substrate digestion by the enzyme.

4.4.4. Activity of Man26A on pretreated and untreated SCG

The hydrolysis of SCG by Man26A was evaluated and was more efficient after pretreatment with NaOH (Figure 4.6).

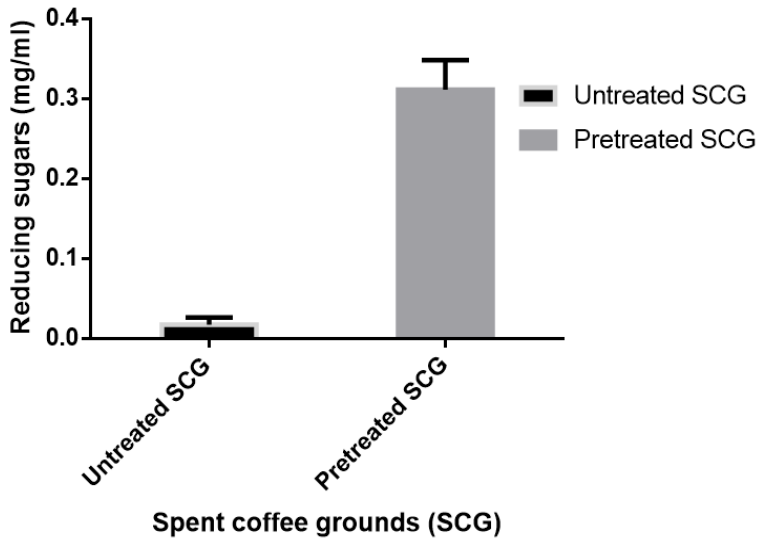

Figure 4.6: Effect of Man26A on pretreated and untreated SCG. Hydrolysis was performed at 50°C, with Man26A (0.25 mg enzyme/g SCG) and 4% (w/v) SCG. Values are represented as means ± standard deviations, n = 3.

Man26A was more active on NaOH pretreated SCG, resulting in 0.37 mg/mL of reducing sugars, while hydrolysis of untreated SCG resulted in only 0.02 mg/mL reducing sugar. NaOH pretreatment resulted in pore formation and increased the surface of SCG, allowing the enzyme to efficiently hydrolyse SCG mannan (Wongsiridetchai et al., 2018).

4.4.5. Optimisation of the enzymatic hydrolysis of SCG

The effect of different concentrations of endo-1,4-β-mannanase, Man26A, derived from *Bacillus* sp. was investigated (Figure 4.7A) and the enzyme concentration of 2 mg enzyme/g SCG resulted in the highest amount of reducing sugars (0.30 mg/mL) being released from 4% (w/v) SCG. Man26A (2 mg enzyme/g SCG) was used to hydrolyse different concentrations of SCG (2-10% (w/v)) (Figure 4.7B). The concentration of Man26A and SCG that resulted in the highest amount of reducing sugars was 2 mg enzyme/g SCG and 10% (w/v), respectively, which resulted in 0.906 mg/mL reducing sugars being released after 48-hour incubation at 50°C. The

concentration of SCG above 10% (w/v) could not be investigated because SCG would swell and absorb all the liquid in the reaction mixture.

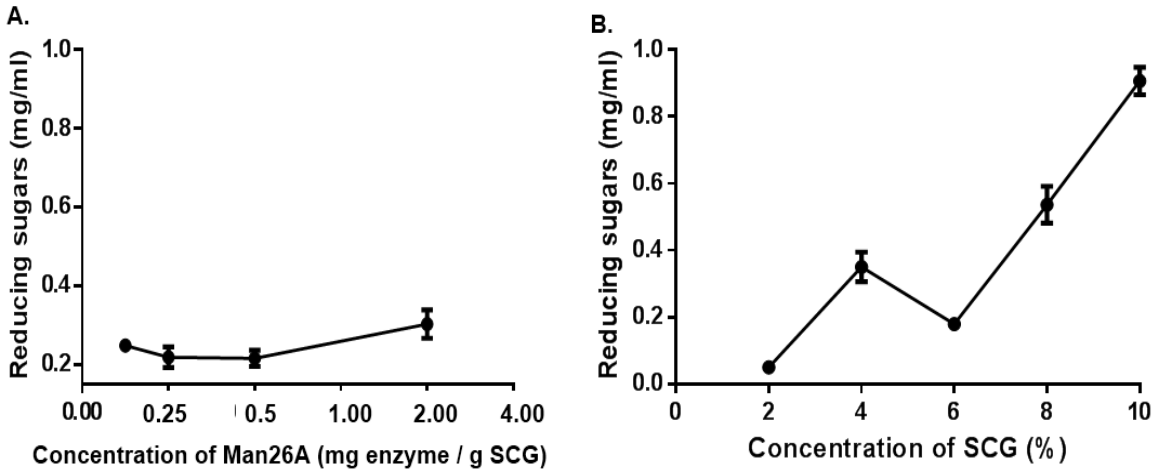

Figure 4.7: Amount of reducing sugars released from the hydrolysis of SCG (4%(w/v)) using different concentrations of *Bacillus sp*. derived Man26A (0.25-2 mg Man26A/g SCG) (A) and different SCG concentrations (2-10% (w/v) (B), at 50^{o}C for 48 hours. Values are represented as means ± standard deviations, n=3.

4.4.6. Analysis of the hydrolysis products on TLC

The hydrolysis products of Man26A on SCG were qualitatively and quantitatively analysed using thin layer chromatography (TLC) and high-performance liquid chromatography (HPLC), respectively. The hydrolysis of this agro-industrial waste using *Bacillus* sp. Man26A released mannobiose (M2) and mannotriose (M3) as the predominant MOS. This agreed with the findings of Chauhan et al., 2014), who also reported that M2 and M3 were the predominant MOS produced from coffee extract using a *Bacillus nealsonii* PN-11 β-mannanase. Wongsiridetchai et al. (2018) also reported that SCG hydrolysis using a *Bacillus sp.* GA2 (1) mannanase results in M2 and M3. As observed in Figure 4.8, M1, M4 and M5 were produced to a lesser extent than M2 and M3. The products observed on TLC were quantified on HPLC (Table 4.1) (HPLC chromatogram in Appendix D (Figure D.1), and standard curves in Appendix A (Figure B5)).

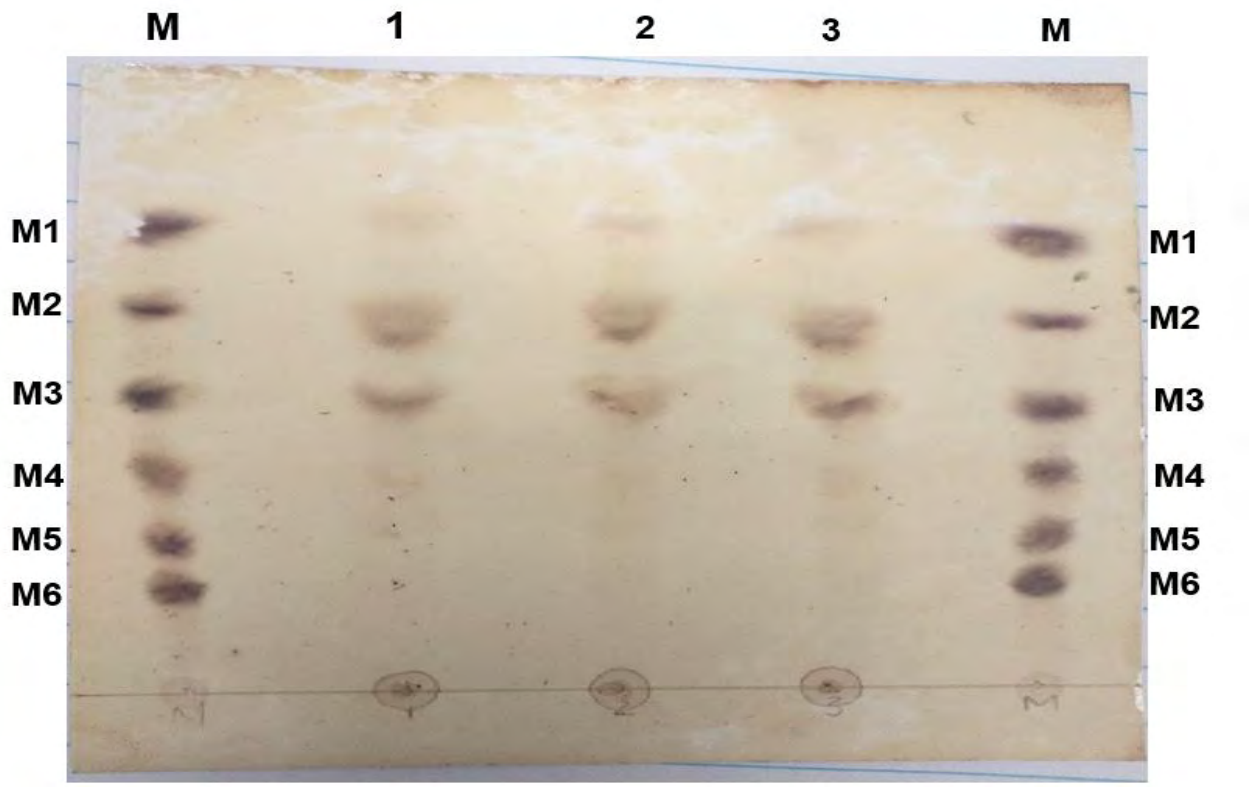

Figure 4.8: Thin-layer chromatography (TLC) profile of the hydrolysate products obtained from SCG hydrolysis using *Bacillus sp.* Man26A. Lane M: MOS standards (M1-M6); and lanes 1, 2 and 3: SCG MOS (in triplicate). M1-mannose, M2-mannobiose, M3-mannotriose, M4-mannotetraose, M5-mannopentaose and M6-mannohexanose.

4.4.7. Analysis of the hydrolysis products on HPLC

The hydrolysis products were separated (simultaneously) using HPLC. Table 4.1 below shows the separated and quantified MOS produced from SCG.

Table 4.1: Summary of the HPLC results showing the concentration of MOS (mg/mL) produced as a result of Man26A hydrolysis. Values are represented as means ± standard deviations, n = 3.

	MOS produced from SCG (mg/mL)
M1	0.18 ± 0.03
M2	1.04 ± 0.03
M3	1.20 ± 0.04
M4	-
M5	0.03 ± 0.00
M6	0.02 ± 0.00
GM	+
TRS	1.80

M1: mannose, M2: mannobiose, M3: mannotriose, M4: mannotetraose, M5: mannopentaose, M6: mannohexaose, GM: galactosyl-manno-oligosaccharides, +: high quantities, -: not produced, TRS: total reducing sugars as determined by the DNS method.

The HPLC method (developed and validated in Chapter 2) was used to quantify the MOS obtained from the hydrolysis of SCG using *Bacillus sp*. Man26A (see chromatogram in Appendix D (Figure D.2). The MOS obtained from SCG hydrolysis were successfully resolved as they eluted at different times; M1 (31.721 min), M2 (26.710 min) and M3 (22.636 min), while the peak at 23.834 was unknown. Interestingly, M5 (17.562) and M6 (15.904) peaks could not be really observed in the chromatogram, but the retention times are present, meaning these MOS were below the LOD. The M4 peak, with a retention time of 19.692 (according to the developed HPLC method in chapter 2) was not observed in the SCG MOS chromatogram. In Table 4.1 above, M2 and M3 were produced at a concentration of 1.039 and 1.203 mg/mL, respectively,

and these were the predominant sugars produced from SCG using Man26A. The concentration of M1 produced was approximately 6-fold lower than the concentrations of M2 and M3. M5 and M6 were produced to a lesser extent, with concentrations of 0.028 and 0.023 mg/mL, respectively. The various sizes of oligosaccharides produced from SCG revealed that this mannanase is an endo-mannanase. *Bacillus sp*. derived endo-1,4-β-mannanase, Man26A, is suitable for MOS production from the inexpensive and abundant substrate SCG. The HPLC results shown in Table 4.1 agree well with the TLC results shown in Figure 4.8. There is no literature available on the quantification of MOS produced from SCG.

4.4.8. Gastrointestinal tolerance test of MOS

Prebiotics must also have several other important characteristics such as tolerance to acids, bile salts and other enzymes that may be present in the gastrointestinal tract, in order to reach the bacteria, the growth of which they enhance. The effect of bile salts, α-amylase, trypsin and hydrochloric acid on SCG MOS was investigated *in vitro*. Bile salts, α-amylase, trypsin and hydrochloric acid were incubated for 4 hours at 37˚C, followed by quantification of the sugars using DNS method. The results are shown in Figure 4.9. SCG MOS and mannose showed resistance to bile salts, α-amylase, trypsin and hydrochloric acid. The reducing sugar content of SCG MOS after incubation with bile salts, α-amylase, trypsin and hydrochloric acid is 1.93±0.04, 1.88±0.09, 2.43±0.06 and 1.32±0.18 mg/ml, respectively. The initial amount of sugars used was 1.7 mg/ml - for the effect of HCl, some of the sugars were lost during preparation, and the reducing sugars subsequently decreased to approximately 1.32 mg/ml. The background sugars were also detected in the negative controls (sugar-free), which caused an increase in the reducing sugar content.

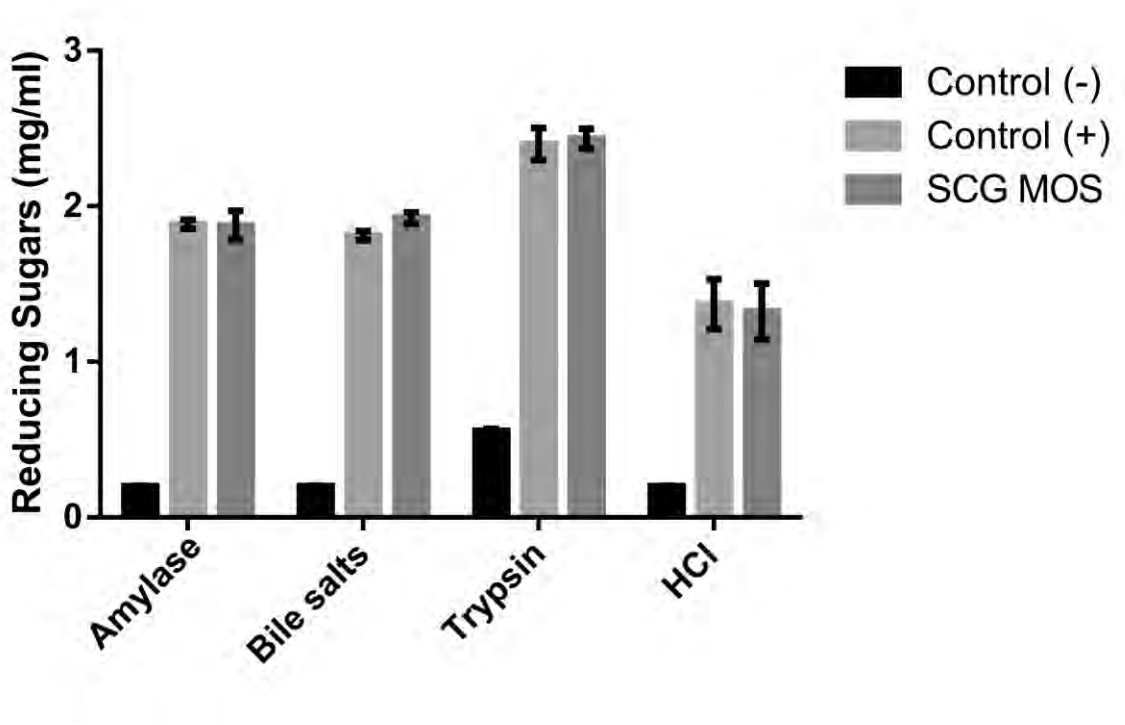

Figure 4.9: Digestion of SCG-derived MOS by bile salts, α-amylase, trypsin and hydrochloric acid. Control (+): mannose, control (-): sugar free. The concentration of bile salts, α-amylase and trypsin were 0.3% (w/v), 1 mg/ml and 1 mg/ml, respectively. 1.7 mg/ml of the sugars (MOS and mannose) were used. DNS method was used to determine the amount of reducing sugars. Values are represented as means ± standard deviations, n = 4.

The results in Figure 4.9 indicate that SCG MOS did not undergo hydrolysis by amylase, bile salts, trypsin and hydrochloric acid, which agree with the findings of Asano et al. (2003) who showed that thermally produced SCG MOS were resistant to human salivary amylase, artificial gastric juice, porcine pancreatic enzymes and rat intestinal mucous enzyme. The ability of SCG MOS to tolerate these gastrointestinal conditions shows that they are indigestible during the initial phase of digestion and will reach large intestine without losing their activity.

4.4.9. Thermogravimetric (TGA) and derivative thermogravimetric (DTA) analysis of SCG MOS

TGA analysis was performed on freeze-dried SCG MOS. The results are shown in Figure 4.10 - Fig. 4.10A depicts the TGA curves, while Fig. 4.10B shows the curves of the derivatives of TGA.

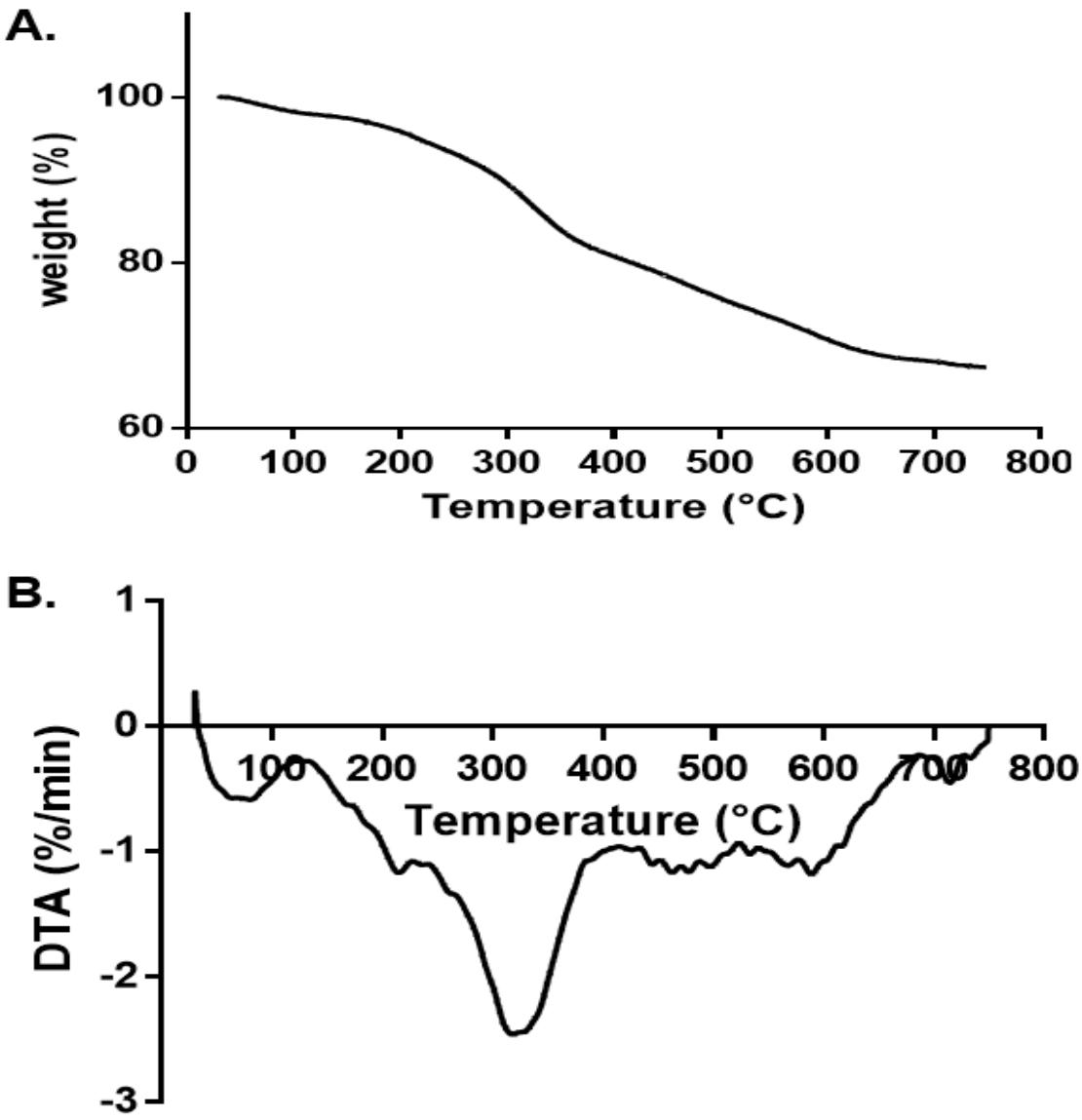

Figure 4. 10: TGA (A) and DTA (B) curves of weight and different temperatures of SCG MOS

The slight loss in the weight of SCG MOS starts at approximately 50°C and this is due to the loss of water and volatiles that may still be present in the sample. This can be observed in Fig. 4.10B. A gradual, but an immense weight loss occurs between 150 and 400°C. López-Sanz et al. (2018) also observed weight loss peaks of Vivinal® GOS at 36, 90 and 135°C. The heat applied by López-Sanz et al. (2018) was up to 200°C. In Fig. 4.10B, a large peak was also observed at 300°C and SCG MOS gradually lost weight until approximately 65% of initial weight. SCG MOS was quite stable against temperature change.

4.5. Conclusion

SCG was successfully pretreated using NaOH. Structural analysis using FT-IR and TGA confirmed the integrity of SCG. MOS were successfully produced from NaOH pretreated SCG using a *Bacillus sp*. derived endo-1,4-β-mannanase, Man26A. M2 and M3 were the predominant MOS species detected in TLC and HPLC. SCG derived MOS could tolerate GI tract conditions, such as resisting hydrolysis by bile salts, α-amylase, trypsin and hydrochloric acid. TGA also revealed that SCG MOS was thermally stable against changes in temperature.

CHAPTER 5: Properties of SCG-derived MOS

5.1. Introduction

Sugars obtained from SCG via hydrolysis are MOS with a mixture of monosaccharides such as glucose and arabinose P rez-Burillo et al., 2019; Tian et al., 2017). Different MOS obtained from SCG have different selective prebiotic activities towards bacterial strains that can utilise them as carbon sources (Tian et al., 2017). Asano et al. (2003) reported that mannobiose (M2), mannotriose (M3), mannotetraose (M4) and mannopentaose (M5) are the MOS obtained from thermal hydrolysis of SCG. MOS (M1-M6) cannot be digested by human α-amylase, artificial gastric juice, and pancreatic enzymes, and so are able to reach the large intestine without being degraded (Asano et al., 2003). Baurhoo et al. (2007) reported that MOS have the ability to increase the growth of *Bifidobacteria* and *Lactobacillus spp*. in the intestines of broilers. MOS obtained from SCG have also been reported to enhance the growth of beneficial bacteria, which, in turn, produce short-chain fatty acids SCF) sa no et al., 2003; P rez-Burillo et al., 2019).

MOS do not only enhance the growth of beneficial bacteria but also have the ability to enhance autoaggregation, the ability of microorganisms of the same strain to cluster together and form aggregates (Cao et al., 2019; Trunk et al., 2018). Cao et al. (2019) reported that these oligosaccharides enhance the rate of autoaggregation of *Lactobacillus plantarum* by an autoaggregation percentage of 23.76%, which is better than the rate of autoaggregation of fructooligosaccharides (FOS, 21.10%) and galactooligosaccharides (GOS, 20.64%). MOS are also reported to be more able to adhere to mucin and Caco-2 cells than FOS and GOS (Cao et al., 2019). The adherence of microbes to surfaces is termed biofilm formation (Trunk et al., 2018). The ability of microorganisms to aggregate and adhere to surfaces is a survival mechanism method that provides them a better chance of survival than planktonic microorganisms, and it also increases their chance of accessing nutrients (Cao et al., 2019; Trunk et al., 2018). The resistance of aggregated bacteria to antibiotics is 1000 x more than that of planktonic bacteria (Trunk et al., 2018). There are multiple components of bacteria associated with their ability to attach to surfaces and these include bacterial surface proteins, peptidoglycan, lipoteichoic acid

and polysaccharide (Cao et al., 2019). Mucin-binding protein is one of the surface proteins found in *Lactobacillus reuteri* 1063 (Roos & Jonsson, 2002). Mucin-binding proteins in bacteria bind to mucins, which form part of the mucus layer in the stomach (Sicard et al., 2017). Beneficial bacteria (i.e. *Lactobacillus* species) and SCFAs (i.e. butyric acid and propanoic acid) enhance the production of mucins in the gastrointestinal tract (Roos & Jonsson, 2002; Sicard et al., 2017). Mucins produced by goblet cells and SCFAs produced by beneficial bacteria contribute in decreasing the number of pathogens in the gastrointestinal tract (Chacher et al., 2017).

Gut bacteria produce a highly toxic compound called hydrogen sulphide (H_2S) in many different ways, which include producing it from cysteine and via the reduction of sulphite (Van den Ende et al., 2011; Winter et al., 2010). When the mucosa is exposed to the produced H_2S, it converts it to thiosulphate to protect itself (Winter et al., 2010). Winter et al. (2010) showed that ROS generated during inflammation oxidises thiosulphate to tetrathionate, which is an electron acceptor. This results in pathogens such as *Salmonella* generating ATP more efficiently than beneficial bacteria (Van den Ende et al., 2011). This is the reason why pathogens always cause intestinal inflammation (Van den Ende et al., 2011; Winter et al., 2010). The ability of beneficial bacteria to flourish in the presence of prebiotics such as FOS and GOS could be also be due to the inhibition of thiosulphate oxidation (Van den Ende et al., 2011).

In this study, we investigated the antioxidant activity of SCG MOS, its effect on the growth of beneficial and pathogenic bacteria *in vitro*, and further evaluated whether the selected bacteria could produce SCFAs upon SCG MOS utilisation. The effect of SCG MOS on the autoaggregation and biofilm formation of these bacteria was also studied.

5.2. Aims of objectives

5.2.1. Aims

The aim of this part of the study was to investigate the prebiotic properties of SCG-derived MOS. In order to achieve this, the following objectives were addressed:

5.2.2. Objectives

- To investigate the radical scavenging activity of SCG-derived MOS;
- To investigate the effect of SCG-derived MOS on the growth, autoaggregation and biofilm formation of beneficial bacteria;
- To investigate the ability of SCG-MOS to tolerate *in vitro* gastrointestinal conditions;
- To investigate the activation of mannan utilisation genes in beneficial bacteria after SCG-MOS utilisation.

5.3. Materials and Methods

5.3.1 Antioxidant activity

The ABTS radical scavenging activity method described previously (Section 3.3.5) was used to determine the scavenging activity of SCG-MOS (3 mg/mL, reducing sugar content). The absorbance was measured at 734 nm.

5.3.2. Prebiotic study

A prebiotic study was performed as described by Li et al. (2020) with some modifications. The bacterial cells were incubated in Luria broth (sodium chloride (0.5 g/L); tryptone (10 g/L) and yeast extract (5 g/L)) and grown overnight at 37^{o}C with shaking at 200 rpm. Bacterial cells (1 mL) were then harvested by centrifugation at 16 060 *g* (Biofuge Pico Heraeus (Hanau, Germany) desktop centrifuge) for 5 minutes and resuspended in 250 µL saline (0.9% (w/v) NaCl) before measuring their growth at 600 nm. The *in vitro* fermentation of probiotics was performed in 1 x M9 minimal media (3.4% (w/v) Na_2HPO_4; 1.5% (w/v) KH_2PO_4; 0.5% (w/v) NH_4Cl; 0.25% (w/v) NaCl) with a pH of 7.4. The samples were supplemented with MOS from SCGs at a concentration of 0.2% ((w/v), reducing sugar content). The initial absorbance (600 nm) of the reaction mixture was adjusted to 0.1 for all the samples. This was followed by incubation of the samples at 37^{o}C for 7 hours, with shaking at 200 rpm. The positive control was supplemented

with 0.4% (w/v) glucose, while the negative control was free of sugars. The OD_{600nm} of the samples was monitored.

The viability of the cells was subsequently tested by adding 50 µL of 0.02% (w/v) of iodonitrotetrazolium chloride (INT) into 96-well plate containing 200 µL of the cells that were quantified at 600 nm. The plate was incubated for 1 hour and the absorbance was measured at 490 nm. This method was adapted from the one reported by Cosa et al. (2020).

5.3.3. Liquid-liquid extraction

A method was developed for SCFA detection after MOS fermentation, where 0.1 mg/mL of acetic acid (AA), butyric acid (BA), lactic acid (LA), citric acid (CA), formic acid (FA) and propanoic acid (PA) standards were prepared, and each standard was mixed with hydrochloric acid (HCl, 0.25 M) in a 1:1 ratio. The spectral scans of the samples were then taken in the UV region of 200 to 400 nm, in 5 nm increments. These results showed that the organic acids absorbed maximally between 205 and 225 nm. Different concentrations of the organic acids were then prepared, mixed with HCl in a ratio of 1:1 and the absorbances were read at 210 nm. The absorbance increased with an increase in the concentration of the organic acids (Appendix C, Table C. 1).

After the prebiotic study, a liquid-liquid extraction was performed to extract SCFAs from the culture broths using diethyl-ether. The method used was adapted from De Baere et al. (2013) with minor modifications. The samples (2 mL) were mixed with 0.2 mL of HCl (0.25 M) and vortexed for 15 seconds. Diethyl-ether (5 mL) was added to extract the acids from the media, via gentle shaking in a shaking incubator (10^{o}C) for 20 minutes, followed by centrifugation for 5 minutes at 1372 x g. The supernatant was added to a new tube and 1 mL of NaOH (0.4 M) was added. Diethyl-ether was added again, samples were gently shaken, and centrifuged as before. The aqueous phase and HCl (0.25 M) were mixed in a 96-well UV plate, in a ratio of 1:1. The absorbance was read at 210 nm.

5.3.4. Biofilm formation

The ability of MOS to influence biofilm formation was monitored using sterile 96-well flat-bottom microtiter plates. Briefly, the plates were prepared for each strain with four replicates of M9 minimal media (3.4% (w/v) Na_2HPO_4); 1.5% (w/v) KH_2PO_4; 0.5% (w/v) NH_4Cl; 0.25% (w/v) NaCl), adjusted to pH 7.4 and supplemented with different 0.2% (w/v) sugars (buffer only, mannose, SCG-MOS) (final OD_{600nm} read of 0.5). A plate for each strain was covered and incubated without shaking at 37°C for 24 h. After the incubation period, the wells in each plate were washed three times with phosphate-buffered saline (PBS) solution to remove unbound cells. The cells attached to the wall of each well were stained for 20 min with 250 µL of 0.1% (w/v) crystal violet in water and washed again three times with the PBS solution to remove unbound crystal violet. Bound cells were quantified by adding 250 µL of acetone/ethanol (20:80 (v/v)), followed by measuring the OD_{540nm} with a microplate reader (Bio-Tek Instruments). For comparison of biofilm formation among strains in each medium, the total growth was monitored first by measuring the OD_{600nm} in each well, and then normalizing the biofilm growth with its total cell growth values. This method was adapted from Balakrishna (2013).

5.3.5. Auto-aggregation of bacteria

The influence of MOS on the auto-aggregation of bacteria was studied as described by Balakrishna (2013). Bacterial cells were harvested by centrifugation at 16 060 *g* for 5 minutes (Biofuge Pico Heraeus desktop centrifuge (Hanau, Germany)) and the pellet was resuspended in 1× M9 minimal media (3.4% (w/v) Na_2HPO_4); 1.5% (w/v) KH_2PO_4; 0.5% (w/v) NH_4Cl and 0.25% (w/v) NaCl) adjusted to pH 7.4. The absorbance of the bacteria was adjusted to an OD_{600nm} reading of 0.5 ± 0.05 in test tubes using 0.4% (w/v) mannose and 0.2% (w/w) MOS derived from SCG hydrolysis, and the total volume of the reaction was 3 mL. Then, the bacterial suspensions were incubated at room temperature, the absorbance readings were measured at t = 0 and t = 1 h. Auto-aggregation percentage was expressed as:

Where A_t represents the absorbance at time t = 1 h and A_0 is the absorbance at t = 0.

5.3.6. Activation of mannan-utilisation genes

After the prebiotic study in section 5.3.2., the activation of mannan-utilisation genes was determined, where the cells were centrifuged at 16 060 *g* using a Biofuge Pico Heraeus desktop centrifuge (Hanau, Germany) and the supernatant was used for endo-1,4-β-mannanase and galactosidase activity. For endo-1,4-β-mannanase activity, 200 µL of the supernatant was mixed with 200 µL of locust bean gum (1%, w/v). The samples were then incubated at 50^{o}C for 60 minutes, and the reducing sugars were quantified using the DNS method as described before (Section 3.3.1). For galactosidase activity, 100 µL of the supernatant was added to the prepared 2.25 mM *p*-nitrophenyl-α-D-galactopyranoside (*p*NPG) (400 µL) (Sigma-Aldrich, St. Louis, USA), and incubated at 50^{o}C for 60 minutes, and the reaction was terminated by adding 500 µL of sodium carbonate (2 M). The absorbance was read at 405 nm. For mannosidase, after centrifugation, the rest of the supernatant was removed and the pellet was resuspended in 50 mM phosphate buffer (pH 7.0) (20 mL buffer /g of pellet) in order to lyse the cells. Lysozyme (Sigma-Aldrich, St. Louis, USA) was added to a final concentration of 1 mg/ml. The samples were incubated at room temperature for 2 hours. After incubation, the samples were stored overnight at -80^{o}C. The samples were then thawed and centrifuged again at 16 060 *g* (Biofuge Pico Heraeus desktop centrifuge (Hanau, Germany)). The supernatant (100 µL) was added to the 2.25 mM *p*-nitrophenyl-β-D-mannopyranoside (*p*NPM) (400 µL) (Sigma-Aldrich, St. Louis, USA) in Eppendorf tubes. The samples were then incubated at 50^{o}C for 60 minutes, and the reaction was terminated by adding 500 µL of sodium carbonate (2 M), after which the absorbance was read at 405 nm.

5.4. Results and discussion

5.4.1. Antioxidant activity

The enzymatic hydrolysis of SCG mannan using Man26A resulted in M2 and M3 as predominant sugars. The MOS obtained from SCG mannan hydrolysis were tested for antioxidant activity using the ABTS radical scavenging method. The decrease in colour change (blue-green to colourless) was measured at 734 nm. SCG-derived MOS exhibited 24.54±1.16% relative scavenging activity. Gallic acid (0.02 mg/mL) was used a positive control and resulted in 61.12±1.18% scavenging relative activity. There are no papers on the effect of SCG-derived MOS as antioxidants on literature. However, Amna et al. (2018) reported that MOS derived from galactomannan, using extracellular carbohydrase derived from *Bacillus* N3, displayed antioxidant activity. SCG also has a branched type of mannan, galactomannan (Redgwell & Fischer, 2006; Nguyen et al., 2019) which, upon *Bacillus* derived endo-1,4-β-mannanase addition, resulted in the production of M2 and M3 as the predominant MOS. These results suggest that SCG-derived MOS obtained from enzymatic hydrolysis transfer a hydrogen atom to stabilise the ABTS radical. The ABTS radical scavenging method involves hydrogen atom transfer (Badhani et al., 2015). ABTS generated using a strong oxidising agent, potassium persulfate, receives hydrogen from antioxidants which causes the colour of the solution to change from blue-green to colourless (Badhani et al., 2015).

5.4.2. Prebiotic activity

The MOS obtained from the hydrolysis of SCG were tested for their effect on the growth of beneficial bacteria (Figure 5.1). MOS (2 mg/mL) were incubated with three different beneficial bacteria: *Streptococcus thermophilus, Bacillus subtilis* and *Lactobacillus bulgaricus*. The absorbance of the cells prior to incubation was 0.1 (A_{600nm}). After incubation, the cells were quantified by measuring the optical density at 600 nm and the metabolic activity of live cells was quantified using iodonitrotetrazolium chloride (wavelength, A_{490} nm).

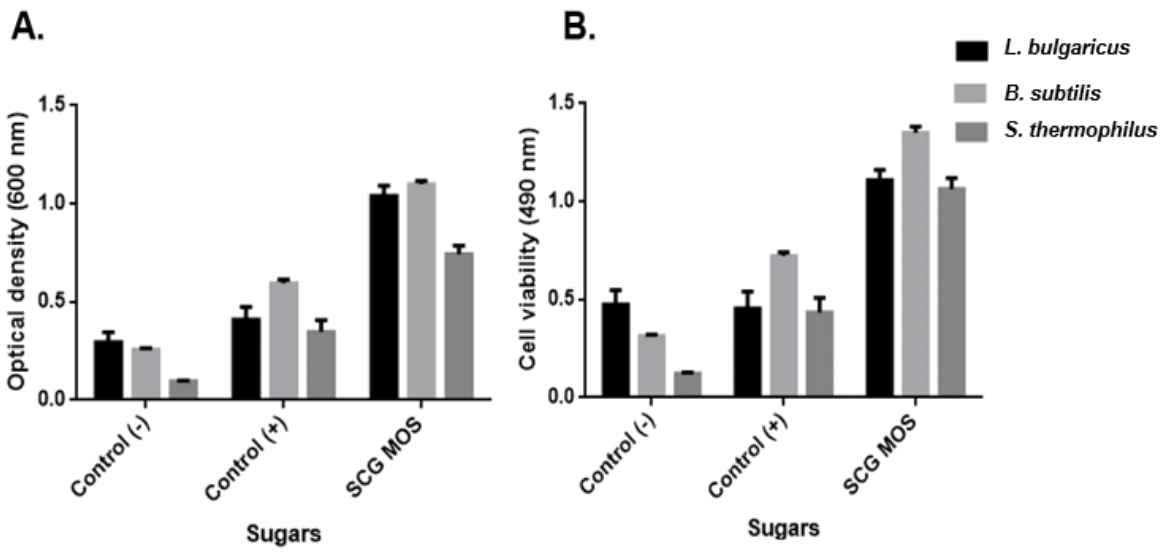

Figure 5.1: Effect of MOS on beneficial bacteria. (A) Absorbance (600 nm) of beneficial bacteria in the presence and absence of sugars. (B) Viability (absorbance at 490 nm) of beneficial bacteria after incubation with the sugars. Control (-): sugar-free, control (+): glucose present and SCG MOS: MOS obtained from SCG. Values are represented as means ± standard deviations, n = 3.

The growth and viability of the cells were measured after 7 hours of incubation with MOS. The use of a tetrazolium salt, INT, to quantify live cells is a simple and cost-effective method. The INT assay involves the conversion of the tetrazolium salt from light yellow into a red formazan dye by metabolically active bacteria (García-Martín et al., 2019). INT is an electron acceptor that changes its colour when it captures two electrons (García-Martín et al., 2019). The electrons captured by INT are from ubiquinone, coenzyme NADH and the cytochrome of bacteria (García-Martín et al., 2019). After INT has captured electrons, it forms a red colour which is quantified. As shown in Figure 5.1, the MOS promoted the growth of *L. bulgaricus, S. thermophilus* and *B. subtilis*. The viability of these beneficial bacteria after incubation with MOS correlates with the optical density, which means the cells do not die after MOS consumption. Cao et al. (2019) and Srivastava et al. (2017) demonstrated similar findings when testing the effect of commercial MOS on *L. plantarum* and low DP MOS (M2 & M3) on seven *Lactobacillus spp*. Pan et al.

(2009b) also reported that MOS enhance the growth of *Lactobacilli* and *Bifidobacteria*, while inhibiting *Enterococcus* and *Enterobacteriaceae*.

Multiple studies (Baurhoo et al., 2007; Chacher et al., 2017; De Baere et al., 2013) have reported that MOS inhibit the proliferation of pathogenic bacteria in the digestive tracts of mammals in many ways, which include the production of SCFA by beneficial bacteria, which contributes to the decrease in pH and inhibition of pathogens from attaching to the intestinal walls. Table 5.1 below (section 5.4.3) illustrates whether the utilisation of MOS by beneficial bacteria resulted in SCFA or not.

5.4.3. Detection of SCFAs produced as a result of MOS fermentation

Liquid-liquid extraction and SCFA detection was performed to determine whether the bacterial cells produce SCFA after MOS utilisation. After the prebiotic study, diethyl-ether was used to extract SCFA from the culture broths. The amount of the carbonyl groups in Table 5.1 below was determined using the butyric acid standard curve in Appendix C, Figure C.1.

Table 5.1: Amount of carbonyl group detected after MOS utilisation by beneficial bacterial. Values are represented as means ± standard deviations, n = 3.

	carbonyl group (mM)		
	B. subtilis	***S. thermophilus***	***L. bulgaricus***
control (+)	0.115±0.00	0.058±0.00	0.081±0.00
control (-)	*ND*	*ND*	0.041 ±0.00
SCG MOS	0.417±0.00	0.344±0.00	0.458±0.00

SCG-spent coffee grounds

The detection of the carbonyl group after MOS utilisation by benefical bacteria means that there are acids produced, which are most likely SCFA. All the bacterial strains, except *L. bulgaricus*,

failed to produce any SCFA in the negative control, which was expected, because these bacteria need to ferment sugars in order to produce SCFA. *L. bulgaricus* produced SCFA even in the absence of sugars, and this is because this is a lactic acid-producing bacterium (Chacher et al., 2017; Pan et al., 2009b). Audisio et al. (2000) and Chacher et al. (2017) reported that *Lactobacillus spp*. and *Bifidobacterium* could utilise glucose and produce lactic acid (LA) and acetic acid (AA) in birds. Production of LA and AA results in a reduction in pH, preventing pathogens from attaching to the host's intestinal walls Chacher et al., 2017).

All bacterial cells produced SCFAs in the presence of SCG-derived MOS, and this was unexpected. SCFAs, such as butyric acid, have been reported to inhibit the activity of pathogens like *Salmonella* and *Clostridium perfringens* in mammals (De Baere et al., 2013). Wu et al. (2020) reported that supplementation of mice drinking water with acetate, butyrate and proprionate reduces their susceptibility to *Klebsiella pneumoniae* infections. Ciarlo et al. (2016) reported that propionate has no effect at all on *K. pneumoniae, Staphylococcus aureus* and *Candida albicans,* but does have the ability to enhance the growth of *Bifidobacterium*. SCFA production by beneficial bacteria was expected, and our results are also in agreement with the findings of Pan et al. (2009a), who reported that MOS intake by *Bifidobacteria* and *Lactobacilli* improves the amount of SCFAs (butyrate, propionate, acetate) and lactate produced. Butyrate, propionate and acetate are the predominant SCFAs produced from bacterial fermentation (Pan et al., 2009a; Wu et al., 2020). Further studies are required to determine which type of SCFAs were produced by which bacteria and to quantify each SCFA because these benefical bacteria could be producing different SCFAs, which probably have different functions in the gut.

5.4.4. Biofilm formation and auto-aggregation

The effect of SCG-derived MOS on biofilm formation and auto-aggregation of beneficial bacteria and pathogens was investigated. The beneficial bacteria used in the study were *L. bulgaricus*, *B. subtilis* and *S. thermophiles*. A 96-well flat-bottom microtiter plate was used to assess biofilm formation, where the bound cells were stained with crystal violet. The results in Table 5.2 show biofilm growth normalised with total cell growth (OD_{540}/OD_{600}) and autoaggregation percentage (%) for each bacterium.

Table 5.2: Effect of SCG MOS on biofilm formation and autoaggregation of beneficial bacteria. Values are represented as means ± standard deviations, n = 3.

	Biofilm formation (OD_{540}/OD_{600})		
	L. bulgaricus.	*B. subtilis*	*S. thermophilus*
Control (-)	0.79±0.01	0.63±0.03	0.62±0.02
Control (+)	0.94±0.40	0.55±0.06	0.66±0.01
SCG MOS	2.19±0.44	1.28±0.14	1.19±0.11
	Autoaggregation (%)		
	L. bulgaricus	*B. subtilis*	*S. thermophilus*
Control (-)	1.63±0.13	1.79±0.43	4.19±0.34
Control (+)	3.06±0.19	2.72±0.23	4.70±0.24
SCG MOS	18.21±1.35	20.98±2.21	17.99±2.73

SCG-spent coffee ground, ND-not detected

SCG MOS enhanced the biofilm formation of *L. bulgaricus, B. subtilis* and *S. thermophilus*. In terms of autoaggregation, *L. bulgaricus, B. subtilis* and *S. thermophilus* grown in SCG derived MOS, showed aggregation percentages of 18.21, 20.98 and 17.99%, respectively, and performed better than percentages recorded on cultures grown in the absence of a carbon source. Cao et al. (2019) reported that MOS enhanced the autoaggregation of *Lactobacillus plantarum* with a rate of autoaggregation of 23.76%, which is slightly higher than that of *L. bulgaricus, B. subtilis and S. thermophilus* reported in this current study. The variations in the rate of autoaggregation could be due to the use of different beneficial bacterial species and the DP of commercial MOS used by Cao et al. (2019) could also be different from the MOS used in our study.

5.4.5. Regulation of mannan utilisation genes in probiotics by MOS

Upregulation of mannan utilisation genes in bacteria after utilisation of SCG MOS was investigated. Table 5.3 beow shows the activities of endo-1,4-β-mannanase, mannosidase and galactosidase.

Table 5.3: The activity of mannan-degrading enzymes produced by beneficial bacteria in the absence and presence of MOS as a carbon source. Values are represented as means ± standard deviations, n = 3.

	Mannanase (U/ml)			**Mannosidase (U/ml)**			**Galactosidase (U/ml)**		
	B. subtilis	*L. bulgaricus*	*S. thermophilus*	*B. subtilis*	*L. bulgaricus*	*S.thermophilus*	*B. subtilis*	*L. bulgaricus*	*S.thermophilus*
Control (-)	0.014±0.0	0.018±0.02	0.020±0.00	*ND*	*ND*	*ND*	0.0027±0.0	*ND*	*ND*
Control (+)	0.016±0.0	0.019±0.0	0.018±0.0	*ND*	*ND*	*ND*	0.0041±0.0	0.0005±0.0	0.0006±0.0
SCG MOS	0.056±0.02	0.049±0.0	0.059±0.01	0.0047±0.01	0.0017±0.0	0.0022±0.00	0.031±0.0	0.026±0.0	0.029±0.0

ND- not detected; SCG MOS- spent coffee ground mannooligosaccharides; control (+)-glucose; control (-)-sugar free

According the results in the table above, MOS utilisation possibly upregulated the expression of mannan utilisation genes by *B. subtilis, L. bulgaricus* and *S. thermophilus*, such as the mannan-degrading CAZymes: endo-1,4-β-mannanase, galactosidase and mannosidase. Song et al. (2018) reported that MOS with a certain degree of polymerisation, for example, M4 and M5, bind to a regulator, which releases its operator sequence resulting in the transcription of the mannan-utilisation gene cluster. This then results in the expression of mannan utilisation enzymes and transporters, causing bacterial cells to utilise mannans efficiently (Song et al., 2018).

The results in Table 5.3 show that some of the MOS produced from the enzymatic hydrolysis of SCG must have bound to the manR regulator in *B. subtilis*, leading to the production of endo-1,4-β-mannanase, galactosidase and mannosidase. ManR is a transcription regulator that represses the mannan utilisation gene cluster (Song et al., 2018). Transportation of MOS during mannan utilisation in bacteria is important. The encoding gene, *ManH*, encodes an extracellular substrate binding domain, that binds MOS and presents them to the transmembrane channel composed of two subunits encoded by *manI* and *manJ* (Song et al., 2018). *ManH*, *manI* and *manJ* genes encode the components of the MOS ABC transporter (Song et al., 2018). In *L. bulgaricus* and *S. thermophiles,* SCG MOS must have also interacted with transcription regulators found in these bacteria, resulting in the production of mannan-utilization enzymes: endo-1,4-β-mannanase, galactosidase and mannosidase

5.5. Conclusion

This study showed that MOS enzymatically produced from NAOH-pretreated SCG exhibited antioxidant activity and had the ability to enhance the growth of beneficial bacteria (*L. bulgaricus, B. subtilis* and *S. thermophilus*), which, in turn, produced SCFAs. These MOS can also cause beneficial bacteria to form microcolonies and adhere to surfaces, protecting them from environmental stress. Mannan-utilisation genes in beneficial bacteria were upregulated after SCG MOS utilisation.

CHAPTER 6: General discussion and future recommendations

6.1 General discussion

SCG has the potential to be utilised for the production of VAPs. SCG is an agro-industrial waste generated during the production of one of the world's most popular beverages, coffee Jooste et al., 2013; McNutt & He, 2019, Sachslehner et al., 2000). This agro-industrial waste (SCG) is mostly composed of galactomannan, arabinogalactan and cellulose as the three main polysaccharides that make up approximately 50% of the polysaccharides in SCG (Nguyen et al., 2019; Redgwell & Fischer, 2006). There are many other substrates containing different types of mannan, e.g. ivory nut, which contains linear mannan known for structural functions, locust bean gum and guar gum which contains galactomannan and are used as gelling agents (Van Zyl et al., 2010). LBG is cheap and easily accessible (Van Zyl et al., 2010). In this study, INM, LBG and GG were used as substrates to biochemically characterise an endo-1,4-β-mannanase, Man26A, derived from *Bacillus sp*., as they contain different types of mannan and are readily available.

Man26A was biochemically characterised and the results were discussed in Chapter 3. For the yield and specific activity, model mannan substrates (4% w/v) were hydrolysed using 0.01 mg/ml Man26A for 24 hours (yield) and 15 minutes (specific activity). The MOS profiles of the hydrolysates were analysed on TLC and HPLC. The highest reducing sugar yield and specific activity was obtained with partially substituted mannan, LBG, with values of 36.86% and 453.52 µmol/min/mg, respectively. Man26 demonstrated a high binding affinity for LBG, with a K_m value approximately 3-fold lower than that of INM and 5-fold lower than that of GG. The V_{max} and k_{cat}/K_m values of Man26A were the highest with LBG, followed by INM. The difference in the enzymatic parameters and the sugar yield of Man26A on each of these three different substrates is due to the difference in the structure (i.e. substitution) of the substrates. Based on the results obtained, Man26A appears to prefer LBG as a substrate, followed by INM and finally, GG. LBG and GG are both galactomannans, but LBG is partially substituted, while GG has abundant galactose substituents attached to mannan. INM is a linear mannan. Man26A is highly tolerant to galactose substituents of partially substituted mannan (LBG). These results agree with

the findings of Kurakake et al. (2006) and Yoon et al. (2008), which found that the activity of the mannanase is limited by the number of galactose substituents attached to the mannan backbone. The hydrolysis of galactose substituents from substrates containing a high number of galactose substituents using galactosidase can increase the efficiency of Man26A (Malgas et al., 2015b).

The hydrolysis of these substrates (INM, LBG and GG) resulted in the production of MOS, which were analysed by TLC as well as with HPLC. As shown on TLC and confirmed by HPLC, hydrolysis of INM by Man26A resulted in M2 and M3 as predominant sugars, while LBG hydrolysis resulted in M5 and M6 as the predominant sugars, and the enzymatic hydrolysis of GG resulted in M6 as a predominant sugar. Galactosyl-MOS were also observed in the HPLC chromatograms of the LBG and GG hydrolysates. Most of the oligosaccharides were larger than DP6 and could not resolve on the TLC plate. Galactose substitution in the mannan backbone of these substrates affects the production of MOS and the DP of the MOS produced.

The MOS obtained from model mannan substrates (INM, LBG and GG) were highly stable at pH 2 to 10 and at temperatures between 25 and 100°C. The pH of the digestive tract differs depending on the various sections within the digestive tract. The pH of the stomach is highly acid (~pH 2), the ileum has a pH of 7.5, the jejunum has a pH of 6.6, the caecum has a pH of 6.4 and the colons have a pH range of 6.4 - 7.0 (Evans et al., 1988). Asano et al. (2003) reported that MOS (M1-M6) could not be hydrolysed by human α-amylase, simulated gastric juice, pancreatic enzymes or rat intestinal enzymes. This means that MOS are be able to pass through the digestive tract and are stable up to 100°C without losing their function. The relative scavenging activity of MOS from different model mannan substrates (INM, LBG and GG) was determined, where ABTS was used as a radical. INM derived MOS displayed the most relative scavenging activity, followed by LBG derived MOS. GG derived MOS showed very low relative scavenging activity. This study showed that the antioxidant activity was affected by the DP of the oligosaccharides, with oligosaccharides of low DP having more antioxidant activity than oligosaccharides with a high DP. The antioxidant activity also decreased as the number of galactose residues attached to the mannan backbone increased.

Man26A was then employed for the production of MOS from SCG. Before SCG enzymatic hydrolysis, SCG was pretreated using NaOH. SCG is an agro-industrial waste generated during the production process of coffee and is mainly composed of polysaccharides that can be

enzymatically hydrolysed using lignocellulolytic enzymes to produce fermentable sugars (Mussatto et al., 2011; Redgwell & Fischer, 2006; Sachslehner et al., 2000). Pretreated SCG was darker in colour (as expected), because pretreatment of SCG causes structural changes in the structures of the components of SCG, resulting in dark coloured compounds called melanoidins (Moreira et al., 2015). The FT-IR spectra of untreated and pretreated SCG samples were compared. The findings showed the presence of peaks (at 812 and 817 cm^{-1}) that were attributed to α-linked D-galactopyranose units and β-linked D-mannopyranose units in both samples, which indicated that galactomannan was not lost during the pretreatment of SCG. The intensity of a peak (1080 cm^{-1}), which was attributed to the glycosidic bond (-C-O-H), was more pronounced in pretreated SCG. These findings suggested that hemicellulose was retained and more exposed in pretreated SCG.

Pretreatment of SCG using NaOH was successful, as this improved the reducing sugar production 19.5-fold, compared to untreated SCG. NaOH pretreatment resulted in the removal of insoluble solids, and altered the structure of SCG, creating pores and swelling. This allowed Man26A to access SCG galactomannan easily. These results are in good agreement with Wongsiridetchai et al. (2018), who reported that the addition of the pretreatment step before SCG hydrolysis decreased its recalcitrance and increased the efficiency of the mannanases. The pretreatment of agricultural biomass also decreased cellulose crystallinity, caused swelling, formed pores on the surface and decreased the degree of polymerisation (Mosier et al., 2005). After successful SCG pretreatment, SCG (10% w/v) was hydrolysed using Man26A (2 mg protein/g SCG) which resulted in the production of 0.9063 mg/mL reducing sugars.

Hydrolysates resulting from SCG hydrolysis (using Man26A) were qualitatively and quantitatively analysed on TLC and HPLC. M2 and M3 were the predominant sugars in TLC and HPLC. The HPLC chromatogram of SCG also revealed galactosyl-MOS (Appendix D, Figure D.2). The production of M2 and M3 as the predominant sugars agreed with the results obtained by Chauhan et al. (2014), Wongsiridetchai et al. (2018) and Wongsiridetchai et al. (2021) from coffee extract and SCG. Chauhan et al. (2014) and Wongsiridetchai et al. (2018 & 2021) employed *Bacillus nealsonii PN-11* and *Bacillus sp*. GA2 (1) mannanases, respectively, for their mannan hydrolysis. MOS are short oligosaccharides that have gained attention due to their potential to act as prebiotics in mammals (Saeed et al., 2017; Chacher et al., 2017). It is

important that SCG MOS proceed through the digestive tract without losing their activity in order to act as prebiotics in the guts of mammals. The ability of SCG MOS to tolerate gastrointestinal tract conditions was investigated. Bile salts, α-amylase, trypsin and hydrochloric acid could not hydrolyse SCG MOS, showing that SCG MOS could tolerate these biological barriers.

MOS obtained from SCG were investigated for their biological properties: antioxidant activity, prebiotic effect, autoaggregation and biofilm formation. The MOS obtained from SCG interacted with ABTS radicals, illustrating that they have an antioxidant activity. Since SCG MOS have antioxidant activity, they will be able to prevent the oxidation of lipids in the stomachs of humans. Human gastric juice increases the oxidation of lipids in the stomach, resulting in cell damage (Van den Ende et al., 2011). Winter et al. (2010) reported that during an inflammatory response, GI ROS enhanced the growth of *Salmonella. Salmonella* has been reported to use ROS for tetrathionate generation, which further allows pathogens to produce more ATP than beneficial bacteria and outcompeting them (Van den Ende et al., 2011; Winter et al., 2010). The presence of MOS in the stomachs of humans should prevent pathogens such as *Salmonella* from producing things like tetrathionate, hindering their growth. SCG derived MOS (M2 and M3) also enhanced the growth of beneficial bacteria: *Streptococcus thermophilus*, *Bacillus subtilis* and *Lactobacillus bulgaricus*. These results agree with the results obtained by Srivastava et al. (2017) who reported that M2 and M3 produced from LBG, using a GH26 mannanase, improved the growth of seven different *Lactobacillus* spp. *in vitro*. MOS obtained from thermally hydrolysed SCG also improved the growth of *Bifidobacterium*, a probiotic in humans (Asano et al., 2003). The production of MOS from SCG will also benefit the environment because most SCG is disposed in landfills, where it produces toxins and methane, which leads to pollution problems (Mussatto et al., 2011). MOS production is a better strategy to manage this agro-industrial waste.

After utilising MOS, beneficial bacteria were expected to produce SCFAs. SCFAs are well-known for decreasing the pH in the digestive tract, resulting in the competitive exclusion of pathogens as well as triggering a host immune response (Wu et al., 2020). After the prebiotic study, SCFAs were extracted using ethyl-ether and detected spectrophotometrically. Utilisation of SCG MOS resulted in the production of SCFAs by these beneficial bacteria, where *L. bulgaricus* and *B. subtilis* produced more SCFAs than *S. thermophilus*. SCFAs, especially

butyric acid, result in the production of mucin and creation of a sticky layer that protects the intestinal epithelium from the attachment of pathogens, which would then result in these pathogens being easily removed from the GI tract (Markowiak-Kopeć & Śliżewska, 2020). The presence of SCFAs in the gut leads to the decrease of free fatty acids, reducing the risks of getting type-2 diabetes (Van den Ende et al., 2011). Diabetes mellitus is one of the top ten leading causes of death globally (Pheiffer et al., 2021). In Africa, 15.5 million people had diabetes in 2017, while 69.2% were unaware of their statuses. The major contributor to type-2 diabetes is obesity (Pheiffer et al., 2021). The ability of *L. bulgaricus*, *B. subtilis* and *S. thermophilus* to produce SCFAs after MOS utilisation will increase insulin sensitivity by reducing free fatty acids and ghrelin (the hunger hormone), reducing risks of getting type-2 diabetes (Tarini & Wolever, 2010; Van den Ende et al., 2011).

The ability of bacterial cells to autoaggregate and form biofilms in the presence of SCG derived MOS was investigated. Autoaggregation is the aggregating together of cells of the same species, which further attach to surfaces, producing biofilms (Galdiero et al., 1988; Trunk et al., 2018). SCG-derived MOS enhanced the ability of *S. thermophilus*, *B. subtilis* and *L. bulgaricus* to form microcolonies. These three probiotic bacteria could also form biofilms in the presence of MOS. It has been reported that the ability of beneficial bacteria to attach to surfaces, i.e. epithelial cells, provides them with a chance to block pathogens from also attaching to these surfaces (Balakrishna et al., 2013). There is no literature available on the effect of SCG-derived MOS on autoaggregation and biofilm formation of bacteria. However, Cao et al. (2019) reported that commercial MOS enhanced autoaggregation of *L. plantarum* ATCC14917. MOS also had a positive effect on biofilm formation of *L. plantarum* ATCC14917 on mucin (24.65%) and Caco-2 cells (14.71%) (Cao et al., 2019).

In conclusion, *Bacillus sp*. derived endo-1,4-β-mannanase, Man26A, was shown to be more catalytically active on partially substituted mannan, compared to linear and highly substituted mannan. Enzymatic hydrolysis of NaOH-pretreated SCG by Man26A resulted in the release of more reducing sugars, compared to untreated SCG. Enzymatic hydrolysis of SCG resulted in mannobiose and mannotriose as the predominant MOS. SCG MOS could not be hydrolysed by bile salts, α-amylase, trypsin and hydrochloric acid, and were stable against temperature change. MOS derived from SCG hydrolysis displayed antioxidant activity, a prebiotic effect and the

fermentation of these MOS by beneficial bacteria resulted in the production of SCFAs, which also activated mannan utilisation genes in bacteria. SCG-derived MOS also enhanced the rate of autoaggregation and the attachment of beneficial bacteria (*L. bulgaricus*, *B. subtilis* and *S. thermophilus)* to surfaces.

The ability of enzymatically producing MOS from SCG should decrease the disposal of SCG in landfills, decrease global warming and improve the health of mammals through MOS consumption. SCG MOS in the gut will prevent oxidative stress through ROS scavenging and SCFA mechanisms, potentially contributing to the treatment of some diseases.

6.2. Future recommendations

In this study, Man26A was used to produce MOS from NaOH-pretreated SCG. The MOS were characterised for their biological properties. Some future recommendations for addressing challenges that arose during this study are suggested below:

- This research project demonstrated that utilisation of MOS by beneficial bacteria resulted in the production of SCFAs. We recommend that the SCFAs produced by beneficial bacteria are separated and quantified, and that each SCFA is tested for its effect on gut pathogenic bacteria.
- The prebiotic properties of SCG-derived MOS could be investigated using a "gut-on-a-chip" approach. This would mimic the gut more closely structural, absorption, pathophysiological and microbes), or the studies could be performed *in vivo* (i.e. in chickens or human volunteers instead of *in vitro)*, as there may be many other factors that may play a role in the inhibition of pathogenic bacteria and promotion of beneficial bacteria in the gastrointestinal tract of mammals.

6.3. Reference List

Abboo, S., 2016. Development of an enzyme-synergy based bioreactor system for the beneficiation of apple pomace lignocellulosic waste. Doctor of Philosophy Thesis, Rhodes University, Grahamstown, pp.33-35

de mark, P., Larsson, M., Tjerneld, F. and Stålbrand, H., 2001. Multiple α-galactosidases from *Aspergillus niger*: purification, characterization and substrate specificities. *Enzyme and Microbial Technology*, *29*(6-7), pp.441-448.

Alsarrani, A.Q., 2011. Production of Mannan-degrading enzyme by *Aspergillus niger*. *Journal of Taibah University for Science*, *5*(1), pp.1-6.

Amin, F.R., Khalid, H., Zhang, H., u Rahman, S., Zhang, R., Liu, G. and Chen, C., 2017. Pretreatment methods of lignocellulosic biomass for anaerobic digestion. *AMB Express*, *7*(1), pp.1-12.

Amna, K.S., Park, S.Y., Choi, M., Kim, S.Y., Yoo, A.Y. and Park, J.K., 2018. Antioxidant Activity of Manno-oligosaccharides Derived from the Hydrolysis of Polymannan by Extracellular Carbohydrase of *Bacillus N3*. *Journal of the Korean Society of Marine Biotechnology*, *10*(1), pp.9-17

Anon. 2011. Technical bulletin: Bradford Reagent (B6916). Sigma-Aldrich.

Armbruster, D.A. and Pry, T., 2008. Limit of blank, limit of detection and limit of quantitation. *The Clinical Biochemist Reviews*, *29*(Suppl 1), pp.45-49.

Asadpoor, M., Peeters, C., Henricks, P.A., Varasteh, S., Pieters, R.J., Folkerts, G. and Braber, S., 2020. Anti-Pathogenic Functions of Non-Digestible Oligosaccharides *In Vitro*. *Nutrients*, *12*(6), p.1789.

Asano, I., Hamaguchi, K., Fujii, S. and IINO, H., 2003. *In vitro* digestibility and fermentation of mannooligosaccharides from coffee mannan. *Food Science and Technology Research*, *9*(1), pp.62-66.

Asano, I., Umemura, M., Fujii, S., Hoshino, H. and Iino, H., 2004. Effects of mannooligosaccharides from coffee mannan on fecal microflora and defecation in healthy volunteers. *Food Science and Technology Research*, *10*(1), pp.93-97.

Atabani, A.E., Mercimek, S.M., Arvindnarayan, S., Shobana, S., Kumar, G., Cadir, M. and Al-Muhatseb, A.A.H., 2018. Valorization of spent coffee grounds recycling as a potential alternative fuel resource in Turkey: An experimental study. *Journal of the Air & Waste Management Association*, *68*(3), pp.196-214.

Audisio, M.C., Oliver, G. and Apella, M.C., 2000. Protective effect of *Enterococcus faecium* J96, a potential probiotic strain, on chicks infected with *Salmonella pullorum*. *Journal of Food Protection*, *63*(10), pp.1333-1337.

Bååth, J.A., Martínez-Abad, A., Berglund, J., Larsbrink, J., Vilaplana, F. and Olsson, L., 2018. Mannanase hydrolysis of spruce galactoglucomannan focusing on the influence of acetylation on enzymatic mannan degradation. *Biotechnology for Biofuels*, *11*(1), pp.1-15.

Badhani, B., Sharma, N. and Kakkar, R., 2015. Gallic acid: a versatile antioxidant with promising therapeutic and industrial applications. *RSC Advances*, *5*(35), pp.27540-27557.

Bai, W., Fang, X., Zhao, W., Huang, S., Zhang, H. and Qian, M., 2015. Determination of oligosaccharides and monosaccharides in Hakka rice wine by precolumn derivation high-performance liquid chromatography. *Journal of Food and Drug Analysis*, *23*(4), pp.645-651.

Bågenholm, V., Reddy, S.K., Bouraoui, H., Morrill, J., Kulcinskaja, E., Bahr, C.M., Aurelius, O., Rogers, T., Xiao, Y., Logan, D.T. Martens, E.C., Koroparkin, N. M. and Stålbrand, H., 2017. Galactomannan catabolism conferred by a polysaccharide utilization locus of *Bacteroides ovatus*: enzyme synergy and crystal structure of a β-mannanase. *Journal of Biological Chemistry*, 292(1), pp.229-243.

Bågenholm, V., Wiemann, M., Reddy, S.K., Bhattacharya, A., Rosengren, A., Logan, D.T. and Stålbrand, H., 2019. A surface-exposed GH26 β-mannanase from *Bacteroides ovatus*: Structure, role, and phylogenetic analysis of *Bo*Man26B. *Journal of Biological Chemistry*, *294*(23), pp.9100-9117.

Balakrishna, A., 2013. *In vitro* evaluation of adhesion and aggregation abilities of four potential probiotic strains isolated from guppy (*Poecilia reticulata*). *Brazilian Archives of Biology and Technology*, 56(5), pp.793-800.

Ballesteros, L.F., Teixeira, J.A. and Mussatto, S.I., 2014. Chemical, functional, and structural properties of spent coffee grounds and coffee silverskin. *Food and Bioprocess Technology*, 7(12), pp.3493-3503.

Baurhoo, B., Letellier, A., Zhao, X. and Ruiz-Feria, C.A., 2007. Cecal populations of *lactobacilli* and *bifidobacteria* and *Escherichia coli* populations after *in vivo Escherichia coli* challenge in birds fed diets with purified lignin or mannanoligosaccharides. *Poultry Science*, *86*(12), pp.2509-2516.

Becker, C., Sharma, L.N. and Chambliss, C.K., 2010. Analytical monitoring of pretreatment and hydrolysis process in lignocellulose-to-bioalcohol production. *Bioalcohol Production*, pp. 281-314. Woodhead Publishing

Birben, E., Sahiner, U.M., Sackesen, C., Erzurum, S. and Kalayci, O., 2012. Oxidative stress and antioxidant defense. *World Allergy Organization Journal*, *5*(1), pp.9-19.

Bird, I.M., 1989. High performance liquid chromatography: principles and clinical applications. *BMJ: British Medical Journal*, *299*(6702), pp.783.

Bland, E.J., Keshavarz, T. and Bucke, C., 2004. The influence of small oligosaccharides on the immune system. *Carbohydrate Research*, *339*(10), pp.1673-1678.

Bradford, M.M., 1976. A rapid and sensitive method for the quantitation of microgram quantities of protein utilizing the principle of protein-dye binding. *Analytical biochemistry*, *72*(1-2), pp.248-254.

Cao, P., Wu, L., Wu, Z., Pan, D., Zeng, X., Guo, Y. and Lian, L., 2019. Effects of oligosaccharides on the fermentation properties of *Lactobacillus plantarum*. *Journal of Dairy Science*, *102*(4), pp.2863-2872.

Carrier, M., Loppinet-Serani, A., Denux, D., Lasnier, J.M., Ham-Pichavant, F., Cansell, F. and Aymonier, C., 2011. Thermogravimetric analysis as a new method to determine the lignocellulosic composition of biomass. *Biomass and Bioenergy*, *35*(1), pp.298-307.

Castanon, J.I.R., 2007. History of the use of antibiotics as growth promoters in European poultry feeds. *Poultry Science*, *86*(11), pp.2466-2471.

Chacher, M.F.A., Kamran, Z., Ahsan, U., Ahmad, S., Koutoulis, K.C., Din, H.Q.U. and Cengiz, Ö., 2017. Use of mannan oligosaccharide in broiler diets: an overview of underlying mechanisms. *World's Poultry Science Journal*, *73*(4), pp.831-844.

Chauhan, P.S., Puri, N., Sharma, P. and Gupta, N., 2012. Mannanases: microbial sources, production, properties and potential biotechnological applications. *Applied Microbiology and Biotechnology*, *93*(5), pp.1817-1830.

Chauhan, P.S., Sharma, P., Puri, N. and Gupta, N., 2014. Purification and characterization of an alkali-thermostable β-mannanase from *Bacillus nealsonii* PN-11 and its application in mannooligosaccharides preparation having prebiotic potential. *European Food Research and Technology*, *238*(6), pp.927-936.

Chiyanzu, I., Brienzo, M., García-Aparicio, M.P. and Görgens, J.F., 2014. Application of endo-β-1, 4, D-mannanase and cellulase for the release of mannooligosaccharides from steam-pretreated spent coffee ground. *Applied Biochemistry and Biotechnology*, *172*(7), pp.3538-3557.

Correia, D.M., Dias, L.G., Veloso, A.C., Dias, T., Rocha, I., Rodrigues, L.R. and Peres, A.M., 2014. Dietary sugars analysis: quantification of fructooligossacharides during fermentation by HPLC-RI method. *Frontiers in Nutrition*, *1*, pp.11.

Cosa, S., Rakoma, J.R., Yusuf, A.A. and Tshikalange, T.E., 2020. *Calpurnia aurea* (Aiton) Benth Extracts Reduce Quorum Sensing Controlled Virulence Factors in *Pseudomonas aeruginosa*. *Molecules*, *25*(10), pp.2283.

Couturier, M., Roussel, A., Rosengren, A., Leone, P., Stålbrand, H. and Berrin, J.G., 2013. Structural and biochemical analyses of glycoside hydrolase families 5 and 26 β-(1, 4)-mannanases from *Podospora anserina* reveal differences upon manno-oligosaccharide catalysis. *Journal of Biological Chemistry*, *288*(20), pp.14624-14635.

Cross, R. 2001. The Preparation of Biological Material for Electron Microscopy Part 3: The Preparation of Material for Scanning Electron Microscopy (SEM). Grahamstown: Rhodes University Press, South Africa.

De Baere, S., Eeckhaut, V., Steppe, M., De Maesschalck, C., De Backer, P., Van Immerseel, F. and Croubels, S., 2013. Development of a HPLC–UV method for the quantitative determination

of four short-chain fatty acids and lactic acid produced by intestinal bacteria during *in vitro* fermentation. *Journal of Pharmaceutical and Biomedical Analysis*, *80*, pp.107-115.

Dhawan, S. and Kaur, J., 2007. Microbial mannanases: an overview of production and applications. *Critical Reviews in Biotechnology*, *27*(4), pp.197-216.

Du, L., Shen, Y., Zhang, X., Prinyawiwatkul, W. and Xu, Z., 2014. Antioxidant-rich phytochemicals in miracle berry (*Synsepalum dulcificum*) and antioxidant activity of its extracts. *Food Chemistry*, *153*, pp.279-284.

Evans, D.F., Pye, G., Bramley, R., Clark, A.G., Dyson, T.J. and Hardcastle, J.D., 1988. Measurement of gastrointestinal pH profiles in normal ambulant human subjects. *Gut*, *29*(8), pp.1035-1041.

Folin, O. and Ciocalteu, V., 1927. On tyrosine and tryptophane determinations in proteins. *Journal of Biological Chemistry*, *73*(2), pp.627-650.

Galdiero, F., Carratelli, C.R., Nuzzo, I., Bentivoglio, C. and Galdiero, M., 1988. Phagocytosis of bacterial aggregates by granulocytes. *European Journal of Epidemiology*, *4*(4), pp.456-460.

García-Martín, E.E., Aranguren-Gassis, M., Karl, D.M., Martínez-García, S., Robinson, C., Serret, P. and Teira, E., 2019. Validation of the *in vivo* iodo-nitro-tetrazolium (INT) salt reduction method as a proxy for plankton respiration. *Frontiers in Marine Science*, *6*, pp.220.

Gomes, J., Terler, K., Kratzer, R., Kainz, E. and Steiner, W., 2007. Production of thermostable β-mannosidase by a strain of Thermoascus aurantiacus: Isolation, partial purification and characterization of the enzyme. *Enzyme and Microbial Technology*, *40*(4), pp.969-975.

Haghparast, S., Shabanpour, B., Kashiri, H., Alipour, G. and Sudagar, M., 2013. A comparative study on antioxidative properties of carameled reducing sugars; inhibitory effect on lipid oxidative and sensory improvement of glucose carameled products in shrimp flesh. *Journal of Agricultural Science and Technology*, *15*(1), pp.87-99.

Harnpicharnchai, P., Pinngoen, W., Teanngam, W., Sornlake, W., Sae-Tang, K., Manitchotpisit, P. and Tanapongpipat, S., 2016. Production of high activity *Aspergillus niger* BCC4525 β-mannanase in *Pichia pastoris* and its application for mannooligosaccharides production from biomass hydrolysis. *Bioscience, Biotechnology, and Biochemistry*, *80*(12), pp.22

Hlalukana, N., Magengelele, M., Malgas, S. and Pletschke, B.I., 2021. Enzymatic Conversion of Mannan-Rich Plant Waste Biomass into Prebiotic Mannooligosaccharides. *Foods*, *10*(9), p.2010.

Hu, J., Chen, J., Ye, L., Cai, Z., Sun, J. and Ji, K., 2018. Anti-IgE therapy for IgE-mediated allergic diseases: from neutralizing IgE antibodies to eliminating IgE+ B cells. *Clinical and Translational Allergy*, *8*(1), pp.27.

Jana, U.K. and Kango, N., 2020. Characteristics and bioactive properties of mannooligosaccharides derived from agro-waste mannans. *International Journal of Biological MScromolecules*, *149*, pp.931-940.

Jiang, W., Peng, H., Li, H. and Xu, J., 2014. Effect of acetylation/deacetylation on enzymatic hydrolysis of corn stalk. *Biomass and Bioenergy*, *71*, pp.294-298.

Jiang, Z., Wei, Y., Li, D., Li, L., Chai, P. and Kusakabe, I., 2006. High-level production, purification and characterization of a thermostable β-mannanase from the newly isolated Bacillus subtilis WY34. *Carbohydrate Polymers*, *66*(1), pp.88-96.

Joerger, R.D., 2003. Alternatives to antibiotics: bacteriocins, antimicrobial peptides and bacteriophages. *Poultry Science*, *82*(4), pp.640-647.

Jooste, T., García-Aparicio, M.P., Brienzo, M., Van Zyl, W.H. and Görgens, J.F., 2013. Enzymatic hydrolysis of spent coffee ground. *Applied Biochemistry and Biotechnology*, *169*(8), pp.2248-2262.

Kaira, G.S. and Kapoor, M., 2019. How substrate subsites in GH26 endo-mannanase contribute towards mannan binding. *Biochemical and Biophysical Research Communications*, *510*(3), pp.358-363.

Kaira, G.S., Usharani, D. and Kapoor, M., 2019. Salt bridges are pivotal for the kinetic stability of GH26 endo-mannanase (ManB-1601). *International Journal of Biological Macromolecules*, *133*, pp.1236-1241.

Kulcinskaja, E., Rosengren, A., Ibrahim, R., Kolenová, K. and Stålbrand, H., 2013. Expression and characterization of a *Bifidobacterium adolescentis* beta-mannanase carrying mannan-binding and cell association motifs. *Applied and Environmental Microbiology*, *79*(1), pp.133-140.

Kurakake, M., Sumida, T., Masuda, D., Oonishi, S. and Komaki, T., 2006. Production of galacto-manno-oligosaccharides from guar gum by β-mannanase from *Penicillium oxalicum* SO. *Journal of Agricultural and Food Chemistry*, *54*(20), pp.7885-7889.

Lakka, N.S. and Kuppan, C., 2019. Principles of Chromatography Method Development. *Chromatography-Separation, Identification and Purification Analysis*, pp.1-16. *IntechOpen: London, UK*,

Loow, Y.L., Wu, T.Y., Jahim, J.M., Mohammad, A.W. and Teoh, W.H., 2016. Typical conversion of lignocellulosic biomass into reducing sugars using dilute acid hydrolysis and alkaline pretreatment. *Cellulose*, *23*(3), pp.1491-1520.

López-Sanz, S., Moreno, R., de la Mata, M.J., Moreno, F.J. and Villamiel, M., 2018. Stability of oligosaccharides derived from lactose and lactulose regarding rheological and thermal properties. *Journal of Food Quality*, *2018*.

Loyao Jr, A.S., Villasica, S.L.G., Peña, P.L.L.D. and Go, A.W., 2018. Extraction of lipids from spent coffee grounds with non-polar renewable solvents as alternative. *Industrial Crops and Products*, *119*, pp.152-161.

Magengelele, M., Hlalukana, N., Malgas, S., Rose, S.H., Van Zyl, W.H. and Pletschke, B.I., 2021. Production and *in vitro* evaluation of prebiotic manno-oligosaccharides prepared with a recombinant *Aspergillus niger* endo-mannanase, Man26A. *Enzyme and Microbial Technology*, *150*, pp.109893.

Malgas, S., van Dyk, J.S. and Pletschke, B.I., 2015a. A review of the enzymatic hydrolysis of mannans and synergistic interactions between β-mannanase, β-mannosidase and α-galactosidase. *World Journal of Microbiology and Biotechnology*, *31*(8), pp.1167-1175.

Malgas, S., van Dyk, S.J. and Pletschke, B.I., 2015b. β-Mannanase Man26) and α-galactosidase (Aga27A) synergism–a key factor for the hydrolysis of galactomannan substrates. *Enzyme and Microbial Technology*, *70*, pp.1-8.

Malviya, R., Bansal, V., Pal, O.P. and Sharma, P.K., 2010. High performance liquid chromatography: a short review. *Journal of Global Pharma Technology*, *2*(5), pp.22-26.

McNutt, J. and He, Q., 2019. Spent coffee grounds: A review on current utilization. *Journal of Industrial and Engineering Chemistry*, *71*, pp.78-88.

Miller, G.L., 1959. Use of dinitrosalicylic acid reagent for determination of reducing sugar. *Analytical Chemistry*, *31*(3), pp.426-428.

Moosavi, S.M. and Ghassabian, S., 2018. Linearity of Calibration Curves for Analytical Methods: A Review of Criteria for Assessment of Method Reliability. *Calibration and Validation of Analytical Methods: A Sampling of Current Approaches*, pp.109-127. *IntechOpen Limited: London, UK*.

Moreira, A.S., Nunes, F.M., Domingues, M.R. and Coimbra, M.A., 2012. Coffee melanoidins: structures, mechanisms of formation and potential health impacts. *Food & Function*, 3(9), pp.903-915.

Moreira, A.S., Nunes, F.M., Domingues, M.R.M. and Coimbra, M.A., 2015. Galactomannans in coffee. *Coffee in Health and Disease Prevention*, pp.173-182. Academic Press.

Moreira, L.R.S. and Filho, E. X. F., 2008. An overview of mannan structure and mannan-degrading enzyme systems. *Applied Microbiology and Biotechnology*, *79*(2), pp.165.

Mosier, N., Wyman, C., Dale, B., Elander, R., Lee, Y.Y., Holtzapple, M. and Ladisch, M., 2005. Features of promising technologies for pretreatment of lignocellulosic biomass. *Bioresource Technology*, *96*(6), pp.673-686.

Mussatto, S.I., Carneiro, L.M., Silva, J.P., Roberto, I.C. and Teixeira, J.A., 2011. A study on chemical constituents and sugars extraction from spent coffee grounds. *Carbohydrate Polymers*, *83*(2), pp.368-374.

Nguyen, Q.A., Cho, E.J., Lee, D.S. and Bae, H.J., 2019. Development of an advanced integrative process to create valuable biosugars including manno-oligosaccharides from spent coffee grounds. *Bioresource Technology*, *272*, pp.209-216.

Nunes, F.M., Domingues, M.R. and Coimbra, M.A., 2005. Arabinosyl and glucosyl residues as structural features of acetylated galactomannans from green and roasted coffee infusions. *Carbohydrate Research*, *340*(10), pp.1689-1698.

Oosterveld, A., Coenen, G.J., Vermeulen, N.C.B., Voragen, A.G.J. and Schols, H.A., 2004. Structural features of acetylated galactomannans from green *Coffea arabica* beans. *Carbohydrate polymers*, *58*(4), pp.427-434.

Oriez, V., Peydecastaing, J. and Pontalier, P.Y., 2020. Lignocellulosic biomass mild alkaline fractionation and resulting extract purification processes: conditions, yields, and purities. *Clean Technologies*, *2*(1), pp.91-115.

Ozaki, K., Fujii, S. and Hayashi, M.t, 2007. Effect of dietary mannooligosaccharides on the immune system of ovalbumin-sensitized mice. *Journal of Health Science*, *53*(6), pp.766-770.

Ozturk, B., Cekmecelioglu, D. and Ogel, Z.B., 2010. Optimal conditions for enhanced β-mannanase production by recombinant *Aspergillus sojae*. *Journal of Molecular Catalysis B: Enzymatic*, *64*(3-4), pp.135-139.

Pan, X.D., Chen, F.Q., Wu, T.X., Tang, H.G. and Zhao, Z.Y., 2009a. Prebiotic oligosaccharides change the concentrations of short-chain fatty acids and the microbial population of mouse bowel. *Journal of Zhejiang University SCIENCE B*, 10(4), pp.258-263.

Pan, X., Wu, T., Zhang, L., Cai, L. and Song, Z., 2009b. Influence of oligosaccharides on the growth and tolerance capacity of *lactobacilli* to simulated stress environment. *Letters in Applied Microbiology*, 48(3), pp.362-367.

Pandey, S., Do, J.Y., Kim, J. and Kang, M., 2020. Fast and highly efficient removal of dye from aqueous solution using natural locust bean gum based hydrogels as adsorbent. *International Journal of Biological Macromolecules*, *143*, pp.60-75.

P rez-Burillo, S., Pastoriza, S., Fern ndez- r teaga, ., Luz n, G., Jim ne z-Hern ndez, N., D' ur ia, G., Francino, M.P. and Rufi n -Henares, J.A., 2019. Spent coffee grounds extract, rich in mannooligosaccharides, promotes a healthier gut microbial community in a dose-dependent manner. *Journal of Agricultural and Food Chemistry*, *67*(9), pp.2500-2509.

Pena, R.T., Blasco, L., Ambroa, A., González-Pedrajo, B., Fernández-García, L., López, M., Bleriot, I., Bou, G., García-Contreras, R., Wood, T.K. and Tomás, M., 2019. Relationship between quorum sensing and secretion systems. *Frontiers in Microbiology*, *10*, pp.1100.

Pheiffer, C., Pillay-van Wyk, V., Turawa, E., Levitt, N., Kengne, A.P. and Bradshaw, D., 2021. Prevalence of Type 2 Diabetes in South Africa: A Systematic Review and Meta-Analysis. *International Journal of Environmental Research and Public Health*, *18*(11), pp.5868.

Redgwell, R. and Fischer, M., 2006. Coffee carbohydrates. *Brazilian Journal of Plant Physiology*, *18*(1), pp.165-174.

Rodr guez- r talejo, F. and L pe z-Garc a, E., 2017. Coffee consumption and cardiovascular disease: A condensed review of epidemiological evidence and mechanisms. *Journal of Agricultural and Food Chemistry*, *66*(21), pp.5257-5263.

Roos, S. and Jonsson, H., 2002. A high-molecular-mass cell-surface protein from *Lactobacillus reuteri* 1063 adheres to mucus components: The GenBank accession number for the sequence reported in this paper is AF120104. *Microbiology*, *148*(2), pp.433-442.

Sabir, A.M., Moloy, M. and Bhasin, P.S., 2013. HPLC method development and validation: A review. *International Research Journal of Pharmacy, 4*(4), pp.39-46.

Sachslehner, A., Foidl, G., Foidl, N., Gübitz, G. and Haltrich, D., 2000. Hydrolysis of isolated coffee mannan and coffee extract by mannanases of *Sclerotium rolfsii*. *Journal of Biotechnology*, *80*(2), pp.127-134.

Saeed, M., Ahmad F., Arain, M. A., El-Hack, A., Emam, M., Bhutto, A. Z., and Moshaveri, A. 2017. Use of Mannan-Oligosaccharides (MOS) As a Feed Additive in Poultry Nutrition. *Journal of World's Poultry Research*, 7(3), pp.94-99

Santos-Sánchez, N.F., Salas-Coronado, R., Villanueva-Cañongo, C. and Hernández-Carlos, B., 2019. Antioxidant compounds and their antioxidant mechanism. *In Antioxidants*, pp.1-28. *London, UK: IntechOpen*.

Sicard, J.F., Le Bihan, G., Vogeleer, P., Jacques, M. and Harel, J., 2017. Interactions of intestinal bacteria with components of the intestinal mucus. *Frontiers in Cellular and Infection Microbiology*, *7*, pp.387.

Singh, S., Ghosh, A. and Goyal, A., 2018. Manno-oligosaccharides as Prebiotic-Valued Products from Agro-waste. In *Biosynthetic Technology and Environmental Challenges*, pp. 205-221. Springer, Singapore.

Solano, C., Echeverz, M. and Lasa, I., 2014. Biofilm dispersion and quorum sensing. *Current Opinion in Microbiology*, *18*, pp.96-104.

Song, Y., Liu, D., Liu, M., Yang, H., Fan, Y., Sun, W., Xue, Y., Zhang, T. and Ma, Y., 2018. Transcriptional regulation of the mannan utilization genes in the alkaliphilic *Bacillus* sp. N16-5. *FEMS Microbiology Letters*, *365*(4), pp.1-6

Soni, H., Rawat, H.K., Pletschke, B.I. and Kango, N., 2016. Purification and characterization of β-mannanase from *Aspergillus terreus* and its applicability in depolymerization of mannans and saccharification of lignocellulosic biomass. *3 Biotech*, *6*(2), pp.1-11.

Srivastava, P.K., Panwar, D., Prashanth, K.H. and Kapoor, M., 2017. Structural characterization and *in vitro* fermentation of β-mannooligosaccharides produced from locust bean gum by GH-26 endo-β-1, 4-mannanase (ManB-1601). *Journal of Agricultural and Food Chemistry*, *65*(13), pp.2827-2838.

Stoll, D., Boraston, A., Stålbrand, H., McLean, B.W., Kilburn, D.G. and Warren, R.A.J., 2000. Mannanase Man26A from *Cellulomonas fimi* has a mannan-binding module. *FEMS Microbiology Letters*, *183*(2), pp.265-269.

Sultan, A., Ullah, T., Khan, S. and Khan, R.U., 2015. Effect of organic acid supplementation on the performance and ileal microflora of broiler during finishing period. *Pakistan Journal of Zoology*, *47*(3).

Sun, T., Tao, H., Xie, J., Zhang, S. and Xu, X., 2010. Degradation and antioxidant activity of κ-carrageenans. *Journal of Applied Polymer Science*, *117*(1), pp.194-199.

Swartz, M. and Krull, I., 2005. Analytical method validation: Accuracy in quantitation. *LC GC North America*, pp.86-88.

Tailford, L.E., Ducros, V.M.A., Flint, J.E., Roberts, S.M., Morland, C., Zechel, D.L., Smith, N., Bjornvad, M.E., Borchert, T.V., Wilson, K.S. and Davies, G.J., 2009. Understanding how diverse β-mannanases recognize heterogeneous substrates. *Biochemistry*, *48*(29), pp.7009-7018.

Tailford, L.E., Money, V.A., Smith, N.L., Dumon, C., Davies, G.J. and Gilbert, H.J., 2007. Mannose foraging by *Bacteroides thetaiotaomicron*: structure and specificity of the β-mannosidase, BtMan2A. *Journal of Biological Chemistry*, *282*(15), pp.11291-11299.

Tarini, J. and Wolever, T.M., 2010. The fermentable fibre inulin increases postprandial serum short-chain fatty acids and reduces free-fatty acids and ghrelin in healthy subjects. *Applied Physiology, Nutrition and Metabolism*, *35*(1), pp.9-16

Thaipong, K., Boonprakob, U., Crosby, K., Cisneros-Zevallos, L. and Byrne, D.H., 2006. Comparison of ABTS, DPPH, FRAP, and ORAC assays for estimating antioxidant activity from guava fruit extracts. *Journal of food composition and analysis*, *19*(6-7), pp.669-675.

Tian, T., Freeman, S., Corey, M., German, J.B. and Barile, D., 2017. Chemical characterization of potentially prebiotic oligosaccharides in brewed coffee and spent coffee grounds. *Journal of Agricultural and Food Chemistry*, *65*(13), pp.2784-2792.

Trunk, T., Khalil, H.S. and Leo, J.C., 2018. Bacterial autoaggregation. *AIMS microbiology*, 4(1), pp.140.

Tsai, W.T., Liu, S.C. and Hsieh, C.H., 2012. Preparation and fuel properties of biochars from the pyrolysis of exhausted coffee residue. *Journal of Analytical and Applied Pyrolysis*, *93*, pp.63-67.

Tsukagoshi, H., Nakamura, A., Ishida, T., Otagiri, M., Moriya, S., Samejima, M., Igarashi, K., Kitamoto, K. and rioka, M., 2014. The GH26 β-mannanase RsMan26H from a symbiotic protist of the termite *Reticulitermes speratus* is an endo-processive mannobiohydrolase: heterologous expression and characterization. *Biochemical and Biophysical Research Communications*, *452*(3), pp.520-525.

Van den Ende, W., Peshev, D. and De Gara, L., 2011. Disease prevention by natural antioxidants and prebiotics acting as ROS scavengers in the gastrointestinal tract. *Trends in Food Science & Technology*, *22*(12), pp.689-697.

Van Zyl, W.H., Rose, S.H., Trollope, K. and Görgens, J.F., 2010. Fungal β-mannanases: mannan hydrolysis, heterologous production and biotechnological applications. *Process Biochemistry*, *45*(8), pp.1203-1213.

Vidushi, Y. and Meenakshi, B., 2017. A review on HPLC method development and validation. *Research Journal of Life Sciences, Bioinformatics, Pharmaceutical and Chemical Sciences, 2*(6), pp.178.

Winter, S.E., Thiennimitr, P., Winter, M.G., Butler, B.P., Huseby, D.L., Crawford, R.W., Russell, J.M., Bevins, C.L., Adams, L.G., Tsolis, R.M. and Roth, J.R., 2010. Gut inflammation provides a respiratory electron acceptor for *Salmonella*. *Nature*, *467*(7314), pp.426-429.

Wolfrom, M.L. and Patin, D.L., 1965. Carbohydrates of the Coffee Bean. IV. An Arabinogalactan1. *The Journal of Organic Chemistry*, *30*(12), pp.4060-4063.

Wongsiridetchai, C., Chiangkham, W., Khlaihiran, N., Sawangwan, T., Wongwathanarat, P., Charoenrat, T. and Chantorn, S., 2018. Alkaline pretreatment of spent coffee grounds for oligosaccharides production by mannanase from *Bacillus sp*. GA2 (1). *Agriculture and Natural Resources*, *52*(3), pp.222-227.

Wongsiridetchai, C., Jonjaroen, V., Sawangwan, T., Charoenrat, T. and Chantorn, S., 2021. Evaluation of prebiotic mannooligosaccharides obtained from spent coffee grounds for nutraceutical application. *Lebensmittel-Wissenschaft & Technologie*, p.111717.

Wu, T., Xu, F., Su, C., Li, H., Lv, N., Liu, Y., Gao, Y., Lan, Y. and Li, J., 2020. Alterations in the Gut Microbiome and Cecal Metabolome During *Klebsiella pneumoniae*-Induced Pneumosepsis. *Frontiers in Immunology*, *11*, pp.1331.

Xia, W., Lu, H., Xia, M., Cui, Y., Bai, Y., Qian, L., Shi, P., Luo, H. and Yao, B., 2016. A novel glycoside hydrolase family 113 endo-β-1, 4-mannanase from *Alicyclobacillus* sp. strain A4 and insight into the substrate recognition and catalytic mechanism of this family. *Applied and Environmental Microbiology*, *82*(9), pp.2718-2727.

Xu, B., 2002. Endoglucanase and mannanase from blue mussel*, Mytilus edulis*: purification, characterization, gene and three dimensional structure (Doctoral dissertation, Acta Universitatis Upsaliensis).

Yoon, K.H., Chung, S. and Lim, B.L., 2008. Characterization of the *Bacillus subtilis WL-3* mannanase from a recombinant *Escherichia coli*. *The Journal of Microbiology*, *46*(3), pp.344.

Zhang, Y., Ju, J., Peng, H., Gao, F., Zhou, C., Zeng, Y., Xue, Y., Li, Y., Henrissat, B., Gao, G.F. and Ma, Y., 2008. Biochemical and structural characterization of the intracellular mannanase AaManA of *Alicyclobacillus acidocaldarius* reveals a novel glycoside hydrolase family belonging to clan GH-A. *Journal of Biological Chemistry*, *283*(46), pp.31551-31558.

7. Appendices

Appendix A: Reagents and materials used

Bovine serum albumin (BSA)	Sigma (Cat. No. A7906)
Bradford reagent	Sigma (Cat. No. B6916)
3,5-Dinitrosalicylic acid	Sigma (Cat No. D0550)
Di-potassium hydrogen phoshate	Merck (Cat. No. 1.05104.1000)
Di-sodium hydrogen orthophosphate	Saarchem (Cat. No. 5822860)
Endo-1,4 β-mannanase (*Bacillus* sp.)	Megazyme
Ethanol	Merck (Cat. No. 8.18700)
D-Glucose	Saarchem (Cat. No. 2676020)
Glycerol	Saarchem (Cat. No. 2676520)
Guar galactomannan, medium viscosity	Megazyme
Imidazole	Merck (Cat. No. 1.04716)
Ivory nut mannan	Megazyme
D-Galactose kit	Megazyme (Cat. No. K-LACGAR)
Locust bean gum	Fluka (Cat. No. 62631)
D-Mannose	Sigma (Cat. No. M2069)
D-Mannose, D-Fructose & D-Glucose kit	Megazyme (Cat. No. K-MANGL)
mannobiose	Megazyme
mannohaxaose	Megazyme
mannopentaose	Megazyme

mannotetraose	Megazyme
Mannotriose	Megazyme
Methanol	Merck (Cat. No. 8.22283)
p-Nitrophenol	Sigma (Cat. No. 42,575-3)
Nutrient Broth	Biolab, Merck (C24)
Phenol	Sigma (Cat.No. P3653)
Potassium permanganate	Sigma (Cat. No. 223468)
Sodium azide	Merck (Cat. No. 8.22335)
Sodium carbonate	Merck (Cat. No. 1.06392.0500)
Sodium chloride	Saarchem (Cat. No. 5822320)
Sodium chlorite	Sigma (Cat. No. 244155)
Sodium hydroxide	Saarchem (Cat. No. 5823200)
Sodium metabisulfite	Sigma-Aldrich (Cat. No.255556)
Sodium Potassium tartrate	Merck (Cat. No. 1.08087)
Tris (hydroxymethyl) aminomethane	Merck (Cat. No. 1.08382)
Tri-sodium citrate dehydrate	Merck (Cat. No. 1.06448)
Tryptone	Fluka (Cat. No. 70169)
Yeast extract	Biolab (Cat. No. BX6)
α-naphthol	Sigma-Aldrich (N1000)

Appendix B: Standard curves

Dinitrosalicylic (DNS) assay

Sugar concentration was measured using a modified DNS method (Miller, 1959). Mannose was used as a sugar standard. The DNS reagent (100ml) was prepared in a Schott bottle by dissolving the following reagents in 100 ml of distilled water: 2 g sodium hydroxide water, 2 g DNS, 40 g potassium sodium tartrate (Rochelle salt), 0.4 g phenol and 0.1 g sodium metabisulfite. The solution was then made up to 200 ml with distilled water. The Schott bottle was then covered with foil. The mannose standard curve was generated using various concentrations of mannose.

volume of each concentration of mannose standard 150 µl) was added to 300 µl of the prepared DNS reagent and mixed. The mixture was then heated at 100^{o}C for 5 min in a Labnet c cuBlock™ digital dry bath Labnet International. Inc, Woodbridge, US) and then cooled on ice for 5 min. n aliquot 250 µl) was then pipetted into a 96-well microtiter plate and the absorbance readings were then taken at 540 nm using a PowerwaveX microplate reader (BioTek Instruments). The standard curve was generated in GraphPad Prism6.05 software (San Diego, CA, USA).

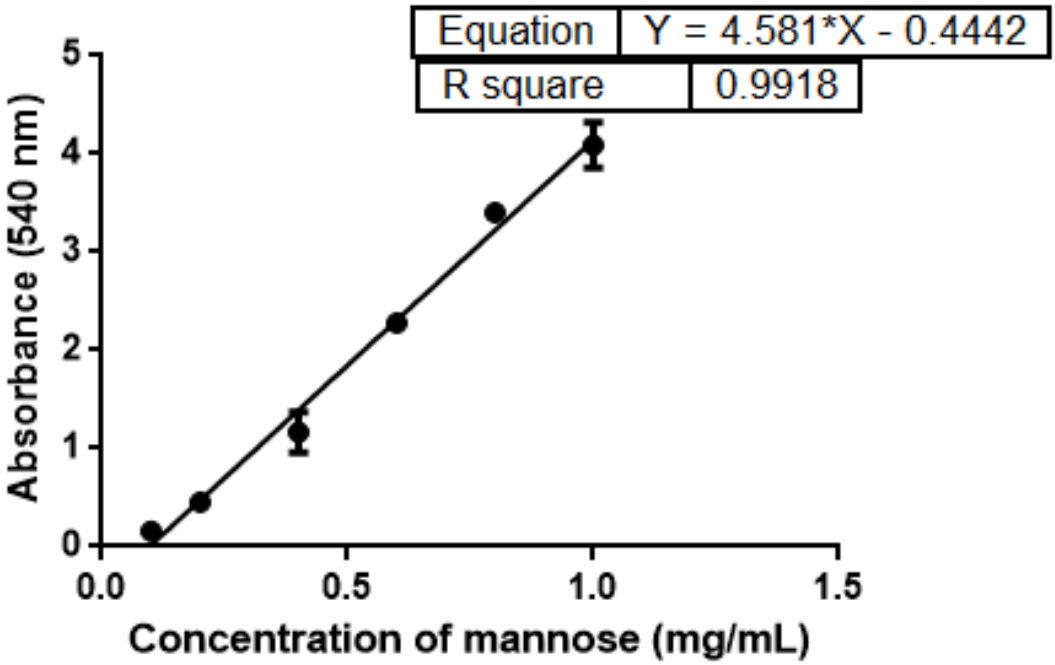

Figure B.1: Standard curve for DNS assay. Mannose was used as a standard and the absorbance was taken at 540 nm. Values are represented as means ± standard deviations, n = 3.

***p*-Nitrophenol assay**

A standard curve was generated using different *p*NP concentrations. A volume of each concentration of *p*NP 400 µl) was mixed with 400 µl of 2 M Na_2CO_3. n aliquot of 250 µl from each Eppendorf tube was pipetted into a 96-well microtiter plate and the absorbance readings were then taken at 405 nm using a PowerwaveX microplate reader (BioTek Instruments). The standard curve was generated in GraphPad Prism 6.05 software (San Diego, CA, USA).

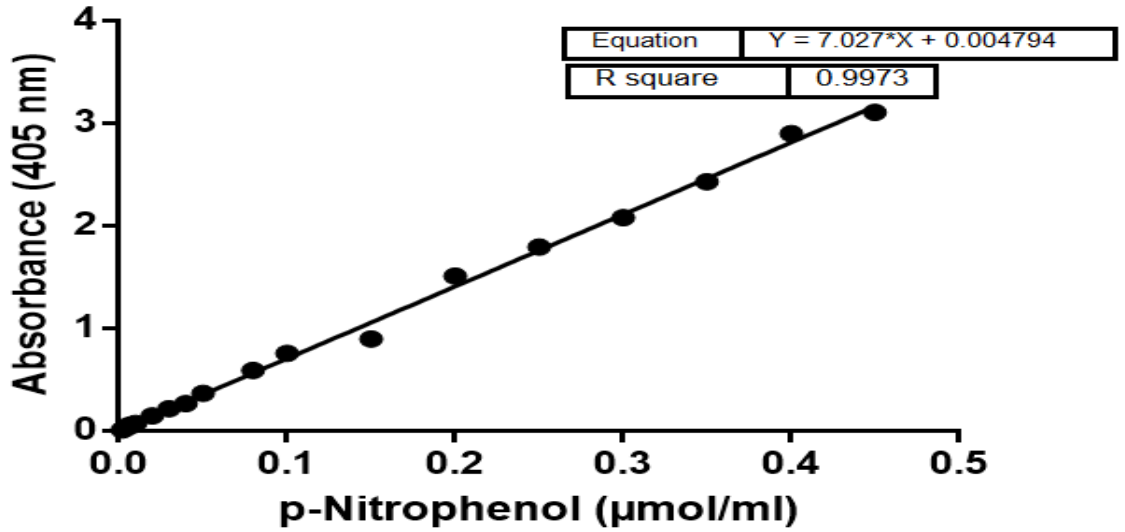

Figure B.2: Standard curve for the quantification of p-nitrophenol. The absorbance was taken at 405 nm (n=3).

Bradford Assay

The Bradford assay was used to determine the protein concentrations and this assay was adapted from Bradford (1976) and Anon (2011). Protein standard: BSA in phosphate buffer (0.05 M, pH 7.0). A standard curve with high protein concentrations (0.05 mg/mL to 0.5 mg/mL) and a sensitive standard curve (0.01 mg/mL to 0.1 mg/mL) were generated. For the low concentration sensitive) range assay, 150 µL of Bradford's reagent was added to 150 µL of each standard solution in a 96-well microtiter plate. For the high concentration range assay, 230 µL of Bradford's reagent was added to 25 µL of each standard solution in a 96-well microtiter plate. The plates were then gently mixed for 5 minutes at room temperature. Absorbance at 595 nm was then read with a PowerwaveX microplate reader (Bio-Tek Instruments). Samples were gently shaken in the microplate reader for 10 seconds prior to absorbance readings being taken. Standard curves were generated using GraphPad Prism 6.05 software (San Diego, CA, USA) and Microsoft Excel.

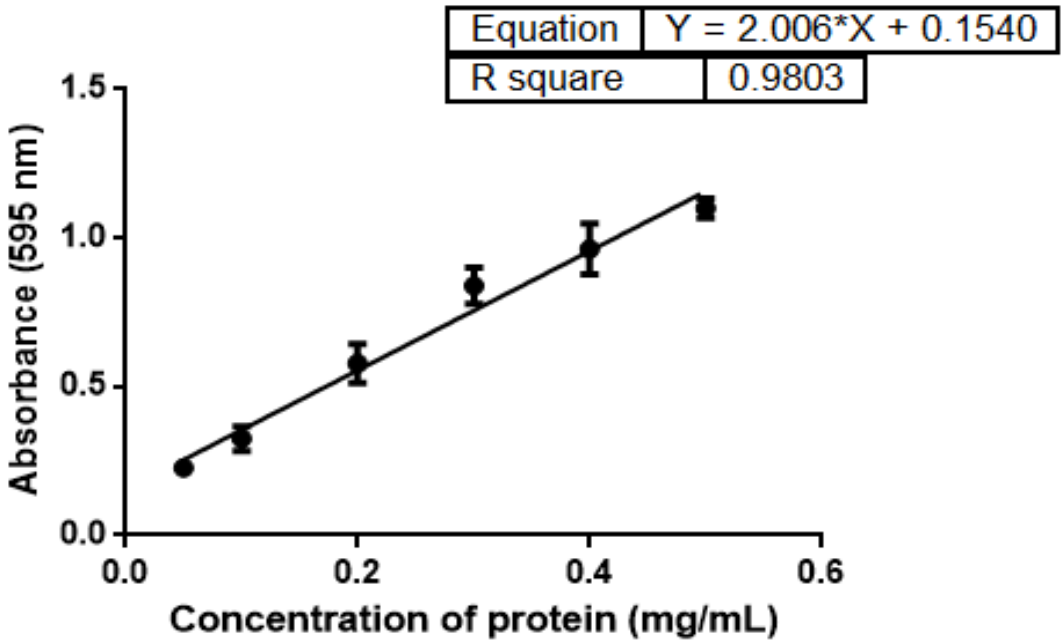

Figure B.3: Bradford standard curve to determine protein concentration, where BSA was used as the protein standard. Values are represented as means ± standard deviations, n = 3.

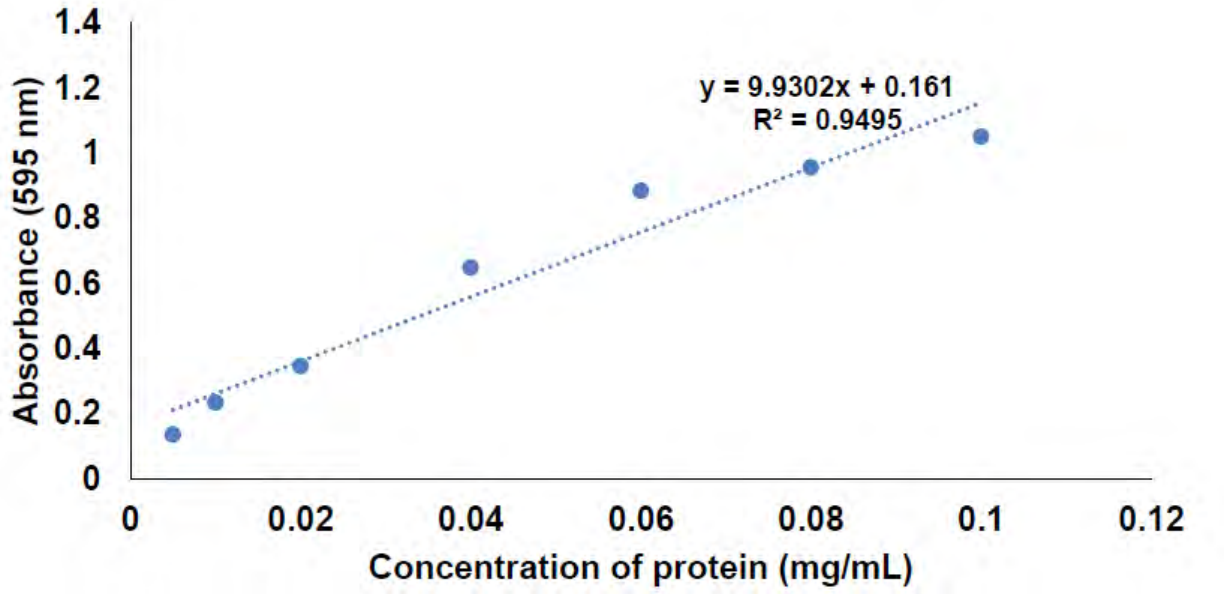

Figure B.4: Sensitive Bradford standard curve to determine protein concentration - BSA was used as the protein standard. Values are represented as means ± standard deviations, n = 3.

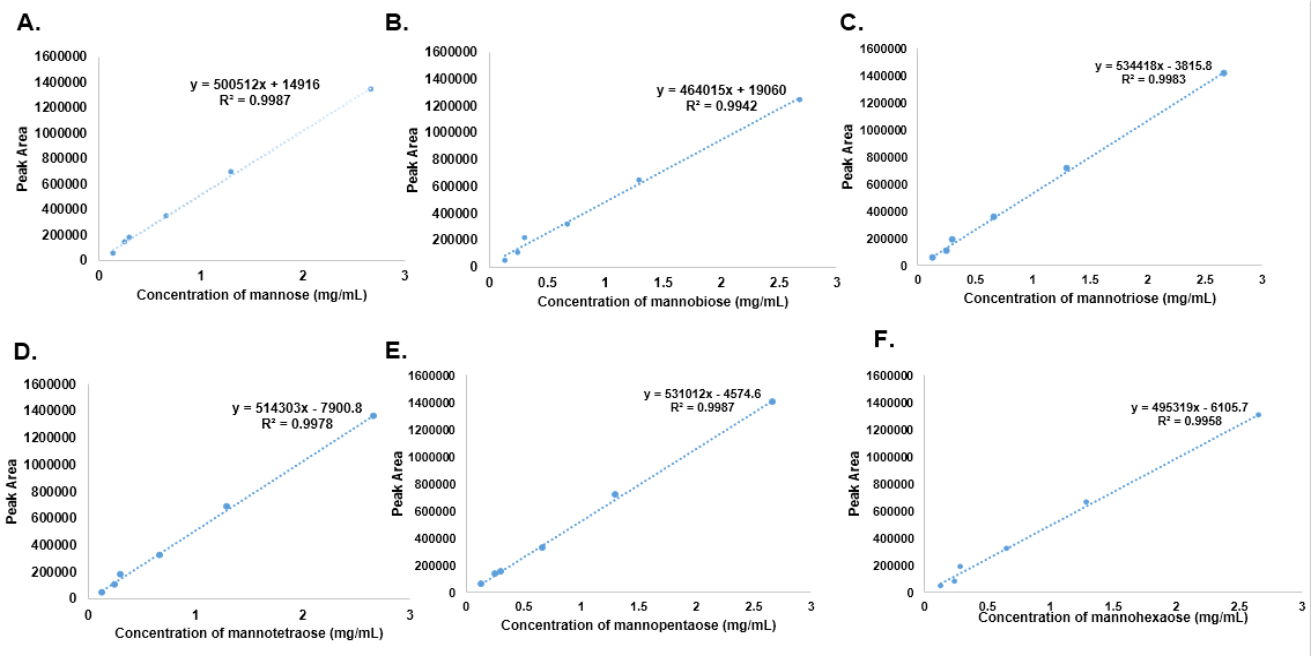

Figure B.5: Standard curves for mannoo-oligosaccharides (MOS). A: mannose (M1), B: mannobiose (M2), C: mannotriose (M3), D: mannotetraose (M4), E: mannopentaose (M5) and F: mannohexaose (M6)

Appendix C: Butyric acid standard curve

Amount of a carbonyl group at different butyric acid concentrations

A method was developed for SCFA detection after MOS fermentation, where 0.1 mg/ml of acetic acid (AA), butyric acid (BA), lactic acid (LA), citric acid (CA), formic acid (FA) and propanoic acid (PA) standards were prepared, and each standard was mixed with hydrochloric acid (HCl, 0.25 M) in a 1:1 ratio. The spectral scans of samples were then taken in the UV region of 200 to 400 nm in 5 nm increments. The results showed that the organic acids absorbed maximally between 205 and 225 nm. Different concentrations (0.0001– 0.01 mmol/mL) of the BA were then prepared, mixed with HCl in a ratio of 1:1 and the absorbance was read at 210 nm to determine the amount of the carbonyl group present. The absorbance values increased with an increase in concentrations of the acids.

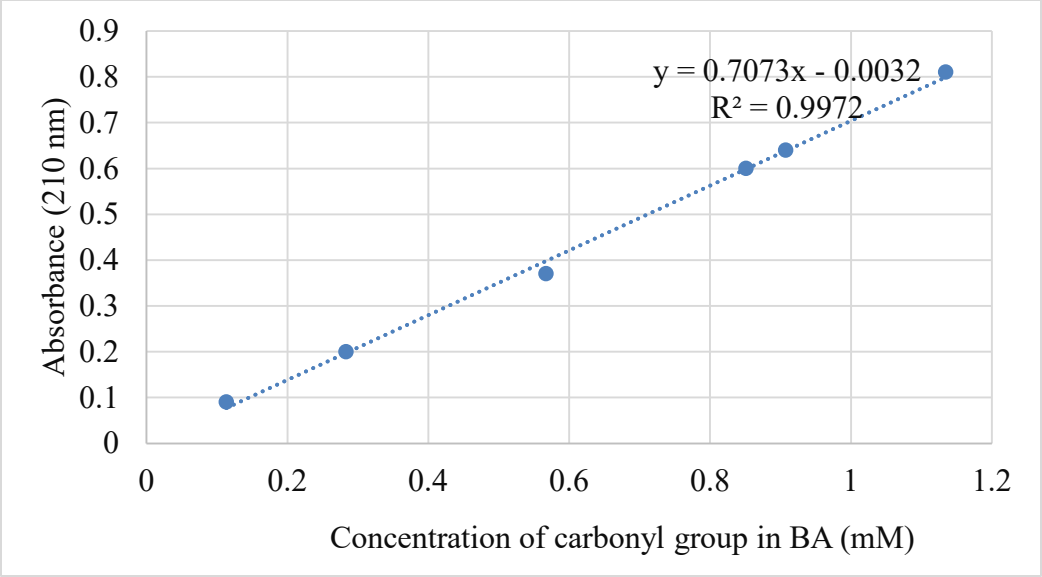

Figure C. 1: Detection of carbonyl groups present in butyric acid (BA). The absorbance values increased with increased concentrations of each acid. Values are represented as means ± standard deviations, n = 3.

Appendix D: High Performance Liquid Chromatograms (HPLC)

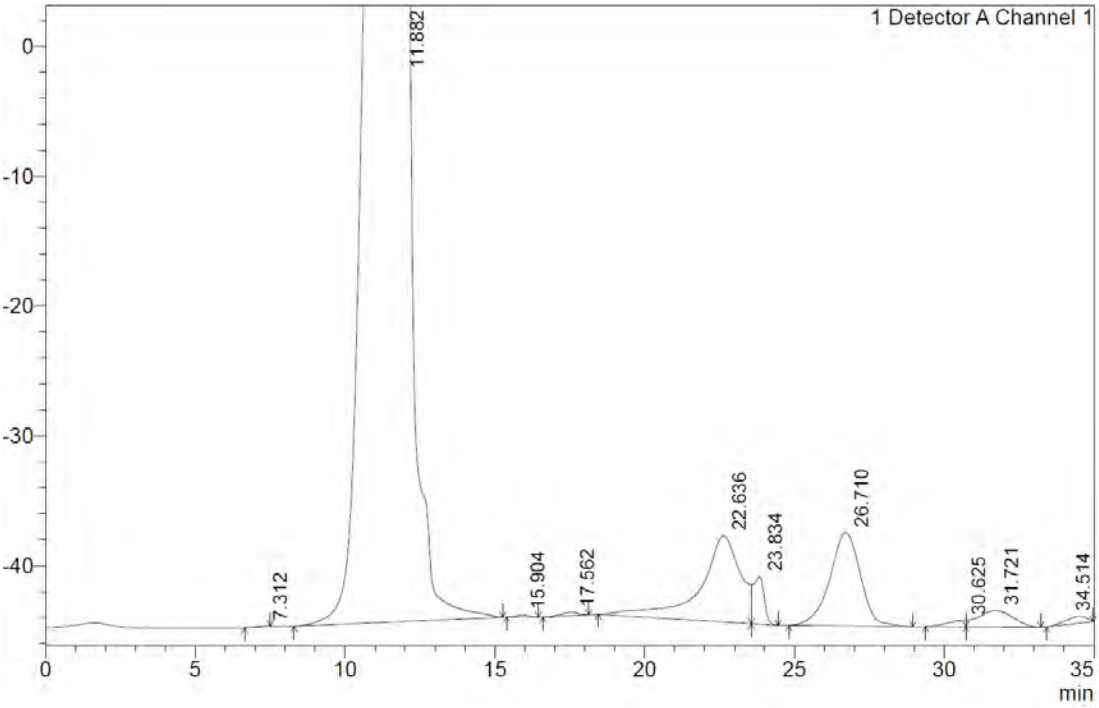

Figure D.1: A representative chromatogram displaying the simultaneous detection and separation of MOS released by SCG hydrolysis. The hydrolysis products were separated using a CarboSep CHO 411 column at a flow rate of 0.3 min/Ml. Distilled water was used as a mobile phase and using a refractive index (RI) detector. MOS: M1-mannose, M2-mannobiose, M3-mannotriose, M4-mannotetraose, M5-mannopentaose and M6-mannohexanose.